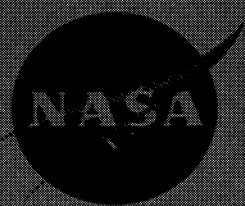


NASA
SPACE VEHICLE
DESIGN CRITERIA
(CHEMICAL PROPULSION)

NASA SP-8115

SOLID ROCKET MOTOR NOZZLES



JUNE 1975

NATIONAL AERONAUTICS AND SPACE ADMINISTRATION

FOREWORD

NASA experience has indicated a need for uniform criteria for the design of space vehicles. Accordingly, criteria are being developed in the following areas of technology:

Environment
Structures
Guidance and Control
Chemical Propulsion

Individual components of this work will be issued as separate monographs as soon as they are completed. This document, part of the series on Chemical Propulsion, is one such monograph. A list of all monographs issued prior to this one can be found on the final pages of this document.

These monographs are to be regarded as guides to design and not as NASA requirements, except as may be specified in formal project specifications. It is expected, however, that these documents, revised as experience may indicate to be desirable, eventually will provide uniform design practices for NASA space vehicles.

This monograph, "Solid Rocket Motor Nozzles," was prepared under the direction of Howard W. Douglass, Chief, Design Criteria Office, Lewis Research Center; project management was by John H. Collins, Jr. The monograph was written by Russell A. Ellis* of Thiokol Chemical Corporation (Wasatch Division) and was edited by Russell B. Keller, Jr. of Lewis. To assure technical accuracy of this document, scientists and engineers throughout the technical community participated in interviews, consultations, and critical review of the text. In particular, William G. Haymes of Rocketdyne Solid Rocket Division, Rockwell International Corp.; Richard J. Owen of Chemical Systems Division, United Technologies; and Robert F. H. Woodberry of Hercules, Incorporated individually and collectively reviewed the monograph in detail.

Comments concerning the technical content of this monograph will be welcomed by the National Aeronautics and Space Administration, Lewis Research Center (Design Criteria Office), Cleveland, Ohio 44135.

June 1975

*Currently with Chemical Systems Division, United Technologies, Sunnyvale, California.

**For sale by the National Technical Information Service
Springfield, Virginia 22161
Price — \$5.75**

GUIDE TO THE USE OF THIS MONOGRAPH

The purpose of this monograph is to organize and present, for effective use in design, the significant experience and knowledge accumulated in development and operational programs to date. It reviews and assesses current design practices, and from them establishes firm guidance for achieving greater consistency in design, increased reliability in the end product, and greater efficiency in the design effort. The monograph is organized into two major sections that are preceded by a brief introduction and complemented by a set of references.

The State of the Art, section 2, reviews and discusses the total design problem, and identifies which design elements are involved in successful design. It describes succinctly the current technology pertaining to these elements. When detailed information is required, the best available references are cited. This section serves as a survey of the subject that provides background material and prepares a proper technological base for the *Design Criteria* and Recommended Practices.

The Design Criteria, shown in italics in section 3, state clearly and briefly what rule, guide, limitation, or standard must be imposed on each essential design element to assure successful design. The *Design Criteria* can serve effectively as a checklist of rules for the project manager to use in guiding a design or in assessing its adequacy.

The Recommended Practices, also in section 3, state how to satisfy each of the criteria. Whenever possible, the best procedure is described; when this cannot be done concisely, appropriate references are provided. The Recommended Practices, in conjunction with the *Design Criteria*, provide positive guidance to the practicing designer on how to achieve successful design.

Both sections have been organized into decimal numbered subsections so that the subjects within similarly numbered subsections correspond from section to section. The format for the Contents displays this continuity of subject in such a way that a particular aspect of design can be followed through both sections as a discrete subject.

The design criteria monograph is not intended to be a design handbook, a set of specifications, or a design manual. It is a summary and a systematic ordering of the large and loosely organized body of existing successful design techniques and practices. Its value and its merit should be judged on how effectively it makes that material available to and useful to the designer.

CONTENTS

	Page
1. INTRODUCTION	1
2. STATE OF THE ART	3
3. DESIGN CRITERIA and Recommended Practices	89
APPENDIX A – Glossary	109
APPENDIX B – Conversion of U.S. Customary Units to SI Units	115
REFERENCES	117
NASA Space Vehicle Design Criteria Monographs Issued to Date	127

<u>SUBJECT</u>	<u>STATE OF THE ART</u>	<u>DESIGN CRITERIA</u>
DESIGN REQUIREMENTS AND CONSTRAINTS	2.1	23
NOZZLE CONFIGURATION AND CONSTRUCTION	2.2	27
Aerodynamic Design	2.2.1	30
Entrance	2.2.1.1	30
Submerged	2.2.1.1.1	33
External	2.2.1.1.2	34
Blast Tube	2.2.1.1.3	34
Throat Region	2.2.1.2	35
Exit	2.2.1.3	35
Thermal Design	2.2.2	39
Throat Insert	2.2.2.1	40
Thermal Liner and Insulator	2.2.2.2	50
Liner Materials	2.2.2.2.1	54
Insulator Materials	2.2.2.2.2	61
Structural and Mechanical Design	2.2.3	62
Basic Nozzle Structure	2.2.3.1	63
Structural Materials	2.2.3.2	65
Adhesives, Sealants, and Seals	2.2.3.3	67

SUBJECT	STATE OF THE ART	DESIGN CRITERIA		
Attached TVC System	2.2.3.4	69	3.2.3.4	
Movable-Nozzle TVC System	2.2.3.5	70	3.2.3.5	
Nozzle-to-Chamber Attachment	2.2.3.6	71	3.2.3.6	
Nozzle Closure	2.2.3.7	74	3.2.3.7	
NOZZLE ANALYSIS	2.3	75	3.3	103
Aero-thermal Analysis	2.3.1	76	3.3.1	103
Thermochemical Analysis	2.3.1.1	76	3.3.1.1	103
Transport-Property Analysis	2.3.1.2	76	3.3.1.2	103
Theoretical Aerodynamic Analysis	2.3.1.3	78	3.3.1.3	104
Inviscid Flow Field	2.3.1.3.1	78	3.3.1.3.1	104
Viscous Flow Field	2.3.1.3.2	80	3.3.1.3.1	104
Experimental Aerodynamic Analysis	2.3.1.4	80	3.3.1.4	105
Theoretical Thermal Analysis	2.3.1.5	81	3.3.1.5	105
Heat Transfer	2.3.1.5.1	81	3.3.1.5.1	105
Material Response	2.3.1.5.2	83	3.3.1.5.2	106
Experimental Thermal Analysis	2.3.1.6	84	3.3.1.6	106
Structural Analysis	2.3.2	85	3.3.2	107
NOZZLE QUALITY ASSURANCE	2.4	87	3.4	107

LIST OF FIGURES

Figure	Title	Page
1	Illustration of basic nozzle configurations and nozzle nomenclature	4
2	Basic exit configurations	5
3	Typical configurations for a liquid injection system attached to nozzle	6
4	Basic configurations for flexible-joint nozzles	7
5	Three possible locations for splitleine of a movable nozzle	9
6	Nozzle for orbital boost motor	11
7	Condor nozzle	11
8	Sidewinder 1C nozzle	12
9	Phoenix nozzle	12
10	Nozzle for apogee motor, HS-303A satellite	13
11	Sparrow nozzle	13
12	Nozzle for BE-3A4 motor	14
13	Nozzle for Extended-Range ASROC	14
14	Nozzle for main retro motor on Surveyor	15
15	Nozzle for Polaris A-3 second stage	16
16	Nozzle for Pershing first stage	17
17	Nozzle for Minuteman wing VI stage I	18
18	Nozzle for Minuteman wing VI stage II	19
19	Flexible-joint nozzle for TVC on Poseidon C-3 first stage	20
20	Nozzle for 260 SL-3 motor	21
21	Deployment of combination rolling-diaphragm extendible exit cone and fluted expandable exit cone	24

Figure	Title	Page
22	Flow chart of nozzle design sequence showing major iteration loops	28
23	Throat and entry geometry for external and submerged nozzles	31
24	Gimbal nozzle incorporating blast tube	32
25	Regions of separated and potential flow in a submerged nozzle (ref. 10)	32
26	Submerged nozzle designed to locate splitline for TVC in separated-flow region	33
27	Delivered thrust coefficient of a conical nozzle as a function of expansion ratio, exit half-angle, and exit length normalized on throat radius	38
28	Nozzle machined from polycrystalline-graphite cylinder	41
29	Prevention of thermal cracking of graphite by segmenting the graphite section into rings	42
30	Provisions for thermal expansion of throat insert	44
31	Nozzle incorporating pyrolytic graphite throat	47
32	Cross-section drawings of nozzle exit showing interface configurations for thermal materials	53
33	Various methods for tape wrap and layup of reinforced-plastic parts	58
34	Large submerged nozzle with honeycomb exit structure	68
35	Three methods for thermal protection of a flexible joint	72
36	Basic methods for attaching nozzle to chamber	73
37	Types of nozzle closures	75
38	Steps in aerothermal analysis of a nozzle	77

LIST OF TABLES

Table	Title	Page
I	Chief Design Features of Representative Operational Nozzles	10
II	Typical Properties of Materials Used for Throat Inserts	46
III	Typical Properties of Phenolic Resin with Various Reinforcement Materials	55
IV	Typical Room-Temperature Properties of Nozzle Structural Metals	66

SOLID ROCKET MOTOR NOZZLES

1. INTRODUCTION

A solid rocket motor nozzle is a carefully shaped aft portion of the thrust chamber that controls the expansion of the exhaust products so that the energy forms produced in the combustion chamber are efficiently converted to kinetic energy, thereby imparting thrust to the vehicle. Approximately 65 to 75 percent of total vehicle thrust is developed by acceleration of the chamber products to sonic velocity at the nozzle throat; the remainder is developed in the nozzle expansion cone. The usual objective in nozzle design is to control the expansion in such a manner that range or payload of the total vehicle is maximized within envelope, weight, and cost constraints. The nozzle is thus an integral component of a larger system and cannot be optimized independently of that system. Because of this interrelationship, nozzle design is an iterative process in which aerodynamic, thermodynamic, structural, and fabrication considerations are manipulated within the constraints to produce a preliminary nozzle configuration. This configuration is subsequently analyzed in detail, first for thermal and structural overdesign or underdesign and second for its contribution to total vehicle performance. This dual iteration process is continued until a thermally and structurally adequate nozzle design evolved within vehicle constraints is as close to optimum as is practical.

This document details the steps in the nozzle design process, and the organization of the material parallels the order in which a designer proceeds. The monograph thus begins with the nozzle designer's role in defining design requirements and constraints. Then follow discussions of each of the three basic phases of the nozzle design process itself: (1) aerodynamic design, in which the gas-contacting surfaces are configured to produce the required performance within the envelope limits; (2) thermal design, in which thermal liners (materials that form the physical boundary for the exhaust products) and thermal insulators are selected and configured to maintain the surfaces as closely as practical against effects of erosion and to limit the structure temperature to acceptable levels; and (3) structural design, in which materials are selected and configured to support the thermal components and to sustain the predicted loads. The influences of fabrication methods, capabilities, and

limitations on nozzle components are treated as part of the discussion of the characteristics of thermal and structural materials. Special design considerations for thrust vector control (TVC) are presented.

Discussion of the analytical techniques that are used to establish thermal and structural design integrity and to predict nozzle performance follows the treatment of nozzle configuration and construction. The concluding section describes the methods for nozzle quality assurance. Relevant material from other pertinent monographs in the chemical propulsion series is indicated by reference throughout the monograph.

Throughout the document, major emphasis is placed on nozzle design and materials for modern high-temperature ($\geq 5500^{\circ}\text{F}$) aluminized propellants; nozzles for older, low-energy propellants are given less attention. Particular attention is given to recurring nozzle design problems including graphite cracking and ejection, differential erosion at material interfaces, lack of sufficient proven nondestructive testing (NDT) techniques, the uncertainty of adhesive bonding, and inadequate definition of material properties, particularly at high temperatures.

2. STATE OF THE ART

The state of the art of solid rocket motor nozzle design is such that a successful design for a given set of requirements can, in general, be accomplished without first solving problems experimentally. Experimentation is necessary only when unusually severe requirements exceed the state of the art, when new materials must be proven, or when extremely tight flightweight margins of safety must be achieved.

Figure 1 presents the two basic nozzle configurations and illustrates basic nozzle nomenclature. The external nozzle is the classical convergent-divergent or deLaval nozzle and is entirely external to the combustion chamber. In the submerged-nozzle configuration, the nozzle entry, throat, and part or all of the exit are cantilevered into the combustion chamber. The submerged nozzle uses space more efficiently in a volume-limited system (ref. 1). The submerged design is more complex than the external because (1) both inner and outer surfaces of the submerged portion are exposed to hot gases, and (2) the submerged section structurally must withstand external pressure forces in addition to the forces developed by the flow along the inner surfaces.

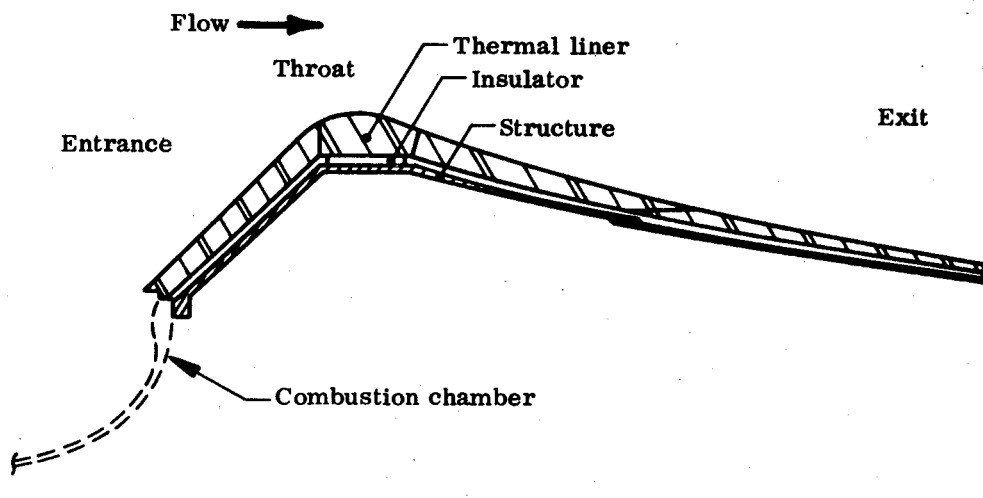
Two basic exit configurations are used, contoured and conical (fig. 2). The contoured nozzle turns the flow so that the exhaust products exit in a more nearly axial direction, thereby reducing divergence losses to a greater extent than does a conical exit.

In many solid rocket motor designs, thrust vector control (TVC) is required. The nozzle can be combined with an attached TVC system, or the nozzle itself can provide TVC (a movable nozzle). The various TVC systems are discussed in reference 2. Of the TVC systems that have achieved operational status, only the liquid-injection TVC (an attached system) and the flexible-joint system (a movable nozzle) have proved to be of continuing interest to NASA. Only these two systems therefore are considered in this monograph. Moreover, since reference 2 treats both TVC systems in detail, only the information essential to the clarity and completeness of this monograph is presented herein.

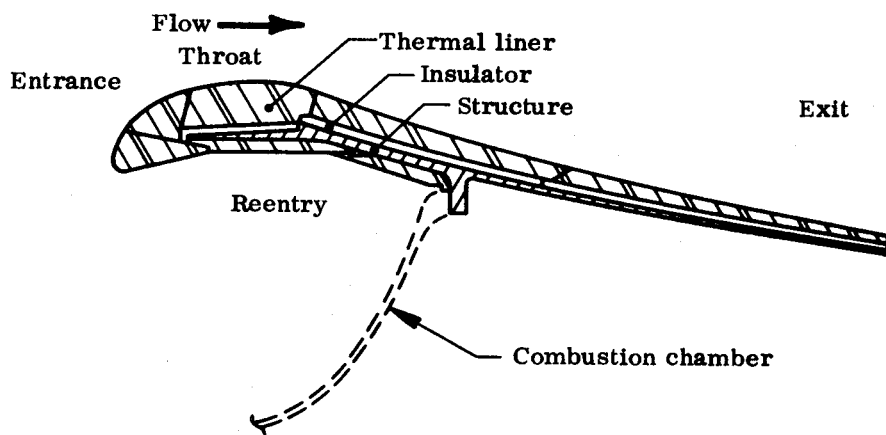
Typical configurations for mounting a liquid-injection system on external and submerged nozzles are shown in figure 3. The effects of an attached TVC system on nozzle design are fivefold: (1) the nozzle exit is subjected to concentrated and asymmetric loading; (2) attachment and support structure must be provided for the TVC system; (3) a suitable flow path through the nozzle wall must be provided for fluid injection (LITVC or HGTVC*); (4) the exit liner is subjected to localized areas of high heat transfer; and (5) the injectant may react chemically with the exit liner.

In the flexible-joint nozzle (fig. 4), the joint – a laminate formed of alternate spherical segments of elastomer layers and rigid reinforcements – attaches the movable part of the

* Symbols, materials, and abbreviations are defined or identified in Appendix A.



(a) External nozzle



(b) Submerged nozzle

Figure 1. - Illustration of basic nozzle configurations and nozzle nomenclature.

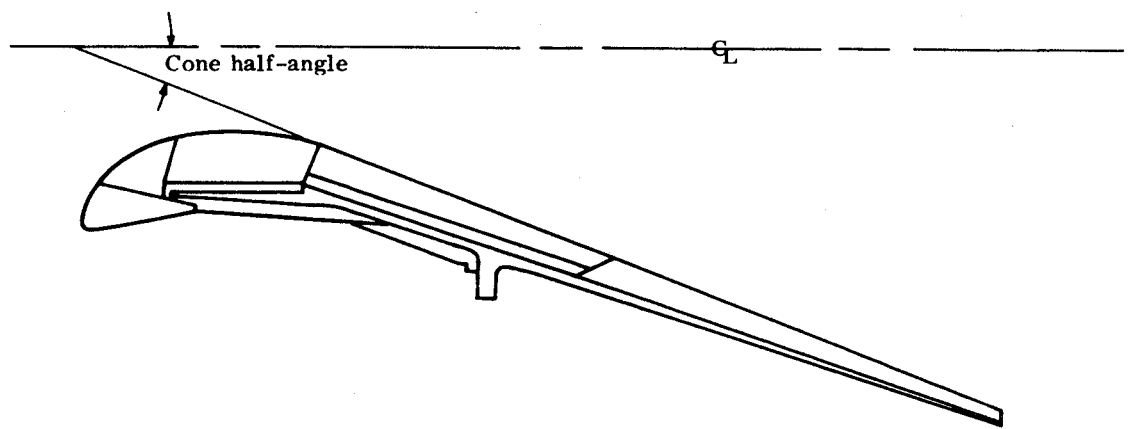
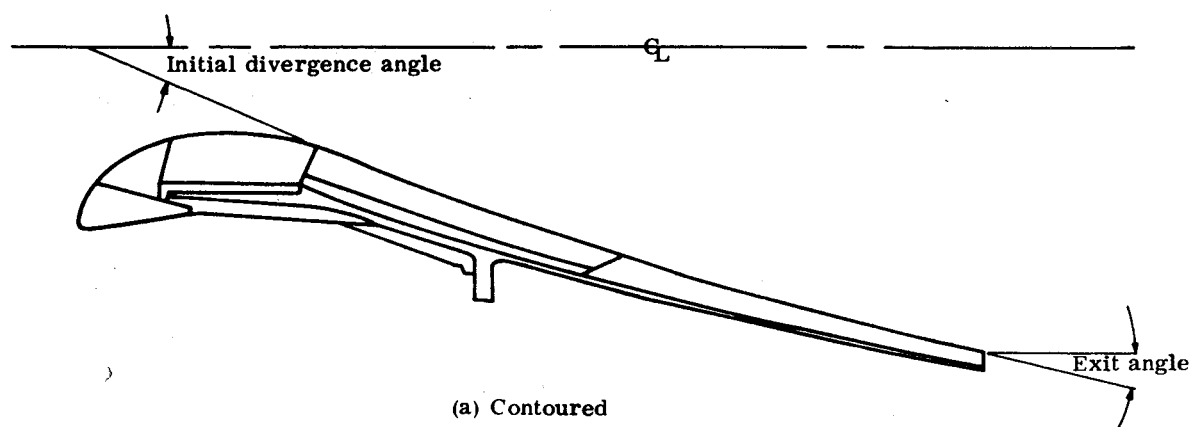
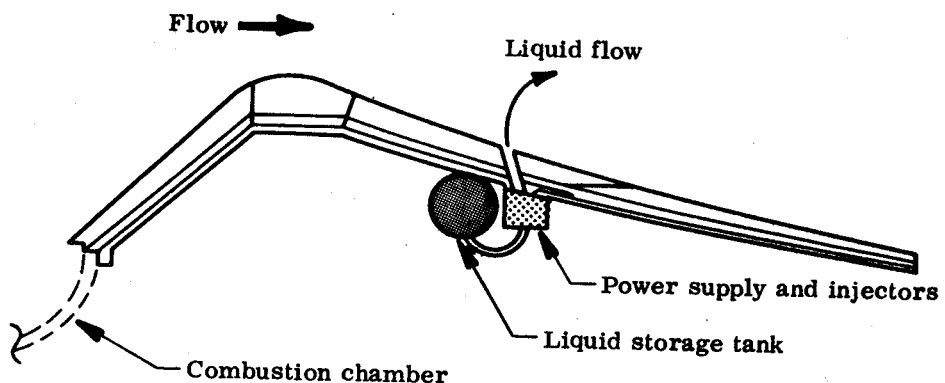
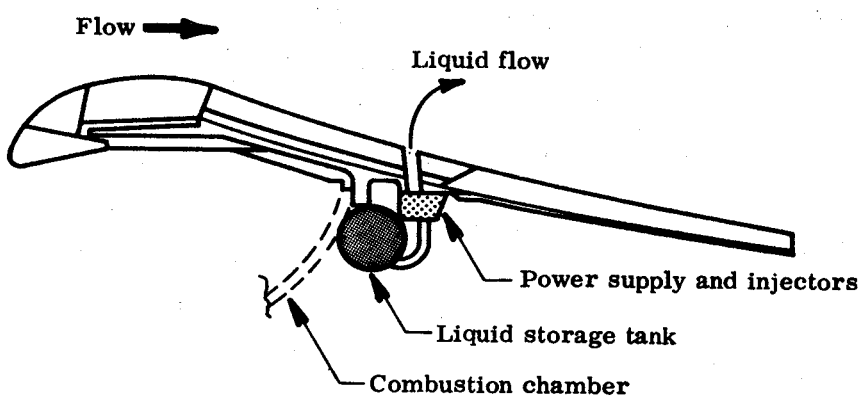


Figure 2. - Basic exit configurations.

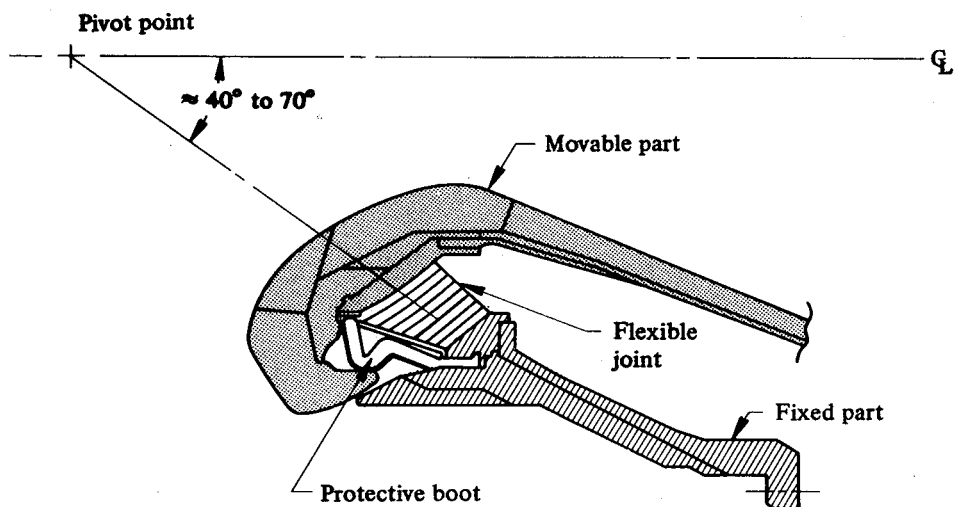


(a) External nozzle

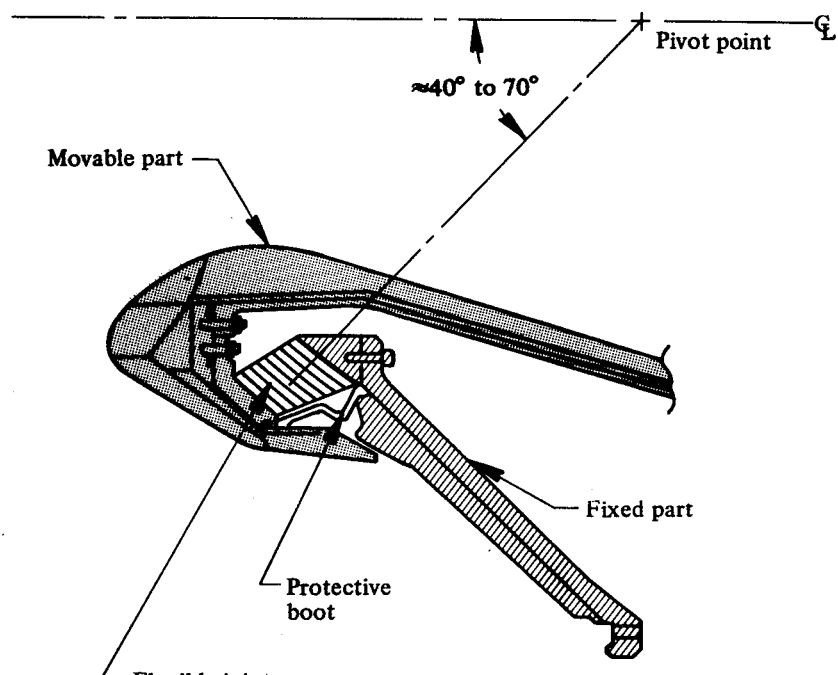


(b) Submerged nozzle

Figure 3. - Typical configurations for a liquid injection system attached to nozzle.



(a) Forward pivot



(b) Aft pivot

Figure 4. - Basic configurations for flexible-joint nozzles.

nozzle to the fixed part, seals between fixed and movable parts, and allows rotational motion about a pivot point by shear strain in the spherical elastomer layers. The dynamics and statics of the flexible-joint element are such that the pivot must be located either forward or aft of the seal, with an angle of approximately 40° to 70° between the nozzle centerline and the line connecting the pivot to the center of the seal cross section (fig. 4). The splitline between the fixed and movable nozzle sections can be located in any one of three places, as illustrated in figure 5:

- (1) In the exit-cone surface (fig. 5(a)) (a supersonic-splitline nozzle)
- (2) In the inlet surface approaching the throat (fig. 5(b)) (a subsonic-splitline nozzle)
- (3) On the chamber side of the submerged part of the nozzle (fig. 5(c)), a location that leaves the inner nozzle surface unbroken or integral (an integral movable nozzle).

The integral movable nozzle has been applied most extensively in recent movable-nozzle work and is of primary interest for future designs. Three successful tests of the supersonic-splitline nozzle have been conducted (refs. 3, 4, and 5); however, this design is not sufficiently well demonstrated and the performance is not characterized well enough to consider supersonic splines state of the art.

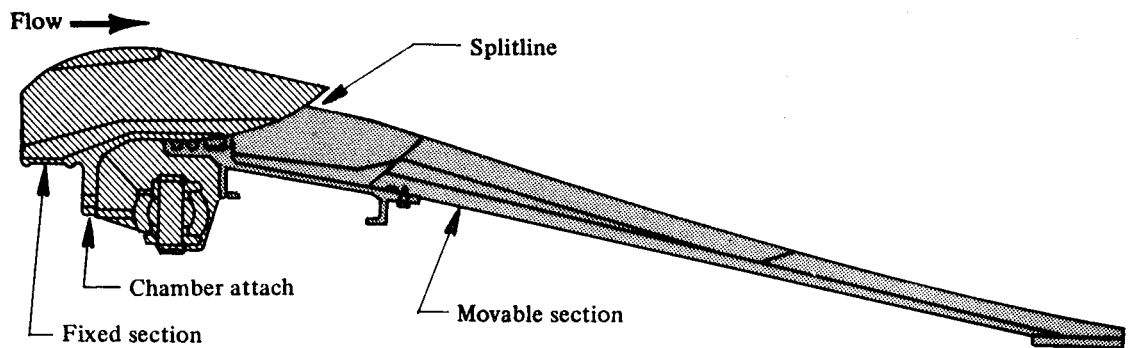
The effects of the incorporation of movable-nozzle TVC in a design are threefold: (1) the nozzle is subjected to concentrated and asymmetric loading; (2) attachment and support structure must be provided for the actuation system; and (3) relative-motion considerations (rather than aerodynamic, thermal, or structural considerations) may determine the detail design of specific areas such as the splitline boundaries.

Table I presents a summary of the chief design features of representative current nozzles. All designs listed are operational except the last two entries, the 260 SL-1 and 260 SL-3, which are included, even though not operational, because they are the two largest nozzles tested successfully to date.

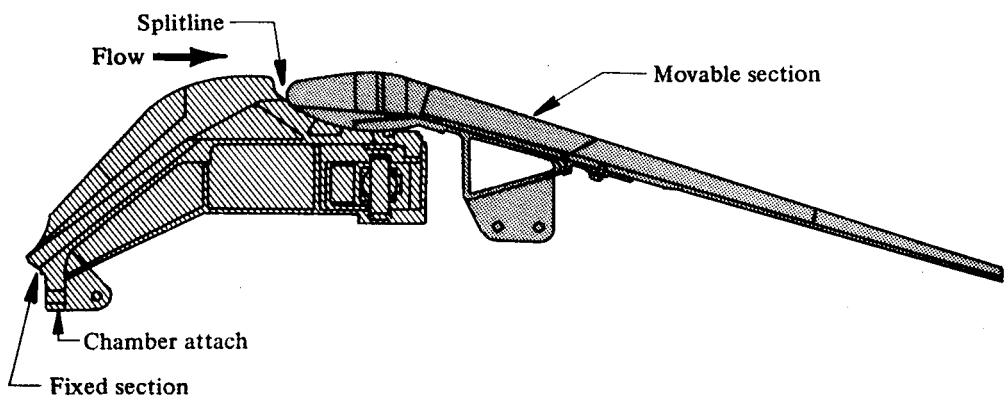
The designs are listed in order of increasing throat diameter. The entries in the table were selected to indicate the range of the design values a designer might encounter: throat diameters from about 1/2 inch to nearly 90 inches*, motor pressures from under 400 pounds per square inch to 2000 pounds per square inch, expansion ratios from less than 4 to over 50, firing durations from less than 1 second to 200 seconds, thrust from a few hundred pounds to over 5 million pounds, flame temperatures from 5100° F to over 6000° F, and a wide variety of propellant compositions.

Figures 6 through 20 illustrate many of the state-of-the-art designs presented in table I. The orbital boost motor nozzle, figure 6, consisting of only three pieces plus an O-ring, is

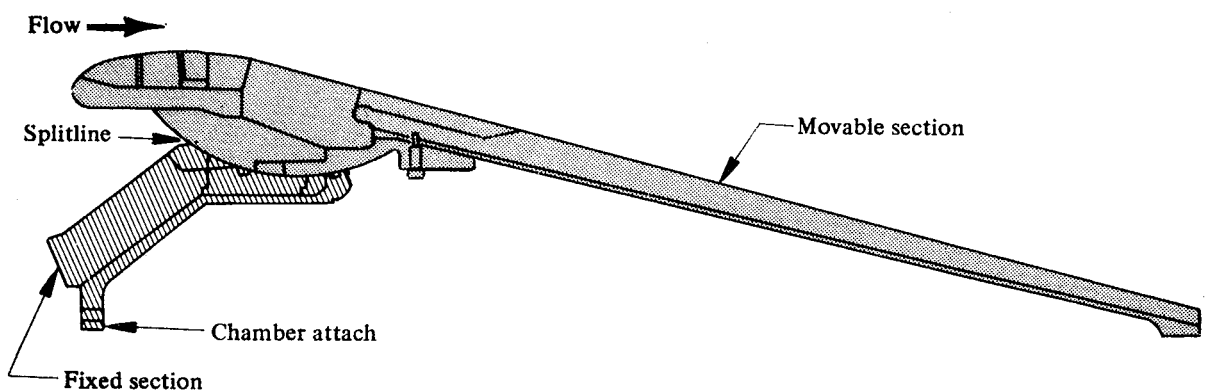
*Factors for converting U.S. customary units to the International System of Units (SI units) are given in Appendix B.



(a) Supersonic splitline



(b) Subsonic splitline



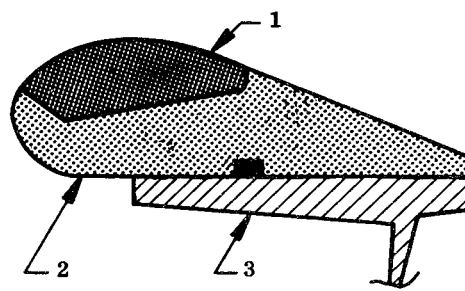
(c) Splitline on chamber side of nozzle
(integral nozzle)

Figure 5. - Three possible locations for splitline of a movable nozzle.

Table I. – Chief Design Features of Representative Operational Nozzles

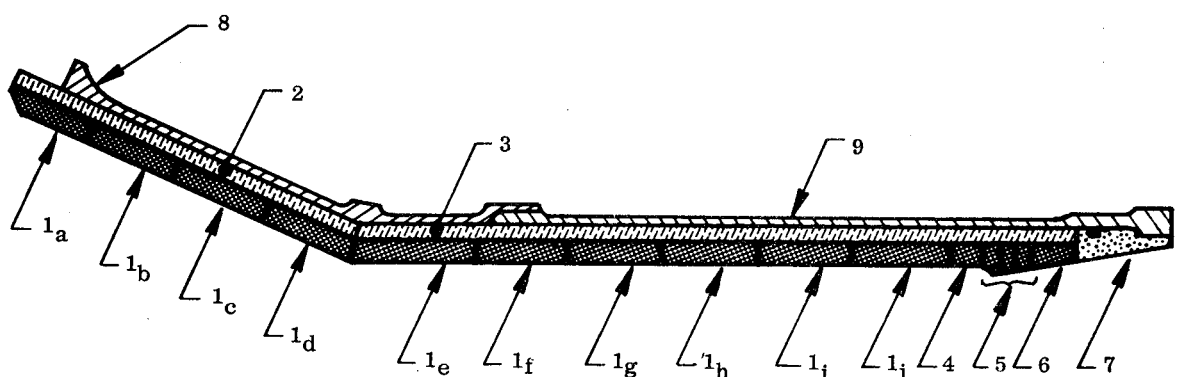
Motor or Vehicle ⁽¹⁾	Type of nozzle	Throat diameter (initial), in.	Maximum pressure, psi	Expansion ratio	Firing duration, sec	Thrust (average), lbf	Propellant flame temperature, °F	Propellant Type ⁽²⁾
Orbital Boost (CO1-1)	Fixed, submerged	0.54	1070	14.9	14.6	330	5251	AP/PBA/A1
Condor	Fixed, external	1.12	790 to 1000	7.5	100 to 200	0 to 1000	5400 to 5700	AP/PBCT/A1
Sidewinder 1C	Fixed, submerged	1.67	1300 to 2000	5.5	5.21	2700	5100	AP/PBCT/A1
Syncon Apogee	Fixed, submerged	1.75	272	35.0	19.6	855	5260	AP/PU/A1
Phoenix (Model 60, Mod 0)	Fixed, external	2.18	700 to 1000	18.5	20 to 30	1000 to 5000	5400 to 5700	AP/PBCT/A1
Apogee (HS-303A satellite)	Fixed, submerged	2.32	389	33.3	17.8	2620	5836	AP/PBCT/A1
Sparrow (Mk 38, Mod 1)	Fixed, external	2.32	1280	5.0	3.04	7085	5333	AP/PBCT/A1
FW 4	Fixed, submerged	2.34	804	50.4	30.2	5730	5698	AP/PBAN/A1
BE-3 A4	Fixed, submerged	2.83	550	18.6	9.15	5770	6300	AP/NG-NC/A1
Extended-Range ASROC	Fixed, submerged, LITVC	3.26	1350	8.6	9.0	15 200	5807	AP/PBCT/A1
Surveyor Main Retro	Fixed, submerged	3.29	556	53.2	40.5	7898	5514	AP/PBCT/A1
ATS Apogee	Fixed submerged	4.08	262	35.0	43.3	6348 (max.)	5260	AP/PU/A1
S-II Stage Ullage	Fixed, external	4.21	1150	8.0	4.2	21 100	5256	AP/PBCT/A1
Polaris A3 Stage 2	Fixed, external, LITVC, 4 per motor	4.50	< 400	14.0	60 to 100	30 000 to 60 000	>6000	AP/HMX/NC/NC/A1
Pershing First Stage	Fixed, external	6.28	400 to 700	7.1	30 to 60	10 000 to 30 000	5400 to 5700	AP/PBAN/A1
Minuteman Stage 1 Wing VI	Movable, external, hinged, 4 per motor	7.23	700 to 1000	10.0	60 to 100	100 000 to 200 000	5700 to 6000	AP/PBAN/A1
Minuteman Wing VI Second Stage	Fixed, submerged, LITVC	9.63	400 to 700	24.8	60 to 100	30 000 to 60 000	5700 to 6000	AP/PBCT/A1
Poseidon C3 1st Stage	Movable, submerged, flexible joint	11.00	700 to 1000	8.2	60 to 100	100 000 to 200 000	5700 to 6000	AP/PBAN/A1
260 SL-1 ⁽³⁾	Fixed, external	71.00	602	6.0	128.2	2 889 000	5536	AP/PBAN/A1
260 SL-3 ⁽³⁾	Fixed, submerged	89.10	643	3.8	80.3	5 884 000	5536	AP/PBAN/A1

⁽¹⁾Identification as given in Rocket Motor Manual(U), CPIA/M1, CPIA, July 1972 (Confidential). No classified information is presented in table.⁽²⁾Symbols, materials, and abbreviations are identified in Appendix A.⁽³⁾Not operational, but successfully tested.



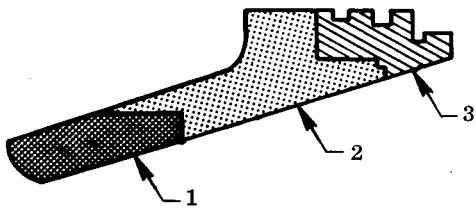
<u>Item</u>	<u>Material</u>	<u>Function</u>
1	Polycrystalline graphite	Throat insert
2	Carbon/phenolic tape	Entrance and exit thermal liner and insulation
3	Steel	Structure

Figure 6. - Nozzle for orbital boost motor.



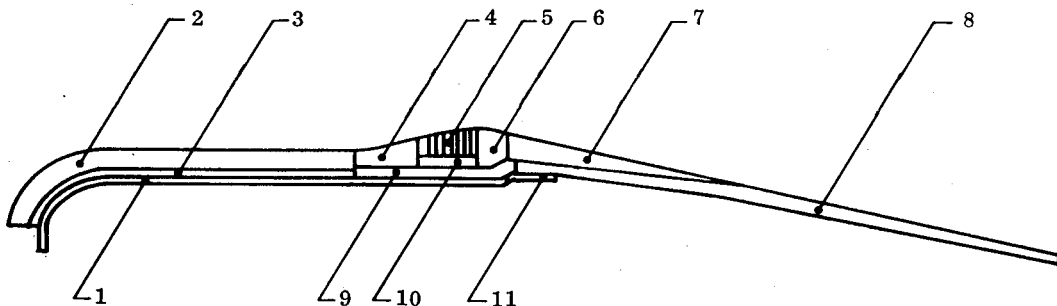
<u>Item</u>	<u>Material</u>	<u>Function</u>
1a-1j	Polycrystalline graphite	Blast tube thermal liners
2	Asbestos/phenolic die molding	Forward blast tube insulation
3	Asbestos/phenolic die molding	Aft blast tube, entrance, and throat insulation
4	Polycrystalline graphite	Throat approach thermal liner
5	Pyrolytic graphite washers	Throat insert
6	Polycrystalline graphite	Throat extension thermal liner
7	Silica/phenolic die molding	Exit thermal liner and insulation
8	Steel	Forward blast tube structure
9	Steel	Aft blast tube, entrance, throat, and exit structure

Figure 7. - Condor nozzle.



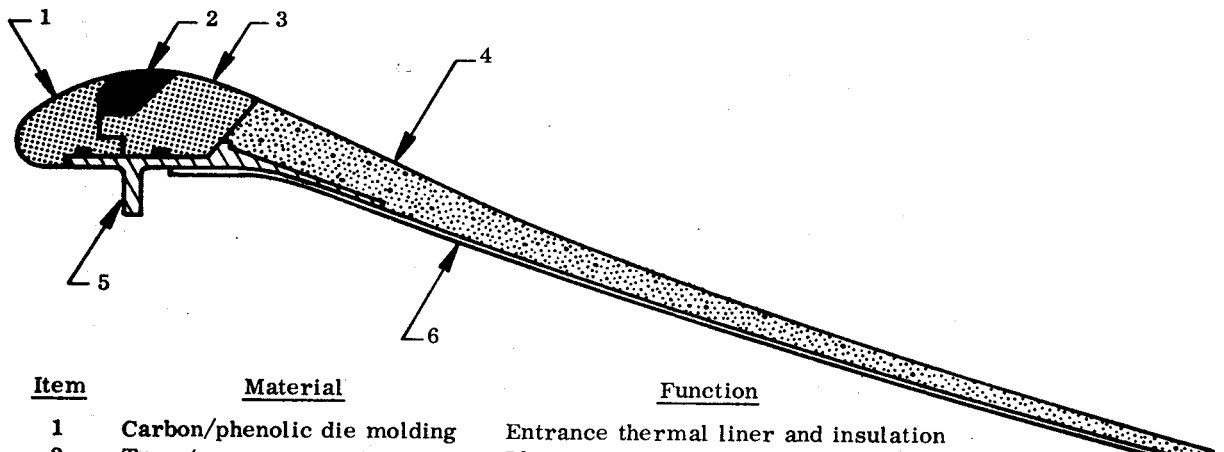
<u>Item</u>	<u>Material</u>	<u>Function</u>
1	Polycrystalline graphite	Throat insert
2	Asbestos/phenolic die molding	Throat insulation and support structure; forward exit thermal liner and insulation
3	Steel	Aft exit thermal liner, insulation, and support structure, and attach structure

Figure 8. - Sidewinder 1C nozzle.



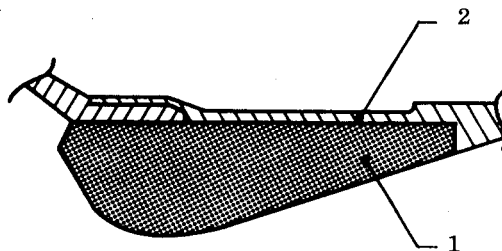
<u>Item</u>	<u>Material</u>	<u>Function</u>
1	Steel	Entrance, blast tube, and throat structure
2	Carbon/phenolic die molding	Entrance and blast tube thermal liner
3	Silica/phenolic tape	Entrance and blast tube insulation
4	Polycrystalline graphite	Throat approach thermal liner
5	Pyrolytic graphite washers	Throat insert
6	Polycrystalline graphite	Throat extension thermal liner
7	Carbon/phenolic tape	Forward exit thermal liner
8	Silica/phenolic tape	Forward exit insulation and structure, and aft exit thermal liner, insulation, and structure
9	Silica/phenolic tape	Throat insulation
10	Polycrystalline graphite	Support ring for washers
11	Aluminum	Exit attach structure

Figure 9. - Phoenix nozzle.



<u>Item</u>	<u>Material</u>	<u>Function</u>
1	Carbon/phenolic die molding	Entrance thermal liner and insulation
2	Tungsten	Throat insert
3	Carbon/phenolic die molding	Throat insulation and throat extension thermal liner
4	Silica/phenolic tape	Exit thermal liner and insulation
5	Aluminum	Attach, entrance, throat, and throat extension structure
6	Glass-cloth/epoxy	Exit structure

Figure 10. - Nozzle for apogee motor, HS-303A satellite.



<u>Item</u>	<u>Material</u>	<u>Function</u>
1	Polycrystalline graphite	Entrance, throat, and exit thermal liner and insulation
2	Steel	Entrance, throat, and exit structure

Figure 11. - Sparrow nozzle.

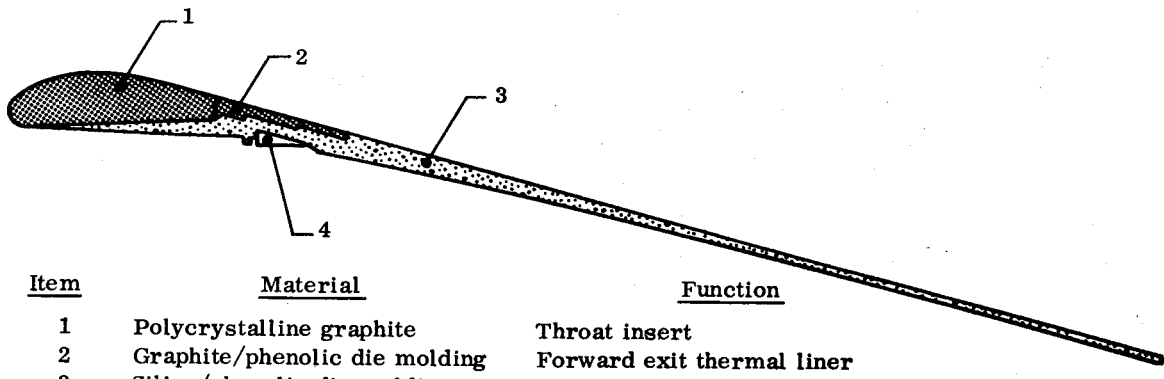
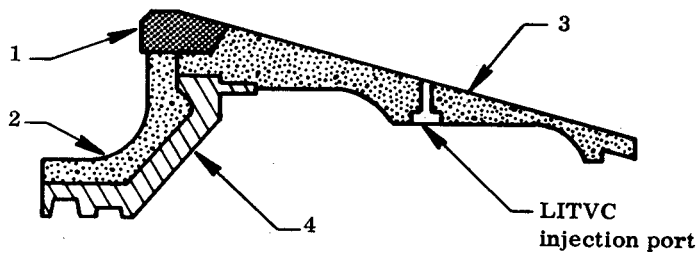


Figure 12. - Nozzle for BE-3A4 motor.



<u>Item</u>	<u>Material</u>	<u>Function</u>
1	Polycrystalline graphite	Throat insert
2	Silica/phenolic die molding	Entrance thermal liner and insulation
3	Silica/phenolic die molding	Exit thermal liner, insulation, and structure
4	Steel	Entrance structure

Figure 13. - Nozzle for Extended-Range ASROC.

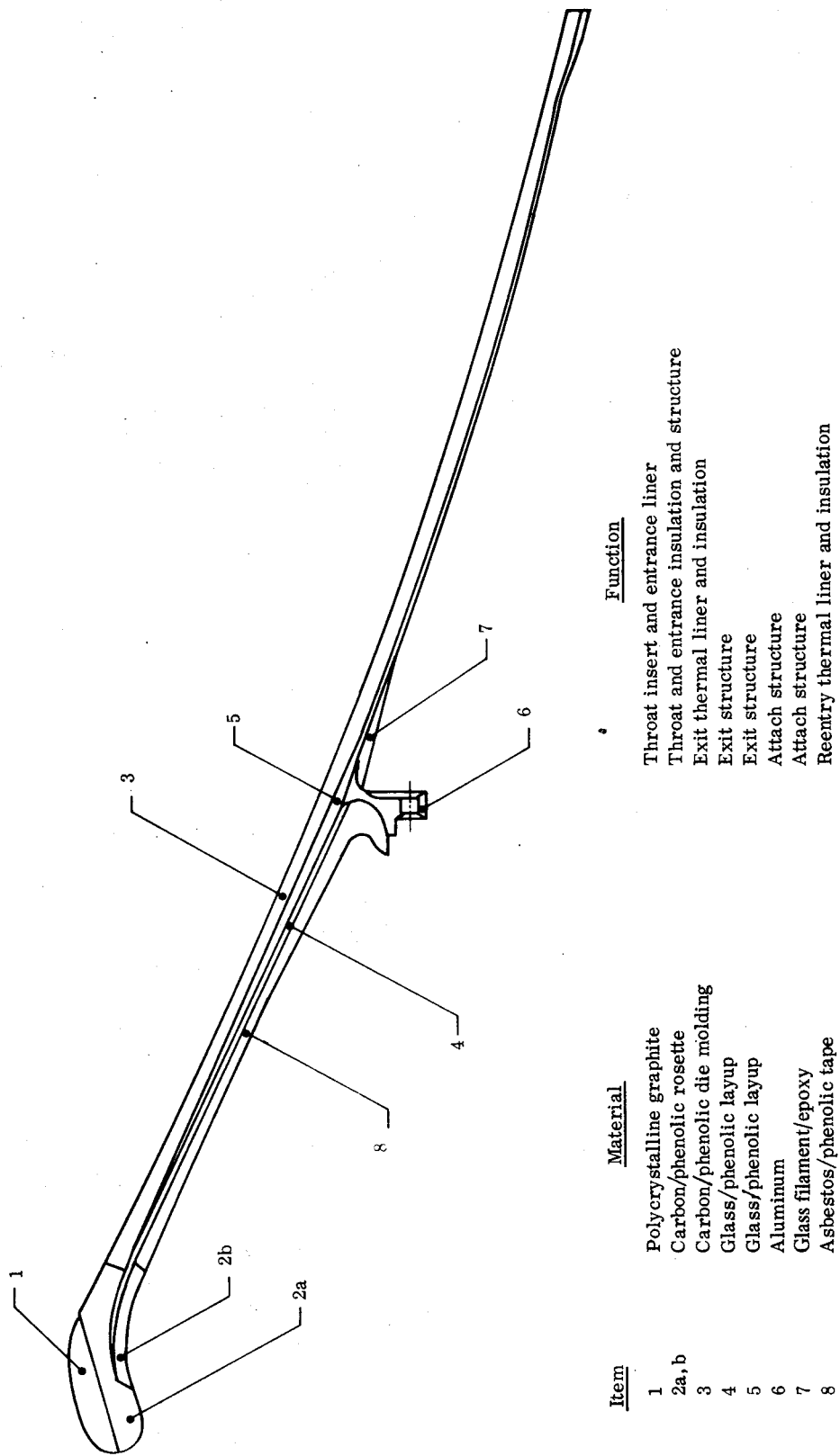


Figure 14. - Nozzle for main retro motor on Surveyor.

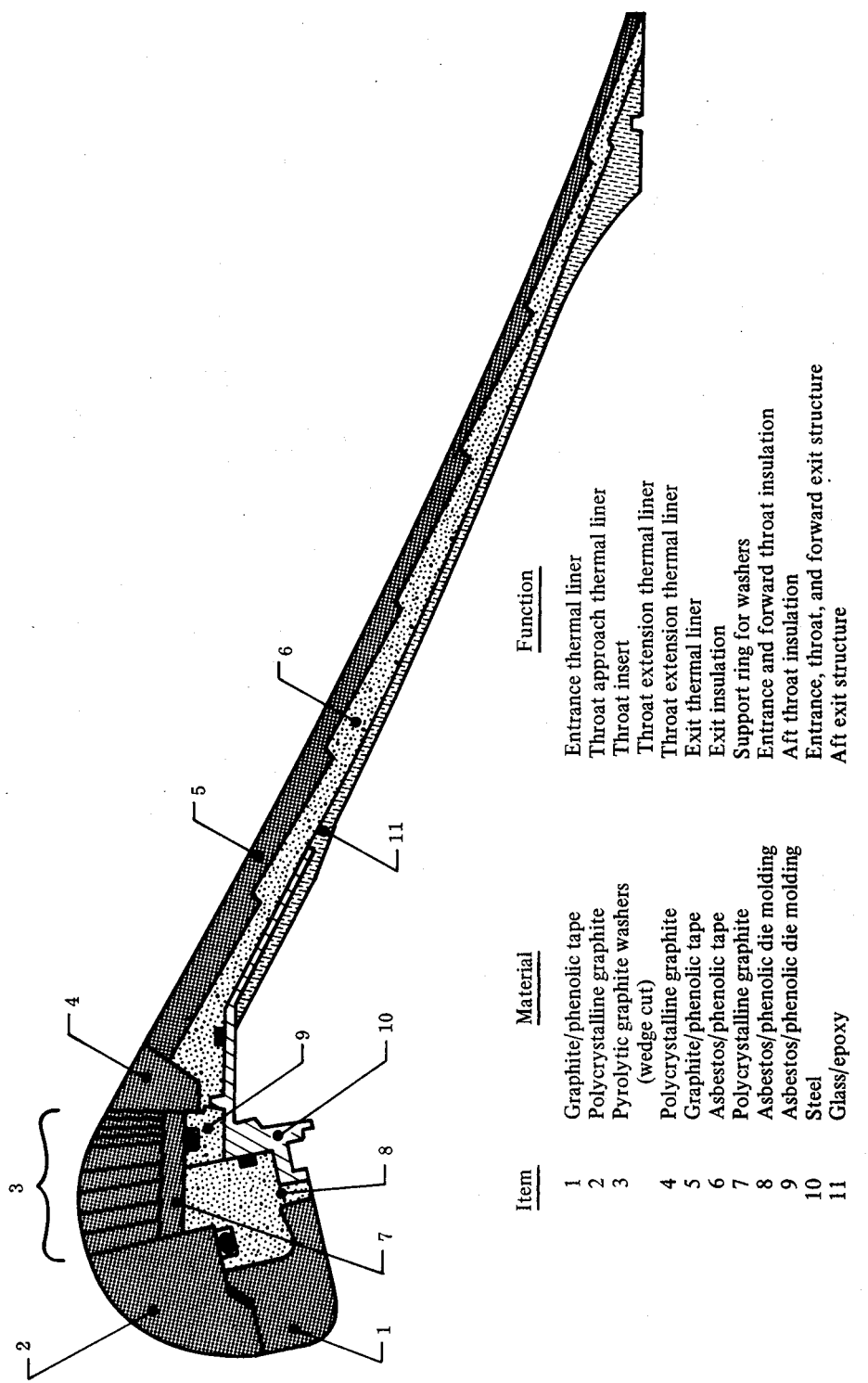


Figure 15. - Nozzle for Polaris A3 second stage.

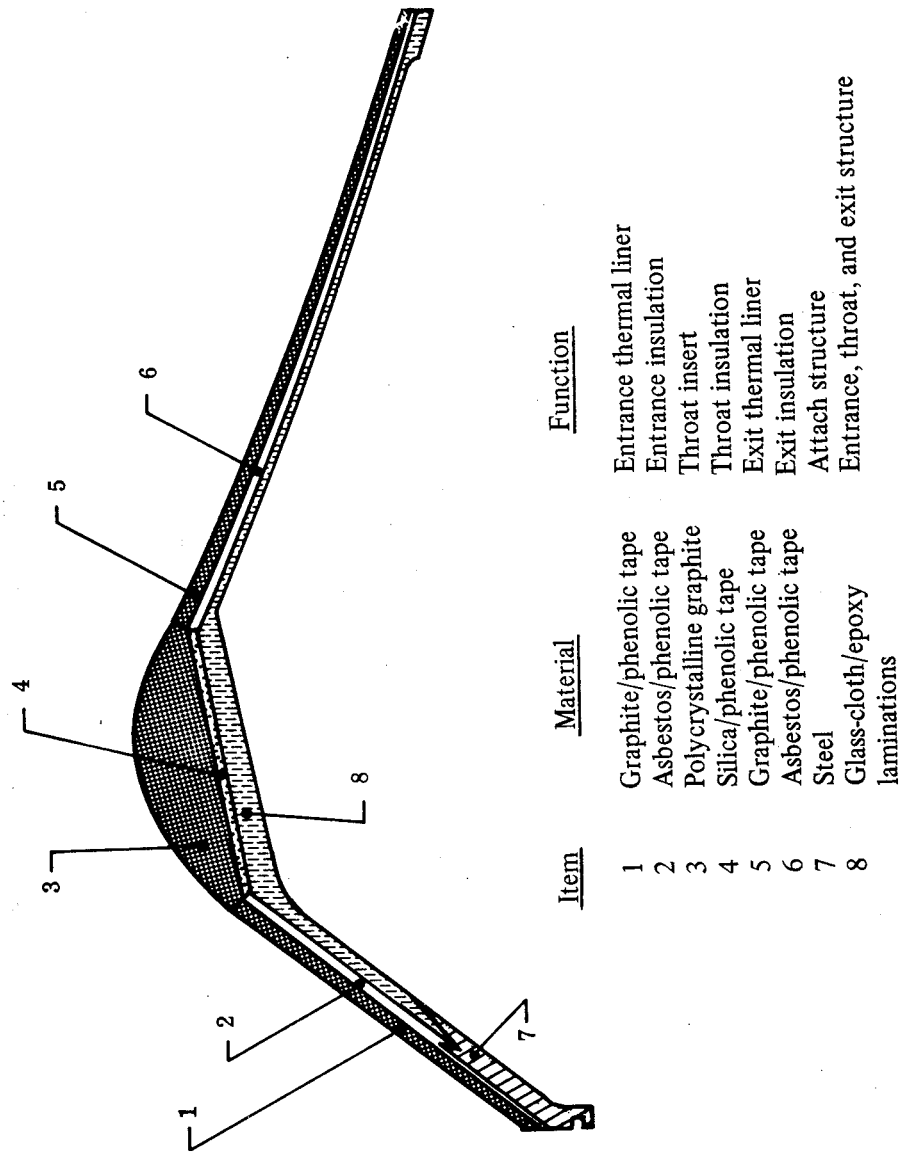
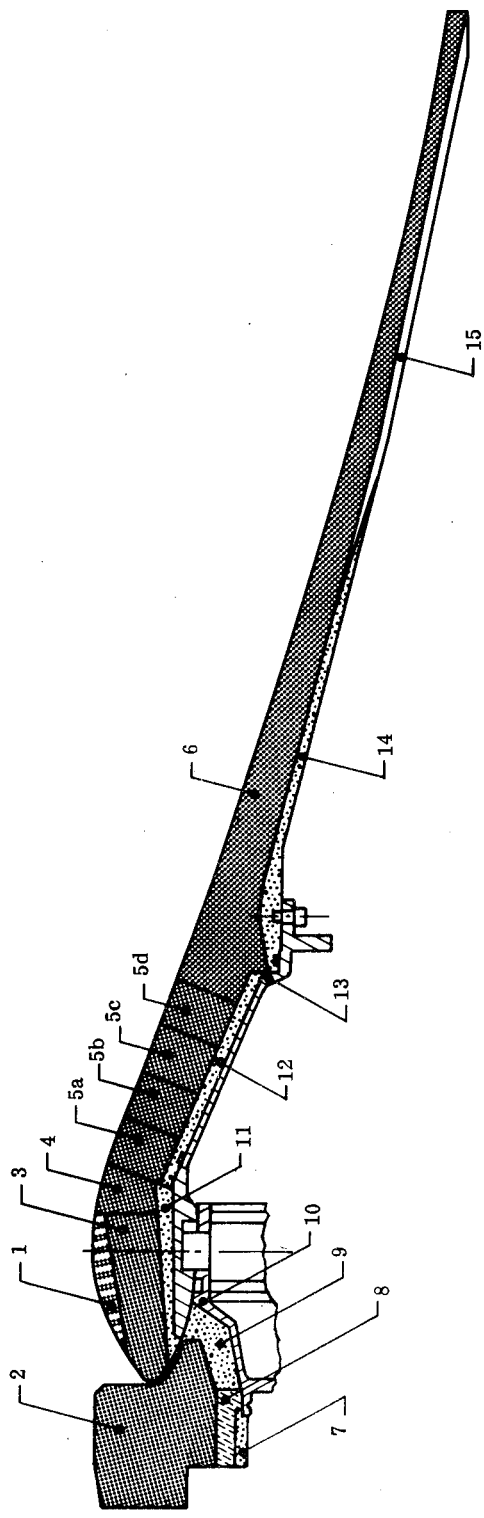


Figure 16. - Nozzle for Pershing first stage.



<u>Item</u>	<u>Material</u>	<u>Function</u>
1	Tungsten	Throat insert
2	Polycrystalline graphite	Entrance thermal liner
3	Polycrystalline graphite	Throat insert support
4	Polycrystalline graphite	Throat extension thermal liner
5a-5d	Graphite/phenolic die molding	Forward exit thermal liner
6	Graphite/phenolic tape	Aft exit thermal liner and insulation
7	Silica/phenolic rosette layup	Forward entrance structure
8	Glass/phenolic die molding	Forward entrance insulation
9	Silica/phenolic tape	Aft entrance insulation
10	Steel	Aft entrance structure
11	Silica/phenolic tape	Throat insulation
12	Silica/phenolic tape	Forward exit insulation
13	Steel	Forward exit structure
14	Silica/phenolic tape	Mid exit structure
15	Asbestos/phenolic tape	Aft exit structure

Figure 17. - Nozzle for Minuteman wing VI stage I.

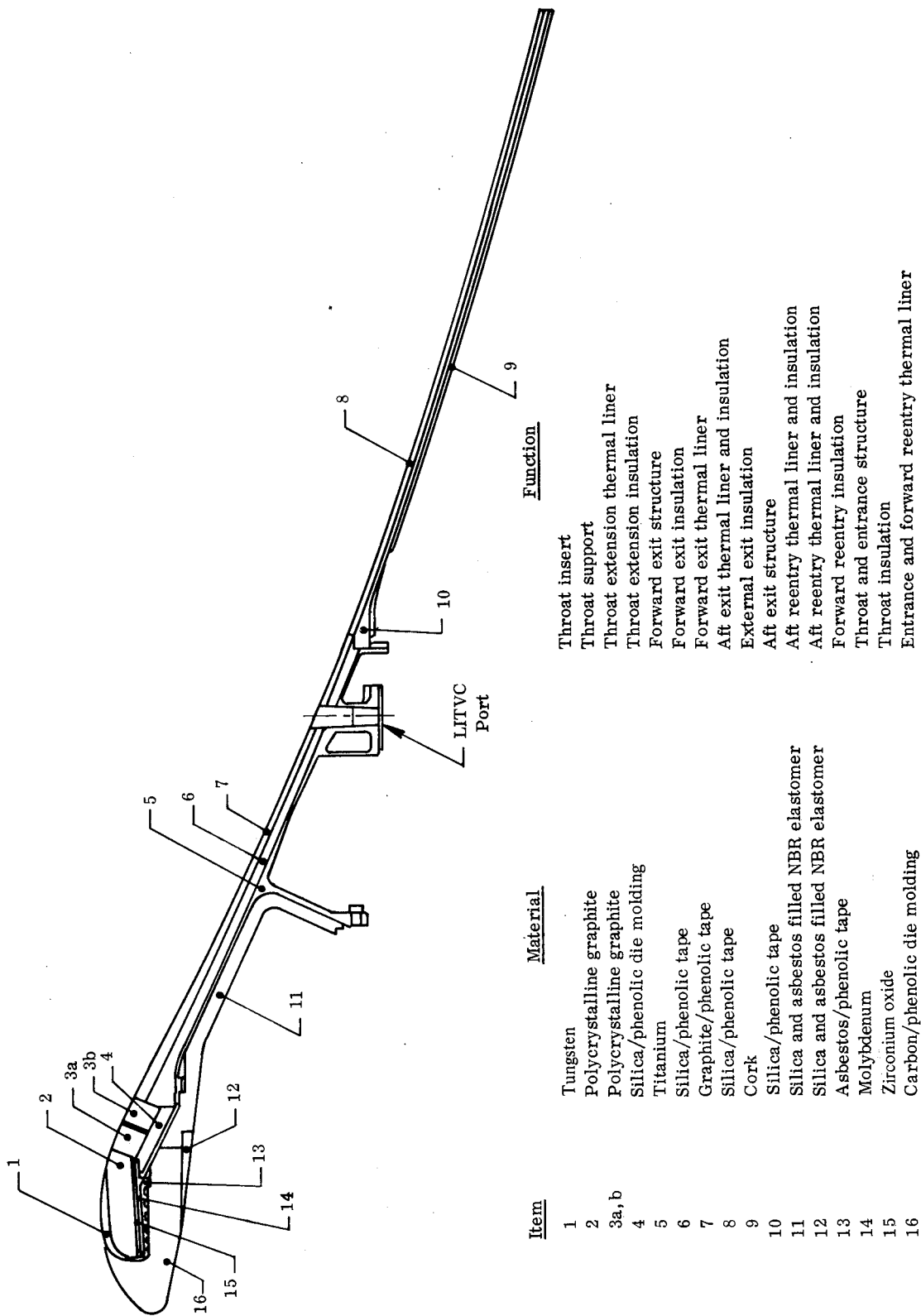


Figure 18. - Nozzle for Minuteman wing VI stage II.

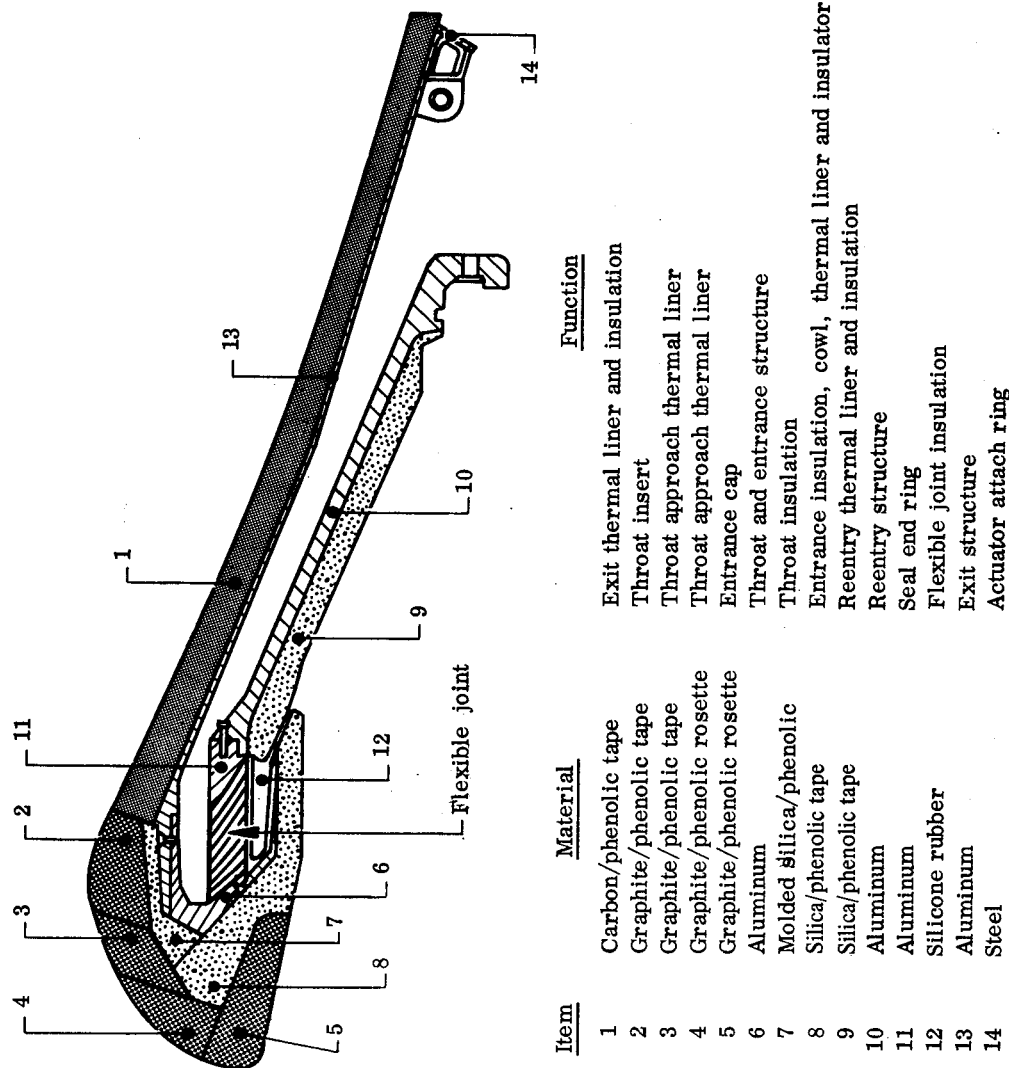


Figure 19. - Flexible-joint nozzle for TVC on Poseidon C-3 first stage.

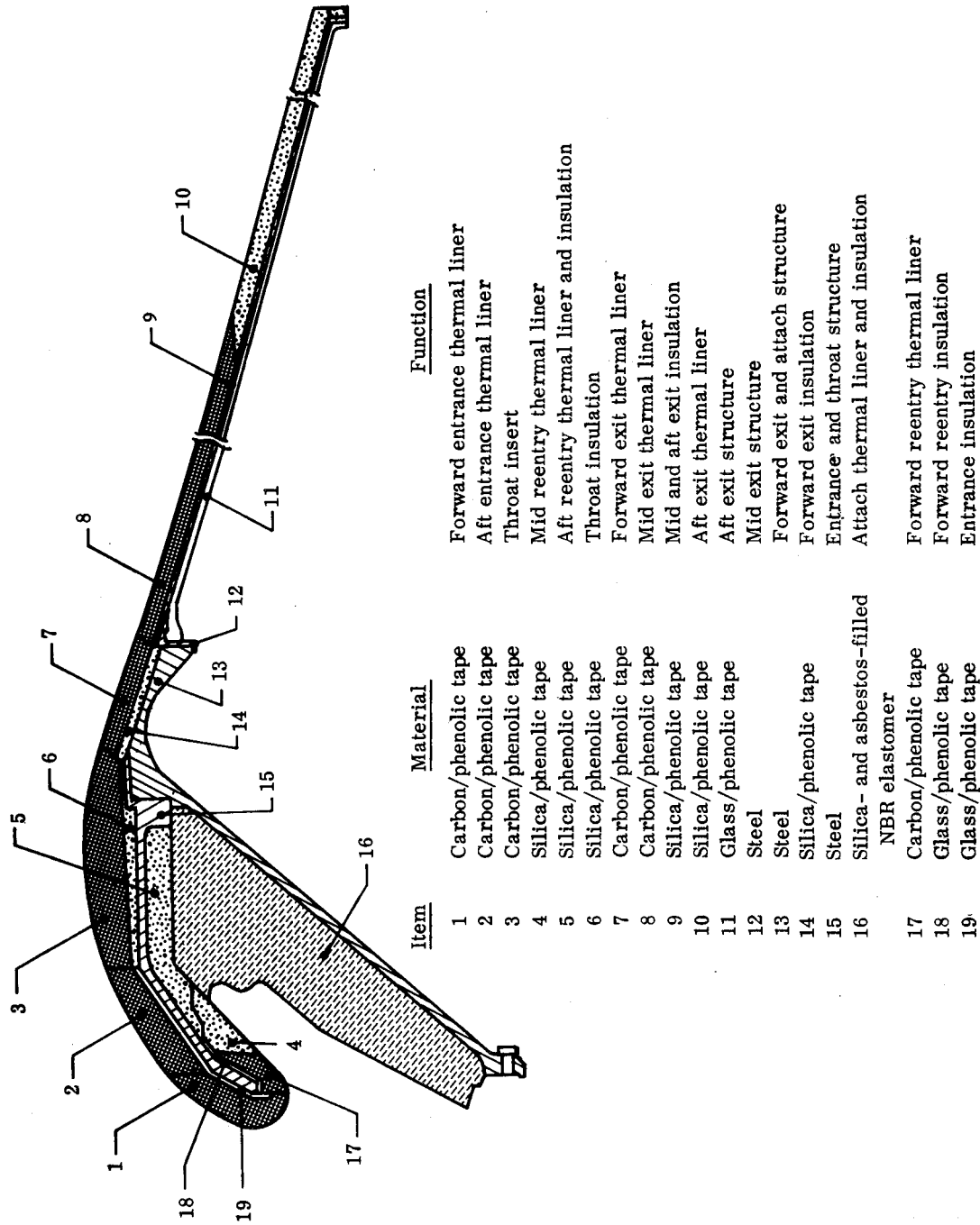


Figure 20. - Nozzle for 260 SL-3 motor.

illustrative of a small, simple, submerged nozzle. On the other hand, the Condor nozzle design, figure 7, demonstrates the complexity of some small-throat-diameter nozzles. The Condor nozzle not only incorporates a blast tube (a long, nearly cylindrical entrance), but the blast tube is bent, a unique design feature. The Condor also features an erosion-resistant pyrolytic graphite throat insert, not the more erodible polycrystalline graphite inserts used in the nozzles of the orbital boost motor and Sidewinder 1C (fig. 8). The Sidewinder nozzle is another example of a simple, relatively low cost, small nozzle.

The Phoenix nozzle, figure 9, is another example of a complex small nozzle; it incorporates a blast tube and a pyrolytic graphite throat.

The nozzle for the apogee motor of the HS-303A satellite, figure 10, is an excellent example of a lightweight nozzle for space application: the use of metal components is minimized, and expansion ratio is high. The apogee motor nozzle also shows the use of (1) a tungsten throat insert that (with most propellants and operating conditions) exhibits zero erosion, and (2) a contoured exit, as opposed to the conical exits of the nozzles in figures 6 through 9.

The Sparrow nozzle, figure 11, exhibits the near ultimate in nozzle simplicity; it is a two-piece nozzle consisting of a polycrystalline-graphite piece retained by a steel shell. Furthermore, since the steel shell is integral with the motor case, many would argue that the Sparrow nozzle is a one-piece nozzle.

The nozzle for the BE-3 A4 motor, figure 12, is another example of a lightweight space-motor nozzle that minimizes the use of metal.

The Extended-Range ASROC nozzle, figure 13, is the first of the nozzles in table I to include provision for TVC (in this case, liquid injection into the exit cone).

The Surveyor main retro nozzle, figure 14, represents another lightweight, high-expansion-ratio nozzle for the use in space.

The Polaris A3 second-stage nozzle, figure 15, is a unique nozzle in that a turn is made in the entrance and throat sections by the use of wedge-shaped stacked pyrolytic graphite washers in the throat. This turn is made so that the nozzle entrances (there are four nozzles per motor) better fit the curved aft dome of the motor and yet exhaust the gases parallel to the motor centerline.

The Pershing first-stage nozzle, figure 16, exemplifies a fairly large, fixed, external nozzle with a contoured exit and a minimum of metal structure.

The Minuteman first-stage nozzle, figure 17, illustrates the complexity of a movable nozzle and the use of a large tungsten throat insert.

The Minuteman Wing VI second-stage nozzle, figure 18, illustrates a large fixed submerged nozzle incorporating LITVC.

The Poseidon C-3 first-stage nozzle, figure 19, incorporates a flexible-joint movable-nozzle system and a graphite/phenolic throat insert.

The 260 SL-3 motor nozzle, figure 20, illustrates the materials and construction used in the largest-diameter nozzle built to date or planned. This nozzle, successfully tested, represents the upper size limit of state-of-the-art nozzles.

A recent advance in nozzle design is the successful development of the rolling-diaphragm metallic extendible exit cone and the fluted metallic expandable exit cone. In three development programs, the extendible exit cone has been successfully test fired, and in one program a combination of the rolling-diaphragm extendible and fluted expandable exit cones has been successfully test fired (refs. 6, 7, and 8). Figure 21 illustrates the deployment of the combination exit cone.

The extendible exit cone is of advantage in length-limited vehicles in that the stowed length of the exit cone is about one-third its extended length; the length thereby saved is available for additional propellant to extend the range or increase the payload of the vehicle. The advantage of the expandable exit cone is that in the stowed position the exit diameter is about two-thirds the expanded exit diameter; exit diameters larger than the motor diameter thereby are made practical. These new nozzle designs thus offer substantial benefits. However, while the development work shows much promise, it must be noted that the operational capabilities of the designs remain to be proven.

2.1 DESIGN REQUIREMENTS AND CONSTRAINTS

Nozzle design requirements and constraints are imposed specifically by contract, are specified by propulsion or vehicle system analysis, or are left to the discretion of the nozzle designer. Requirements from system analyses are, in part, based on estimated nozzle weight, performance, and envelope. An iterative process therefore is involved, and nozzle design parameters can be expected to change during a design effort. The nozzle designer is better prepared to respond to changes when he is acquainted with the source of each design requirement or constraint.

Definition of the following variables is required for nozzle design:

- Design pressure
- Predicted pressure-time trace (defines average pressure, firing duration, restarts, and coast time if any).

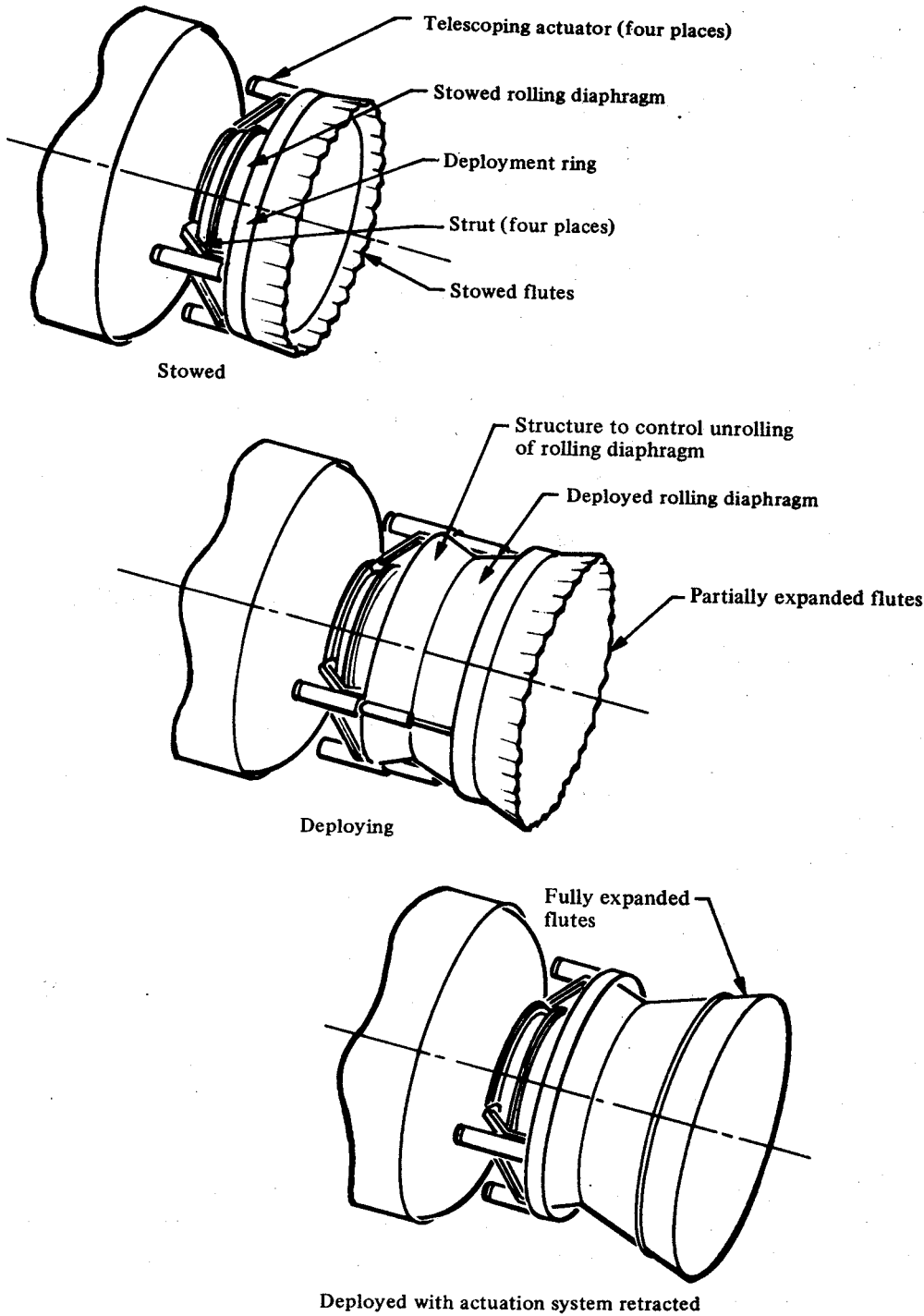


Figure 21. - Deployment of combination rolling-diaphragm extendible exit cone and fluted expandable exit cone.

- Propellant properties
 - Chamber temperature
 - Thermodynamic constants
 - Thermochemical properties (e.g., oxidation ratio, blowing coefficient, corrosivity index) representative of the products of combustion
- Throat size (area or diameter, initial or final)
- Acceptable throat-size change
- Envelope limits
- Expansion ratio
- Exit configuration
- Nozzle submergence (submerged nozzle only)
- Design vector angle or TVC force requirement (movable nozzle only)
- Diameter of interface with case
- Weight, reliability, cost, and development-time guidelines
- Production quantity and rate
- Storage and operating ambient environment.

Each of these parameters is discussed briefly below.

The design pressure for nozzle structural design is usually the motor MEOP (maximum expected operating pressure). If this value is not provided, MEOP is often estimated as 110 percent of the maximum pressure in the trace or as 120 percent of average pressure if only average is provided. In both cases, the pressure trace corresponding to the maximum propellant grain temperature is used.

Throat size, predicted pressure-time trace (or at least duration and average pressure), and estimates of production quantities and rates are mandatory inputs to the designer; but the designer often is expected to estimate his own values as first guesses for the other listed parameters.

In general, constant throat area is desirable in order to maintain a nearly constant chamber pressure; however, there have been motors in which an increase in throat area was desirable

(e.g., first-stage Sprint). Furthermore, the grain designer often can compensate for throat erosion without a significant penalty, so iteration of the grain design and nozzle design tasks may be required. Throat erosion is much more significant in small motors than in large motors, since the relative throat-area change is greater. The prohibitive increases in throat area that occur with some materials limit the designer's choice of throat materials in small motors, and the more-erosion-resistant materials generally are used for small throats unless firing duration is very short. A reverse problem has occurred with tungsten throats: the throat area has decreased as the tungsten heated up. Confined by the backup structure, the thermal growth of the tungsten has taken place inwardly, leading to motor pressure higher than predicted (ref. 9). The designer's criterion for throat-area change, when it is his choice, is predicated on an awareness of these effects.

If the propellant is unknown, the properties of a propellant previously used for a similar application are assumed to be valid.

The envelope limits generally will be defined by the minimum case opening, a 15° to 17.5° half-angle cone, and the expansion ratio. In some systems, the envelope will be further restricted by requirements for packaging instrumentation or guidance around the nozzle. In the absence of other requirements, however, the radial distance to the outside of any point on the nozzle (while it is in the maximum vectored (hard-over) position if a movable nozzle) should not exceed the motor radius.

The best choice of expansion ratio for test nozzles usually is the ratio at which the static pressure at the exit plane equals ambient pressure, because this condition eliminates the need in data reduction to correct for over- or under-expansion losses. For flight nozzles, the designer may have to make an initial choice; the final values will be determined by mission analysts. Previous experience should guide the designer in making the initial choice: expansion ratios in the range of 7 to 10 are usual for first-stage and single-stage low-altitude vehicles, and ratios of 15 to 80 may be used for upper-stage and high-altitude vehicles.

The thrust coefficient corresponding to a specific ambient pressure often is specified rather than the expansion ratio and exit configuration. The designer must then select the necessary expansion ratio and exit configuration to provide the thrust coefficient. Several combinations will be available. The choice of a particular combination usually is dictated by the other constraints discussed herein.

If the exit configuration is not given, a 15° half-angle cone is the usual choice. Use of this more-or-less standard angle makes correlation of the test data to previous data less subject to error and makes the use of existing fabrication tooling more likely. A 17.5° half-angle cone is often used for large nozzles (throat diameter > 10 in.). However, if the nozzle is to be used in a severely-length-limited or high-performance vehicle, the designer chooses a contoured nozzle. A configuration with an initial angle of 25° and an exit angle of 13° is representative of an efficient exit-cone contour.

With submerged nozzles, weight and motor opening usually are minimized when the nozzle is submerged to the extent that the throat plane is axially located near the mating surface between the nozzle and the motor chamber; thus this degree of submergence is used unless envelope limits require greater submergence. The term "submergence" must be used cautiously because several definitions are in common use. The two definitions most often used for submergence are (1) the percentage of the overall nozzle length that is forward of the nozzle-to-chamber interface, and (2) the percentage of the throat-to-exit length that is forward of this interface. Quoted submergence values are best accompanied by definition of the term, or confusion and misunderstanding is likely.

The design vector angle for movable nozzle designs often is left to the nozzle designer in test-nozzle designs and concept-demonstration programs. Industry experience indicates that 4° to 6° is the usual range for the first stage of multistage vehicles, and 2° to 4° for upper stages. Related experience is used as guide for specific applications.

Propulsion system weight usually is minimized when the case opening for the nozzle is minimum; therefore, the smallest opening consistent with the nozzle design and the grain core or mandrel is assumed if the choice is the nozzle designer's.

Weight, cost, reliability, and development-time considerations – reflected in material choices and factors of safety – are estimated by reference to the most nearly similar previous design, unless specific guidance is provided.

A low-temperature ambient storage or operating environment (e.g., space) will limit the material choices available to the designer. Most elastomers and some adhesives are not suitable for use at space temperatures. Storage in a corrosive atmosphere (e.g., salt air) will require special corrosion protection for some materials (e.g., anodizing of aluminum). Most environments require special protection to be taken against galvanic corrosion if dissimilar metals are used. If the environment is not specified, the designer can usually assume it from knowledge of the motor application; for example, low-temperature storage and operating environment usually is assumed for space motors.

2.2 NOZZLE CONFIGURATION AND CONSTRUCTION

Nozzle design is a dynamic, iterative process, as evidenced by the estimate of nozzle designers that they average three major iterations before release of a design. Iteration occurs because of (1) interactions between nozzle and total propulsion systems and (2) interactions between the design and analysis tasks (fig. 22).

The initial values of the design parameters (e.g., throat area, expansion ratio) for the design of the nozzle are based on estimates of the weight, performance, envelope, and (possibly) cost of the nozzle used in analyzing the propulsion system. The weight, envelope, performance, and cost of the design laid out to the initial values rarely match all the original

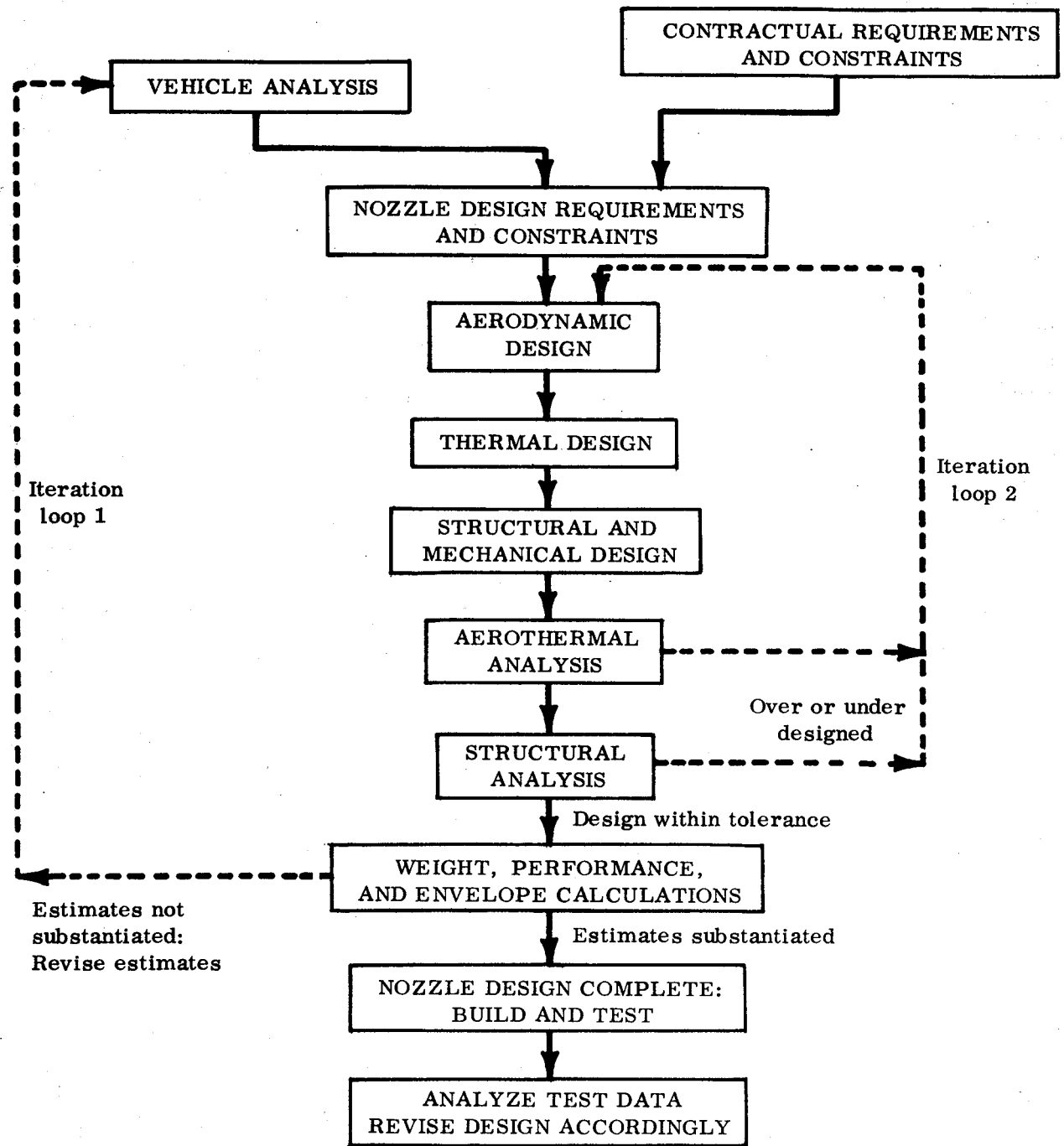


Figure 22. - Flow chart of nozzle design sequence showing major iteration loops.

estimates; therefore, the estimates usually must be revised, the result being a change in the values of the parameters for the nozzle design. Preliminary design using quick sizing methods sometimes is accurate enough to bring estimated and design layout values into agreement close enough that the values can be frozen for detailed design. Some facilities have automated this initial process on the computer, drafting-board layouts thus being eliminated from the initial iteration loop (ref. 10).

The major nozzle design iterations involve the designer and the analysts. The common practice is for the designer to use quick sizing equations, design curves, computer programs, and engineering judgment to lay out the aerodynamic contour, the liners and insulators to form the contour, and the structures to support the liners and insulators. The aerodynamic, thermal, and structural analysts then can apply more refined techniques to identify questionable areas. The designer uses this information to reconfigure the design, changing materials and moving interfaces as needed, and issues an updated drawing. The analysts then analyze the revised configuration, often with techniques even more sophisticated than those used previously, and make further recommendations. Fabrication specialists frequently are consulted at this point for suggestions as to cost reduction, elimination of potentially troublesome areas, and the like.

The incorporation of these suggestions and recommendations in the third revision of the nozzle drawing usually completes the design process. Whether more or less than three iterations are required depends on the sophistication and purpose of the nozzle, its similarity or dissimilarity to previous nozzles, and the importance of the weight and cost budgets for the nozzle. A design for a heavyweight test nozzle, for example, may be completed in one iteration without consultation with aerodynamic, thermal, or structural analysts, whereas a design for a high-performance nozzle submitted in competition with other designs may undergo five or six iterations. Further iterations in design are, of course, usually made after the prototype is test fired.

The nozzle designer develops the initial design in a logical three-phase process beginning at the inside surface and working outward. In the aerodynamic-design phase, the entry, throat, and exit surfaces are sized and configured to provide the desired thrust. In the thermal-design phase, throat inserts, thermal liners, and insulators are selected and configured to maintain the aerodynamic design. In the structural-design phase, structural rings and shells are selected and configured to support the thermal components and to sustain the predicted loads. In all three phases, design is carried forward in keeping with envelope restrictions and weight and cost budgets.

Throughout design, all available data on similar nozzles are used to evaluate critically the design approach, materials application, and analytical methods.

2.2.1 Aerodynamic Design

Aerodynamic design consists of configuring the nozzle surfaces exposed to the exhaust gases in such a manner that the conversion of energy to kinetic energy is a practical maximum consistent with other design constraints. In general terms, maximum practical energy is extracted by maintaining a smoothly accelerating flow through the nozzle. The specific practices used in attainment of the goal are discussed below. The influence of nozzle aerodynamic design on motor performance is discussed further in reference 9.

2.2.1.1 ENTRANCE

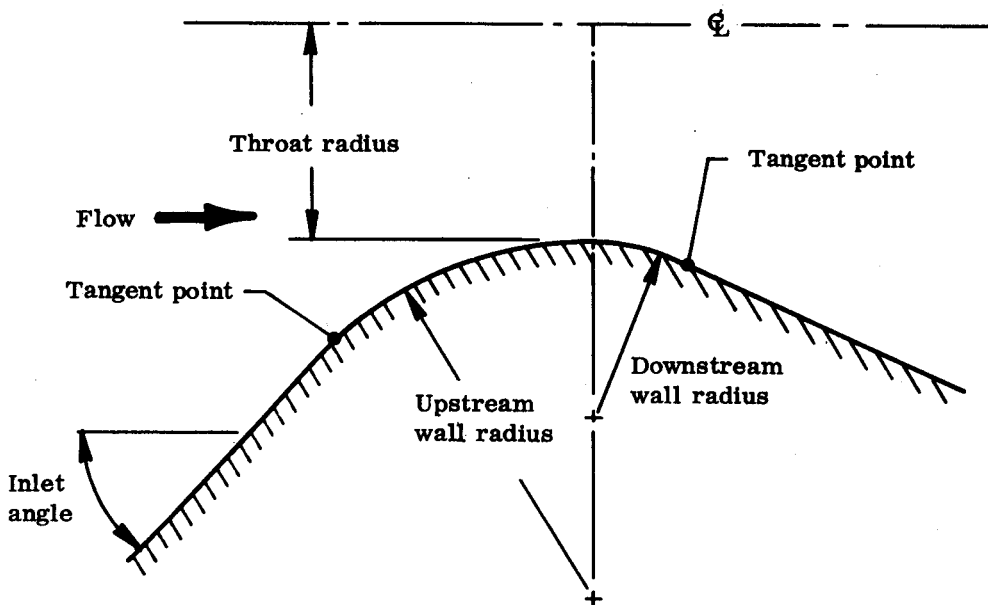
Nozzle entrance sections are either of the convergent-cone type (external to the motor) or of the submerged type (submerged into the motor) (fig. 1). Throat and entry geometry for both types is presented in figure 23. On some systems, a blast tube, a long cylindrical or slightly tapered section of the nozzle entrance (fig. 24), is required.

A potential-flow field characterizes the convergent-cone type of entrance, whereas cold-flow studies have established that the submerged entrance is characterized by a potential-flow region, a separation boundary, and a vortex-flow region, as depicted in figure 25 (ref. 10). Current data and available analytical methods are not adequate to define the flow patterns in these regions; however, cold-flow simulation studies have provided useful data.

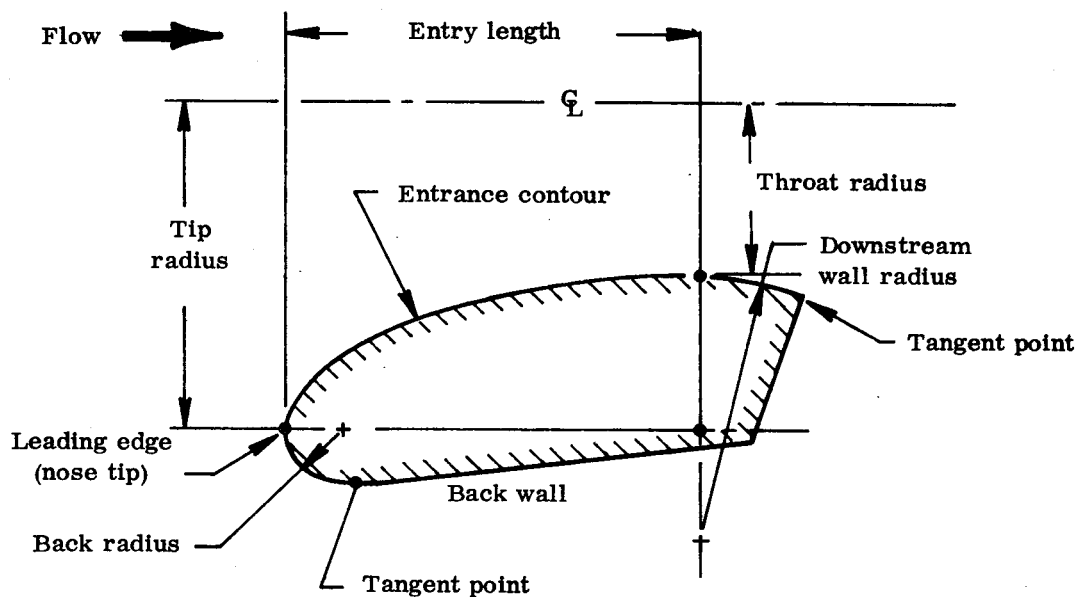
The velocities in the vortex-flow region are relatively low (of the order of Mach 0.01 to 0.10, in typical designs) (ref. 11). In movable submerged nozzles, it is advantageous to locate the splitline between the fixed and movable sections in the separated-flow region, as in figure 26. When the nozzle is vectored, pressure remains essentially constant in the separated-flow region around the periphery of the splitline, so that little circumferential flow is induced and little heat is transferred to the splitline materials. On the other hand, if the splitline is located in a convergent-cone entrance, the pressure around the splitline varies considerably when the nozzle is vectored, considerable circumferential flow is induced, and charring and ablation of splitline materials are increased (ref. 12).

Because of the more desirable flow conditions with the splitline located in the separated vortex-flow region of the submerged nozzle, the submerged movable nozzle, rather than the movable nozzle with the splitline in the entrance cone (fig. 5), has been used in nearly all recent movable nozzle designs even when submergence per se was not required.

A performance loss as great as 1 percent has been reported with nozzles submerged so that a large percentage of the grain length (over 25 percent) was aft of the leading edge (refs. 9 and 13). Submergence losses with 0 to 25 percent of the grain length covered by the nozzle, a condition representative of the majority of submerged nozzles, have not been established.



(a) External nozzle



(b) Submerged nozzle

Figure 23. – Throat and entry geometry for external and submerged nozzles.

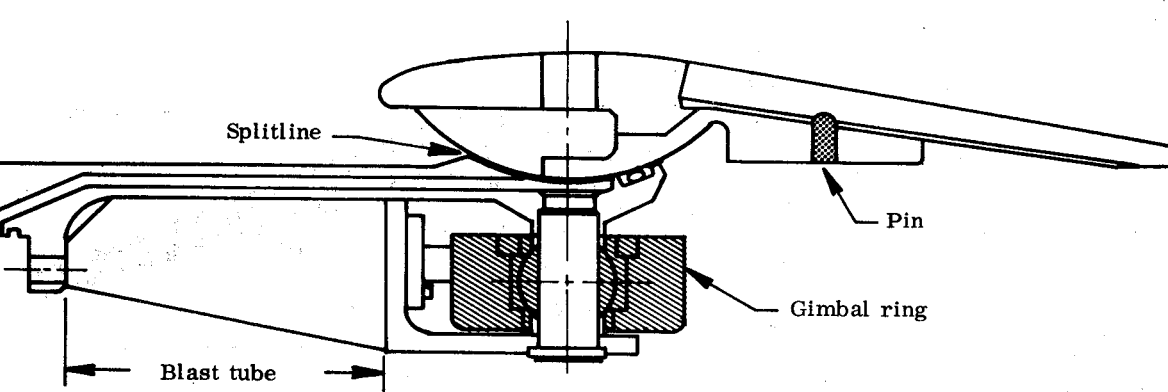


Figure 24. - Gimbal nozzle incorporating blast tube.

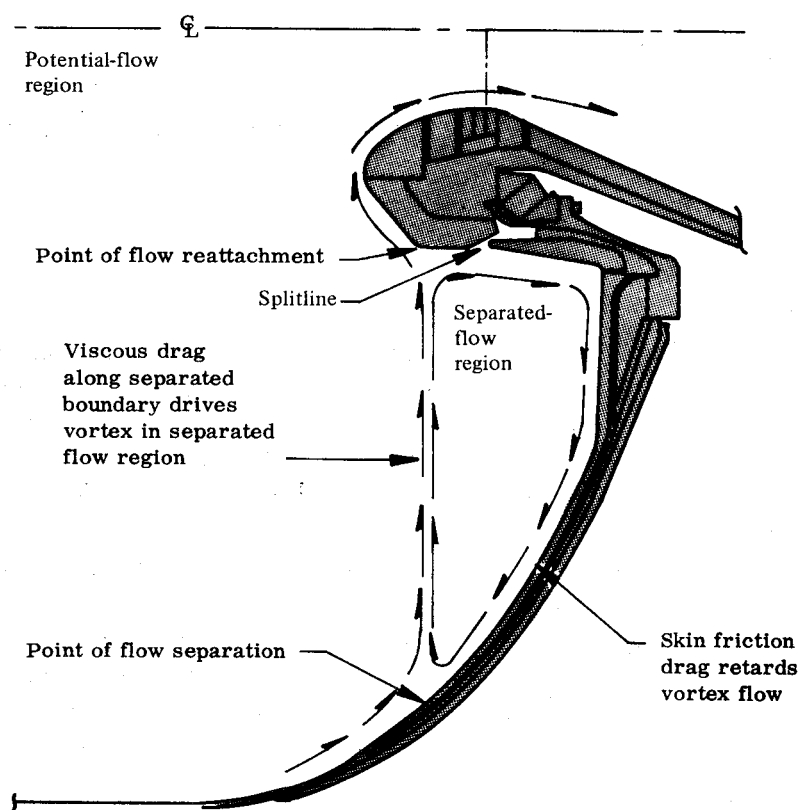


Figure 25. - Regions of separated and potential flow in a submerged nozzle (ref. 10).

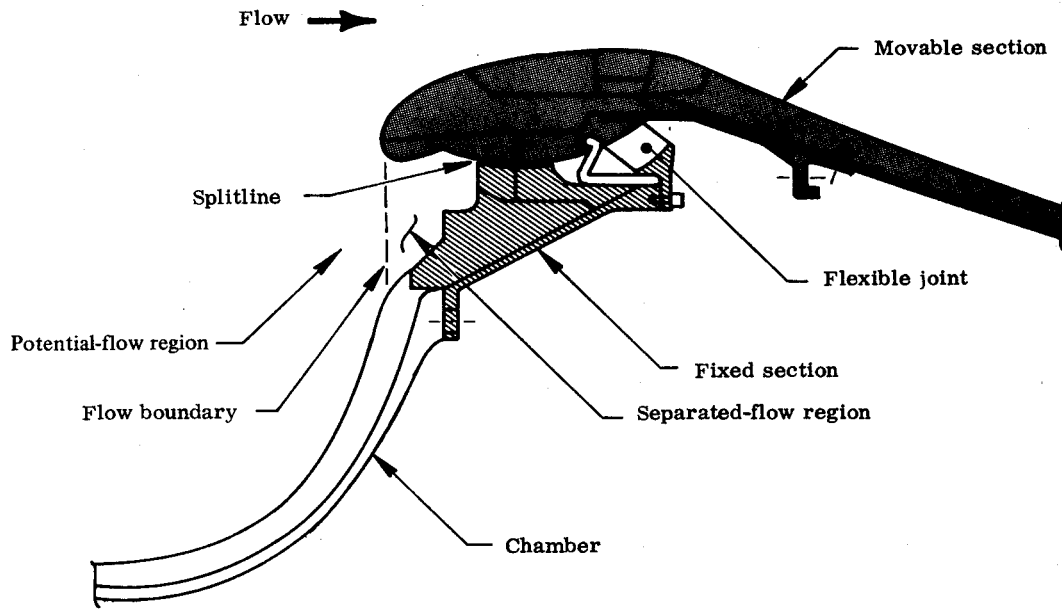


Figure 26. - Submerged nozzle designed to locate splitline for TVC in separated-flow region.

2.2.1.1.1 Submerged

The envelope of the entrance (nose) of a submerged nozzle generally is specified by the axial and radial location of the leading edge (fig. 23b). The length (throat plane to leading edge) of successful submerged entrances has ranged from 0.42 to 5.4 throat radii, with the mean length equal to about 1.0 throat radius. The contraction ratio (ratio of flow areas at leading edge and at throat) has ranged from 1.5 to 8.8, with a mean value of approximately 3.0.

An ellipse, a series of tangent circular arcs, and a hyperbolic spiral have been used successfully as the cross-section shapes connecting the leading edge to the throat (ref. 14). Theoretical studies having some experimental verification indicate that the latter shape induces more nearly uniform acceleration, which produces a more nearly uniform entrance erosion profile and reduces entrance erosion to some degree (ref. 15). However, the differences are not a major consideration, and all of the above shapes are considered suitable.

Theoretical and cold-flow studies indicate that delivered specific impulse is improved by longer entrance lengths and greater contraction ratios (ref. 16); however, experimental

verification of this improvement is lacking. The general practice is to design near to or greater than the mean successfully demonstrated values of tip radius and entry length, the actual values being determined by thermal, structural, or mechanical considerations if such predominate; the alternate practice is to design near to the minimum successfully demonstrated values of tip radius and entry length in order to conserve weight and cost.

In comparison with center-perforated cylindrical grains, the star, slot, and other complex grain designs tend to induce increased and nonuniform erosion on nozzle inlets. These effects are reduced as the entrance length and contraction ratio increase.

2.2.1.1.2 External

The contraction ratio at the interface of the nozzle with the chamber almost always is determined by chamber and system design requirements rather than by nozzle design requirements. The half-angle (inlet angle, fig. 23(a)) of the convergent-cone entrance of successful nozzles has varied between 1° and 75° with most designs near 45° . An empirical study (ref. 17) indicates little variation of delivered specific impulse with inlet angle. However, liner erosion increases with a steeper inlet (probably as a result of a greater number of solid particle impactions or a thinner boundary layer or both). The erosion increase is particularly significant at high pressure (≥ 1500 psi), so steep inlets are avoided.

2.2.1.1.3 Blast Tube

In older, four-nozzle motor designs, the blast tube (fig. 24) serves as a flow straightener to remove part of the asymmetry that results from flow being divided and turned from the center port into each of the nozzles. Blast tubes for four-port systems may vary significantly from the cylindrical shape, particularly in the inlet. The aerodynamic configuring of flow-straightening blast tubes has been accomplished by means of cold-flow studies and empirical test firings (refs. 18 and 19).

With the development of omni axial TVC systems and submerged nozzles, four-nozzle systems have declined in usefulness, because single-nozzle systems provide significantly higher delivered specific impulse efficiency at a lower cost (ref. 20). In single-nozzle propulsion systems incorporating movable aerodynamic surfaces for attitude control, a blast tube often is required to provide aft-end packaging envelope for the surfaces and their control system.

Minimization of blast-tube diameter usually is desired by the system designer. The diameter is determined by tradeoffs among weight budgets, cost budgets, and envelope requirements. As diameter is decreased, the increase in Mach number is accompanied by increased erosion and char and may force the use of expensive liner materials. Furthermore, frictional flow

effects and the associated pressure drop become significant as the blast-tube Mach number increases, and motor performance may suffer. Some experience indicates that long, low-Mach-number blast tubes reduce throat and entrance erosion.

2.2.1.2 THROAT REGION

The aerodynamic design of the throat region (in longitudinal cross section) usually consists of an upstream circular arc tangent to a downstream circular arc at the geometric throat (smallest area of the nozzle), as in figure 23. Many designs, however, include a finite cylindrical length at the throat. The cylindrical section has the following advantages:

- It aids nozzle alignment, as it facilitates location of the geometric throat.
- In some cases, it facilitates machining of the throat region contour because a contour can be machined tangent to a flat more easily than it can be machined tangent to another arc. Throat-diameter tolerances can therefore be met more easily.
- Relatively long cylindrical sections (0.5 throat radius in length and greater) have been reported to reduce the throat erosion rate significantly.

In most nozzles, a cylindrical throat increases total nozzle length, and any benefits must be traded against this disadvantage. When a blast tube is required for packaging purposes, part of the blast-tube length can instead be used for a cylindrical throat. As no increase in overall nozzle length is incurred, this configuration is often beneficial.

The radius used for the upstream arc in successful nozzles has varied from zero (sharp throat) to 5.0 throat radii, with most designs between 1.0 to 2.0 throat radii. The downstream arc radius has varied from zero to 6.0 throat radii, with most designs between 1.0 and 2.0 throat radii. Studies have shown conflicting results: negligible differences in delivered specific impulse with arcs down to 0.5 throat radius (ref. 14), and improvements with radii of 0.5 and 0.6 throat radius (ref. 21). The trend in recent years has been to use smaller radii, since the overall nozzle length (and thus weight and cost) is reduced without apparent performance penalties.

2.2.1.3 EXIT

The choice between a conical exit configuration and a contoured configuration (fig. 2) is made by tradeoffs of performance, weight, and cost. Weight tradeoffs are straightforward; however, with a contoured exit, the liner immediately forward of the exit plane is subject to increased erosion, and this effect must be considered in the weight tradeoff.

The cost differences involved often have been exaggerated. The cost difference for a contoured exit is primarily the difference in cost between a contoured mold and straight mold or between a contoured-wrap mandrel and a conical-wrap mandrel. These differences tend to be insignificant, especially in quantity production. In large nozzles, however, cost differences may be significant if honeycomb structure is used or if metal structure continues to the exit plane.

There is no general agreement on the magnitude of the performance advantages of contouring an exit, although there is general agreement that contouring a nozzle improves delivered specific impulse. For a given throat-to-exit length, the estimates of the increase obtained with a contour range from 0.5 percent to more than 1.0 percent. There is no conclusive evidence from tests in which substitution of an equal-length contour for a cone was the only variable.

The nozzle exit also may be contoured to reduce nozzle length, since a contoured exit is shorter than a conical exit that provides an equal thrust coefficient.

In test nozzles, conical exits (usually of a 15° half-angle) are more-or-less standard. Use of a standard helps isolate the effects of the variables under test. Use of nonstandard nozzles introduces additional variables and clouds the data.

Conical exit. — The half-angle of successful nozzle exits has varied from 6° to 28°, but most designs are either 15° or 17.5°. Small exit angles result in long (and therefore heavy and costly) exits. The divergence loss is approximated by the one-dimensional formula

$$\text{divergence loss} = 1 - \lambda \quad (1)$$

where

$$\lambda = \frac{1 + \cos \alpha}{2} = \text{divergence loss factor}$$

α = nozzle-divergence or exit half-angle, deg

Divergence loss, which increases rapidly at larger angles, is additive to other nozzle losses (including wall friction and two-phase effects) that are discussed more fully in reference 9.

For a given throat-to-exit length, ambient pressure, and chamber pressure, the half-angle that maximizes the delivered thrust coefficient $C_{F\ del}$ can be estimated by using the one-dimensional formula

$$\max C_{F \text{ del}} = \lambda \left[C_{F \text{ vac}} - \epsilon \frac{P_e}{P_c} \right] + \frac{\epsilon}{P_c} (P_e - P_{\text{amb}}) \quad (2)$$

where

$C_{F \text{ del}}$ = delivered thrust coefficient

$C_{F \text{ vac}}$ = vacuum thrust coefficient with zero divergence loss

ϵ = expansion ratio corresponding to α and the given throat-to-exit length

P_e = static pressure of exhaust gas at exit plane, psi

P_{amb} = ambient pressure, psi

P_c = chamber pressure, psi

A performance map (fig. 27) constructed from the formula gives the relationship among calculated delivered thrust coefficient, optimum half-angle, and corresponding expansion ratio for any throat-to-exit length. The optimum value usually lies in the range of 15° to 20° (refs. 22 and 23).

If performance maximization is not important and if the choice of half-angle is the nozzle designer's, then 15° for nozzles up to 10-in. throat diameter and 17.5° for larger nozzles have been more-or-less standard. Data from motor firings can then be more confidently compared to previous data.

Contoured exit. — Circular arcs, parabolas, and streamlines of method-of-characteristics flow nets have all been used to define an exit contour (refs. 24 through 28). The wall angle at the point of tangency with the downstream throat arc is referred to as the initial divergence angle or maximum exit angle (fig. 2). The wall angle at the exit plane is referred to as the exit angle.

Initial divergence angles up to 32° have been successful, although the most common angles range from 20° to 26° . The difference between initial and exit angles has significant effect on performance. Experimental data as discussed in reference 9 indicates severe losses in delivered specific impulse if the difference between the initial divergence angle and the exit angle exceeds 12° (refs. 29 and 30).

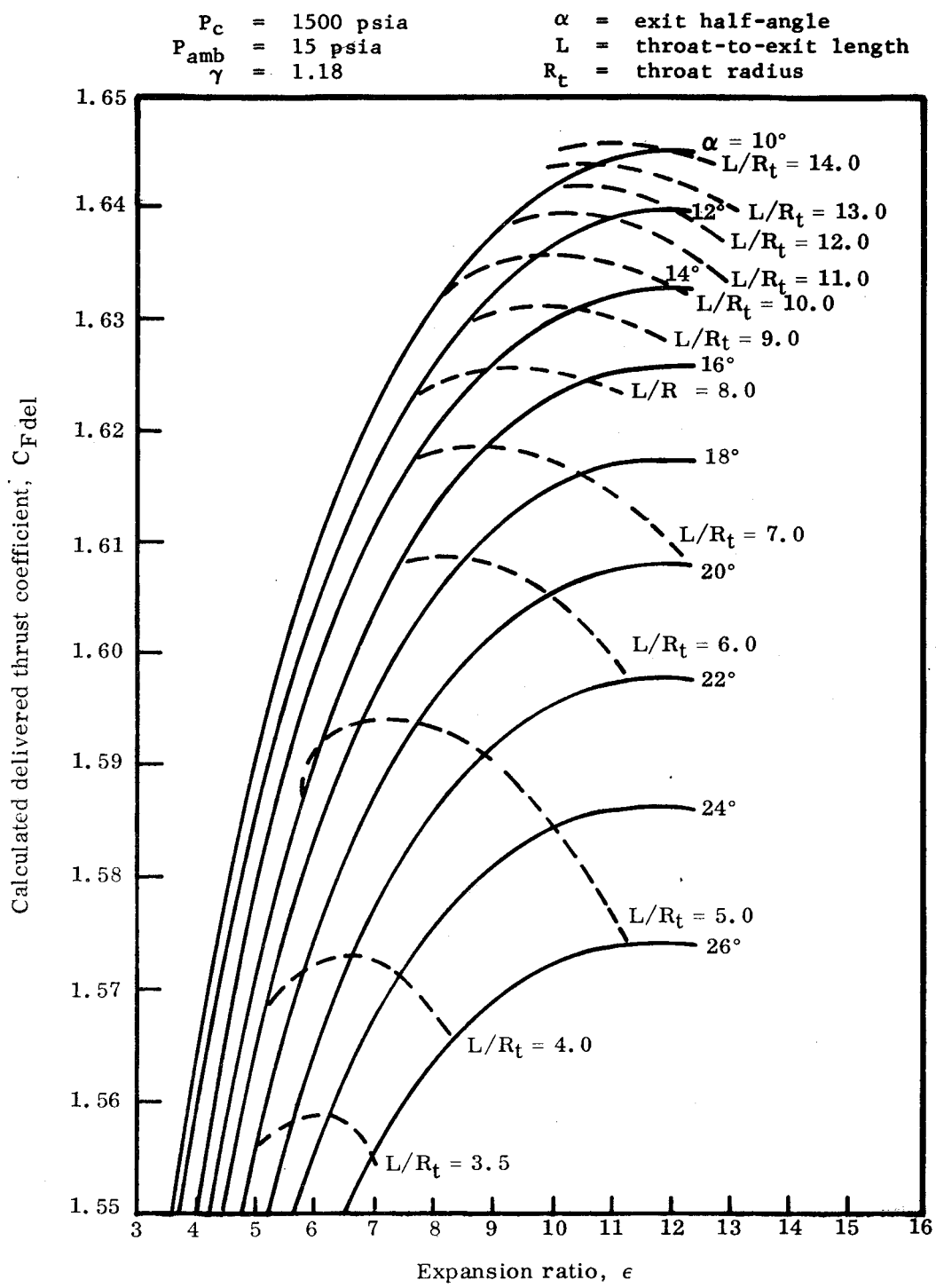


Figure 27. - Delivered thrust coefficient of a conical nozzle as a function of expansion ratio, exit half-angle, and exit length normalized on throat radius.

For a given initial divergence angle and exit angle, there is no conclusive experimental evidence that any one of the contour geometries outperforms the others. The particular choice of curve is not considered significant. The best choice is to use shapes for which the designer has accumulated experimental data, and for which he can therefore predict performance with confidence.

2.2.2 Thermal Design

The objective of the thermal-design phase is to maintain nozzle aerodynamic design insofar as is practical and to limit the temperature of the structure to acceptable levels. A thermal liner* forms the nozzle aerodynamic contour; the surface of a thermal liner is exposed to the exhaust-product flow. An insulator is a material placed behind a liner to serve as a thermal barrier to protect the structural member from excessive temperature; a single material thickness often serves as both liner and insulator (and sometimes as structure also). A throat insert is a special erosion-resistant liner placed in the throat region of a nozzle to limit the increase in throat area that results from erosion of the throat liner.

In practice, the throat insert and other liners usually are designed first, then the insulators. Liner and throat-insert materials usually are selected for erosion resistance, and insulator materials for low thermal diffusivity. The materials suitable for liners are, in general, considerably more expensive than those suitable for insulators, so liner use is generally minimized. The use of throat inserts usually is limited to the throat region because of the high cost of inserts and the special support and retention provisions required for use.

Available data (ref. 31) indicates that efficiency of a nozzle with a tungsten, pyrolytic graphite, or polycrystalline throat, with phenolics fore and aft of the throat, drops by one to three percent during a firing lasting 30 seconds or more. In recent years, increasing attention has been directed toward design of nozzles that will maintain an efficient aerodynamic contour against the effects of erosion and charring. This design approach has become known as "contour control". Contour control has become increasingly of interest because newer materials such as carbon/carbon and pyrolytic graphite coatings offer a degree of control not possible with previous materials. Test of a carbon/carbon nozzle with a pyrolytic graphite throat described in reference 31 indicates a one-percent improvement in nozzle efficiency. The improvement was assigned to four differences between the carbon/carbon nozzle and a conventional phenolic nozzle tested under similar conditions: the carbon/carbon nozzle exhibited (1) less change from initial contour, (2) less severe erosion discontinuities fore and aft of the pyrolytic graphite throat, (3) less surface roughness in the eroded condition, and (4) no char layer.

* "Liner" as used herein is not to be confused with the propellant grain liner.

Current thermal design practices include consideration of contour-control effects and selection of materials to minimize losses. Particular attention is paid to minimization of erosion discontinuities in the throat region, since these discontinuities are believed to be a major source of efficiency loss.

2.2.2.1 THROAT INSERT

Six groups of materials have been evaluated as nozzle throat inserts:

- (1) Reinforced plastics
- (2) Polycrystalline graphite
- (3) Pyrolytic graphite and pyrolytic graphite codeposited with silicon carbide
- (4) Refractory metals
- (5) Carbon/carbon composites
- (6) Ceramics.

The first four materials are in common usage, and the carbon/carbon composites (also called fibrous graphites or prepyrolyzed composites) are in advanced development. The ceramics, however, have poor thermal-shock characteristics; currently they are not considered by nozzle designers to be suitable for solid rocket application. Only the first five therefore are treated in the following discussion.

Reinforced plastics. — Reinforced-plastic throats are treated in the general discussion of thermal liners (sec. 2.2.2.2). For clarity, the material at the throat that forms the gas boundary will be referred to herein as the throat insert even if it is made of reinforced plastic.

Polycrystalline graphite. — The polycrystalline graphites (also called bulk graphites or monolithic graphites) are relatively inexpensive materials formed by either compression molding or extrusion. The fine-grain grades are used in many nozzle designs in limited areas because of their relatively low cost, high erosion resistance, and the unique characteristic (shared with pyrolytic graphite and carbon/carbon) of becoming significantly stronger as temperature increases (up to about 4500° F).

However, the relatively low strength of polycrystalline graphite requires that relatively thick sections be used or that the sections be well supported structurally. These restrictions limit

the use of polycrystalline graphite in flight-type nozzles to throats, throat approaches, throat extensions, and blast tubes. However, polycrystalline graphite often is used in all sections of small test nozzles. Furthermore, nozzles for propellant or grain-design test motors and some small operational motors often consist of nothing more than a nozzle shape machined from a cylinder of graphite held in a flanged steel shell (figs. 11 and 28).

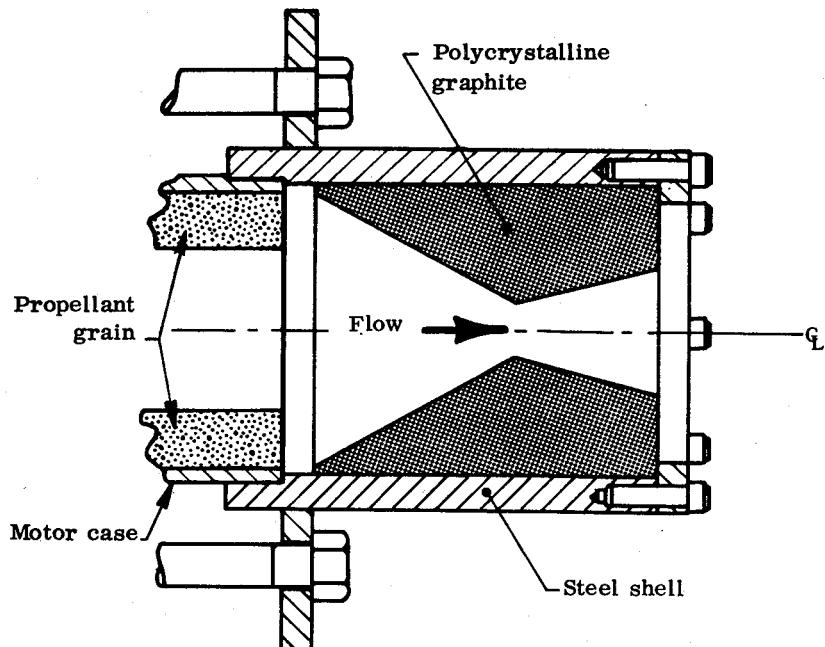
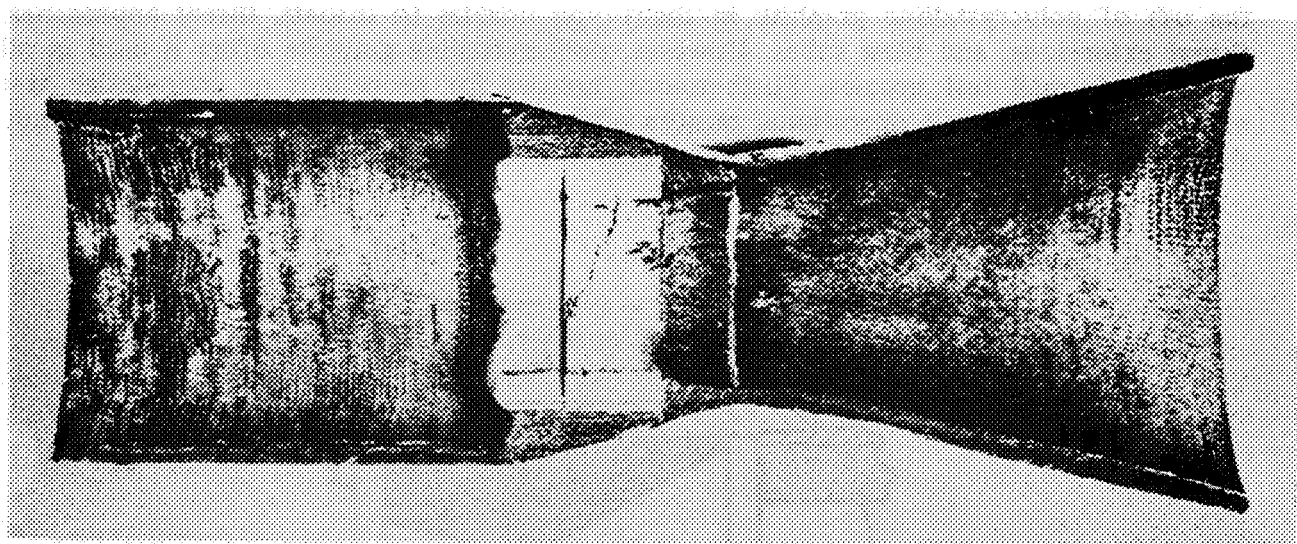


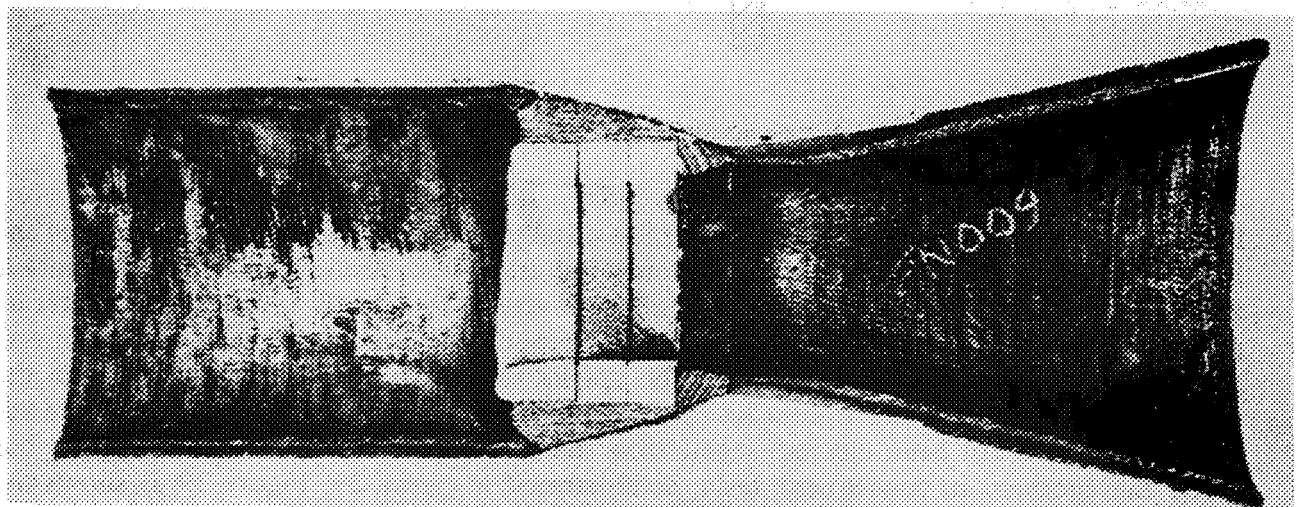
Figure 28. - Nozzle machined from polycrystalline-graphite cylinder.

Failures of polycrystalline graphites in nozzles usually have occurred in the early part of the firing when the graphite surface first becomes hot and the backside is still cool. Graphite is relatively brittle, and the thermally induced stress frequently cracks the material, particularly if the graphite is not uniformly supported along its length. Furthermore, graphite often does not crack cleanly. The cracks tend to propagate spirally through the material, resulting in severe fracturing that usually leads to ejection. When the graphite has cracked and has not been ejected, segmenting the graphite at the crack location often has cured the problem in subsequent tests, as illustrated in figure 29. Figure 29(a) shows the cracked graphite after a test run. Segmenting the aft section of graphite before the next test corrected the problem (fig. 29(b)). Reference 32 discusses a similar example.

Sections of graphite therefore often are segmented axially into rings; ring cross sections varying from square to a 2:1 rectangle (axial length:radial thickness) are typical. Axial



(a) Nozzle with circumferential crack in aft graphite section



(b) Redesigned nozzle with crack eliminated by segmenting the aft section into rings

Figure 29. - Prevention of thermal cracking of graphite by segmenting the graphite section into rings.

segmentation reduces stress levels and allows better escape of gases pyrolyzed from charring backup insulators. Failure of one nozzle was attributed to collapse from the external pressure built up by the gas released from the insulator (ref. 33). Segmentation of the graphite and provision of gas bleedoff paths eliminated the problem.

Analysis of polycrystalline graphite to predict cracking is imperfect because of (1) the lack of accurate high-temperature properties, (2) the wide variation in the material from piece to piece and within pieces, and (3) the lack of well-established failure criteria. Such analysis is often impractical because of the usually prohibitive expense of exacting plastic analysis. With increased size, the variability within a single piece increases, strength decreases, and NDT becomes more difficult, so that confidence in the survivability of large-diameter inserts is much less than the confidence with small-diameter inserts (refs. 34 and 35). Among nozzle designers, confidence in the successful use of polycrystalline graphite as a throat insert drops sharply if the inside diameter exceeds 12 in.

A further reason for limiting the use of graphite is its relatively high thermal diffusivity. Except in firings of very short duration, the graphite outer surface is at a high temperature throughout most of the firing. Most designs require a substantial thickness of insulation behind the graphite to drop the temperature to an acceptable level at the interface with the support structure. The relatively high coefficient of thermal expansion requires special design consideration. Provisions for the thermal growth of graphite in the axial direction relative to adjacent materials must be made. Gaps filled with an elastomeric material or other material that breaks down at low operating temperature are provided to allow for the graphite thermal growth in the axial direction. Inadequate allowance or no allowance for thermal growth has been a cause of nozzle failure.

Designers usually provide also for growth in the radial direction, since such growth (or restraint of it) can significantly affect stresses in the insert. Two methods are in use (fig. 30). One technique is to provide a cylindrical annulus behind the cylindrical graphite rings; the annulus may or may not be filled with a material such as that used in the axial gaps. The other method is to shape the back of the graphite rings as a ramp with the greater diameter at the forward end and support the rings with a matching ramp of insulation. The axial gap is placed at the forward end of the graphite-ring pack. The graphite-ring pack then thermally grows forward on the ramp into the axial gap. An additional advantage of this technique is that pressure forces on the rings push them against the ramp, thereby providing a pressure seal behind the insert.

One facility reports that the thermal-shock sensitivity of graphite is reduced by coating the inner surface with zirconium oxide (ref. 36); however, coating is not a general practice in industry.

References 37 through 40 discuss the effects of processing on graphite properties. References 41 through 43 discuss erosion characteristics of graphite.

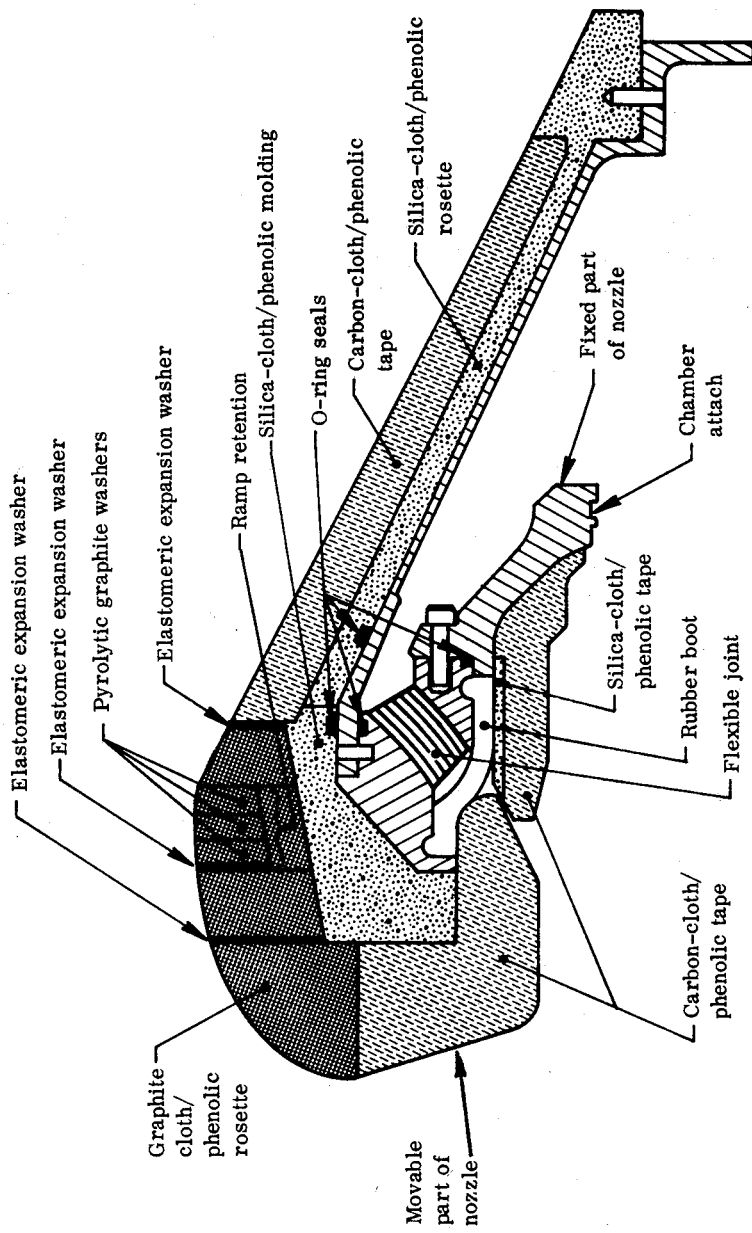


Figure 30. - Provisions for thermal expansion of throat insert.

Pyrolytic graphite. — Pyrolytic graphite is a very-high-density (2.2 gm/cm^3), erosion-resistant, expensive form of graphite formed by the deposition of gaseous carbon on a substrate. This layer-by-layer deposition results in a highly anisotropic material that differs greatly from polycrystalline graphite. The properties in the direction perpendicular to the layers (commonly referred to as the "c" direction) differ significantly from the planar properties ("a" and "b" directions). Table II, which presents typical properties of throat-insert materials, compares the properties of pyrolytic graphite in the "c" and "a,b" directions to typical properties of polycrystalline graphite.

Pyrolytic graphite has been used in nozzles in two forms: washers and coatings. Washers have been state of the art for some time, whereas coatings are still under development. Pyrolytic-graphite coatings on a polycrystalline-graphite substrate (with throat diameters up to 4 in.) have been fired successfully in solid rocket test motors with high-performance propellants (refs. 44 through 50); less success has been achieved with larger throat diameters. The current status of the pyrolytic-graphite coating efforts is presented in reference 51.

The properties of pyrolytic graphite are sensitive to the material processing conditions. Among the more important process variables are the geometry of the substrate, carbon deposition temperature, gas flowrate, and impurities in the gas stream (ref. 52). The geometry of a deposit of pyrolytic graphite reflects the geometry of the surface of the substrate, so that foreign particles on the substrate or in the deposit lead to changes in the material structure. At low temperatures ($< 1700^\circ \text{ C}$) of deposition, the material is characterized by moderate orientation and small crystallite sizes, whereas at high temperatures ($> 2300^\circ \text{ C}$) a highly graphitic structure with exceedingly high orientation results. A low flowrate of gas through the furnace results in a singularly nucleated structure; at high flowrates, soot particles tend to deposit in the pyrolytic materials and thereby reduce its strength. The controlled use of small amounts of impurity in the gas stream can change the structure and properties of pyrolytic graphite.

Figure 31 presents a typical design for a pyrolytic-graphite throat insert; see also figures 7, 9, and 15. The maximum thickness of each individual washer generally has been $3/8$ in., although suppliers report capability to produce thicker plate. Washers of approximately $3/8$ -in. thickness generally are relatively low in cost and perform satisfactorily.

Individual washers are stacked to obtain the desired total thickness. In order to effect economy, procurement specifications often are written such that the total thickness of the pack of washers is tightly controlled but considerable variation in the number and thickness of individual washers within the pack is allowed.

The use of pyrolytic-graphite washers in nozzle design is somewhat similar to the use of polycrystalline graphite. Axial-expansion provisions are even more critical because the thermal expansion in the axial direction is relatively much greater; inadequate provision for thermal expansion has been a recurrent cause of nozzle failures. Backup insulators and

Table II. — Typical Properties of Materials Used for Throat Inserts⁽¹⁾

Property	Tungsten		Pyrolytic graphite ⁽³⁾	Polycrystalline graphite ⁽³⁾	Carbon/carbon composite ⁽³⁾
	Forged or extruded	Pressed and sintered ⁽²⁾			
Density, gm/cm ³	19.0	17.4	2.2	1.75	1.45
Sublimation or melting temp., °F	6170	6170	6600	6600	6600
Specific heat, Btu/(lbm·°F)	0.033 (0.047)	0.033 (0.047)	0.22 (0.5)	0.25 (0.6)	0.31 (0.54)
Thermal conductivity, Btu·ft/(hr·ft ² ·°F)	96 (60)	54 (33)	—	—	—
with grain or ply (warp)	—	—	200 (40)	70 (16)	18
across grain or ply	—	—	1.2 (.03)	40 (15)	8
Thermal expansion, μ in./(in.·°F)	2.5	2.3	—	—	—
with grain or ply (warp)	—	—	—	—	—
across grain or ply	—	—	1.33 20.0	1.50 2.2	0.5 (1.7) 1.4 (2.8)
Ultimate tensile strength, ksi	160 (10)	55 (10)	—	—	—
with grain or ply (warp)	—	—	10 (15)	4.5 (7.0)	13.5 (16.0)
across grain or ply	—	—	0.4	3.0 (5.0)	0.7 (1.3)
Tensile modulus, 10 ³ ksi	59	40	—	—	—
with grain or ply (warp)	—	—	4.0 (2.5)	0.75 (0.80)	2.3 (2.1)
across grain or ply	—	—	1.7 (1.0)	0.90 (1.25)	1.6 (1.8)
Compressive strength, ksi	NA	NA	—	—	—
with grain or ply (warp)	—	—	10	9.0 (11.0)	13.5 (13.5)
across grain or ply	—	—	45	10.0 (12.0)	6.5 (9.0)
Compressive modulus, 10 ³ ksi	NA	NA	—	—	—
with grain or ply (warp)	—	—	4.8	0.9 (1.1)	2.5 (2.2)
across grain or ply	—	—	1.9	0.8 (1.0)	1.5 (0.65)

⁽¹⁾All values shown are for room-temperature properties except that the values in parentheses refer to properties at 4000°F.⁽²⁾Properties for 90-percent-dense, unalloyed, pressed-and-sintered tungsten.⁽³⁾Typical properties, not design properties. Density, strengths, and moduli can be varied over a wide range by changing the processing methods.
NA = not available.

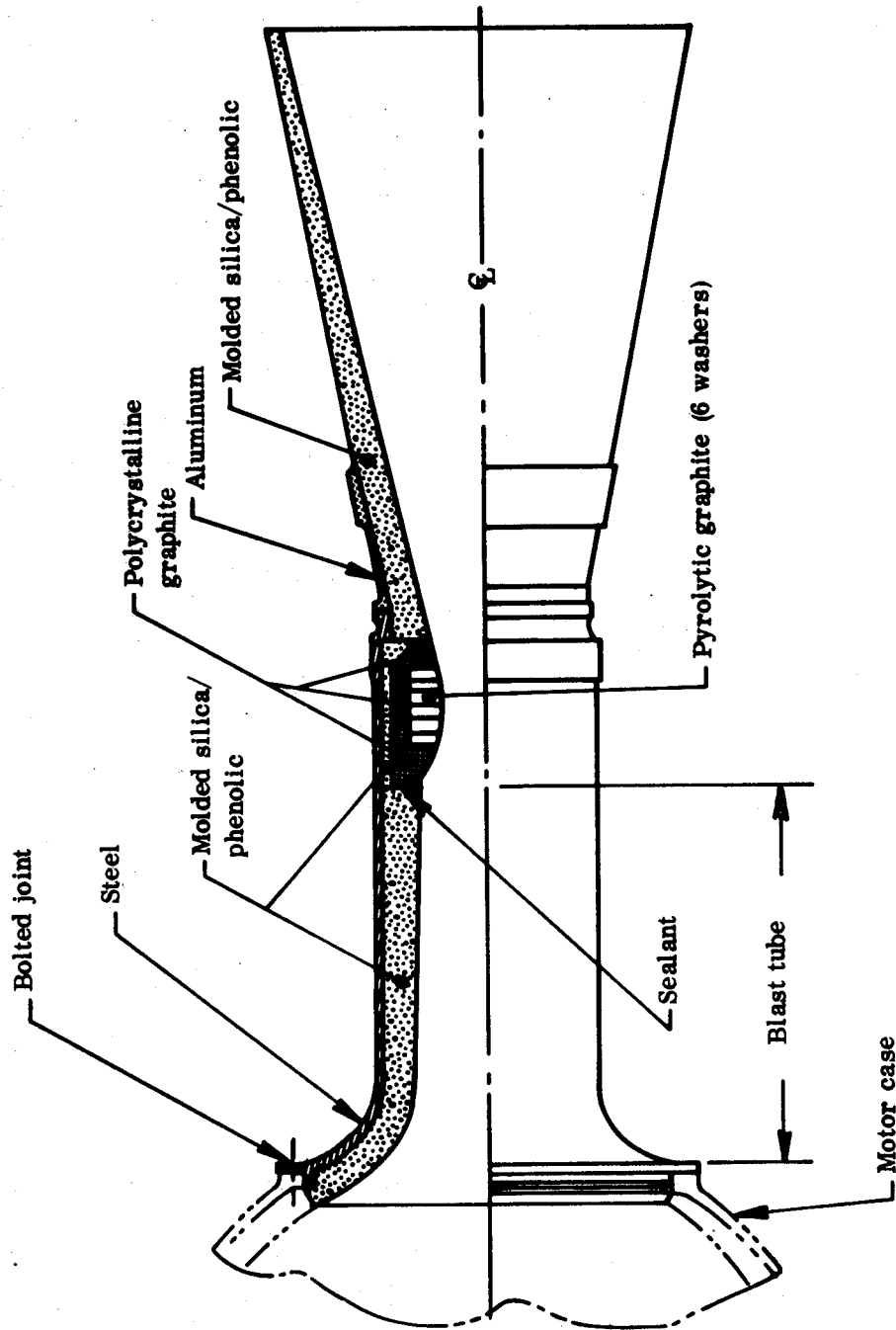


Figure 31. - Nozzle incorporating pyrolytic graphite throat.

structural support must be provided. Because of greater erosion resistance and greater strength, pyrolytic-graphite washers are useful in many designs where polycrystalline graphites are unsatisfactory.

In the usual design with pyrolytic-graphite washers (fig. 31), a polycrystalline-graphite or phenolic backup ring runs the length of the washer pack, and polycrystalline-graphite or carbon/carbon rings are located fore and aft of the washer pack. The backup ring helps to provide uniform support for the washer pack, and the fore, aft, and backup rings can function as heat sinks to reduce the temperature of the washer pack. Use of polycrystalline-graphite or carbon/carbon rings fore and aft prevents an excessive step from forming at the faces of the pyrolytic washers and reduces the tendency to delaminate. The most common failure in pyrolytic-graphite throats has been excessive delamination of the washers.

A pyrolytic-graphite ring with the "a,b" orientation parallel to the nozzle axis rather than a polycrystalline backup ring has been used in several designs to back up the washer pack. The pyrolytic backup ring's orientation makes it a more efficient conductor of heat to the fore and aft polycrystalline-graphite rings; this property helps reduce both the temperature of the washer pack and the heat flux to the backup insulator.

Pyrolytic-graphite washers up to 18 in. in outside diameter are available. To date, successful tests have been conducted with pyrolytic graphite throats as large as 12.5 in. in diameter at chamber pressures exceeding 1000 psi.

Refractory metals. — Molybdenum, tungsten, alloys of tungsten, infiltrated tungsten, and flame-sprayed tungsten have been used as throat inserts to eliminate or minimize throat erosion. The use of molybdenum is limited to the relatively low-temperature, low-energy propellants rarely used in current solid rocket applications and to short-duration small-scale motor tests.

Tungsten and tungsten alloys currently are used in forged, extruded, and pressed-and-sintered forms, and successful tests with a tungsten-wire/plasma-spray-tungsten matrix have been conducted (refs. 53 through 55). Since forgings and extrusions have quite similar properties (table II), extrusions (which cost less) usually are employed up to the maximum available diameter of a little over three inches. Forging and extrusions have higher strength and more desirable grain orientation than the pressed, sintered, and infiltrated tungsten, so the former normally are used unless the exhaust temperature at the insert is so high that forged or extruded tungsten might become plastic and be ejected. (Extruded tungsten has been used successfully, however, with propellant flame temperatures as high as 6500° F (ref. 56)). At these high temperatures, silver-infiltrated tungsten (and, to a lesser extent, copper- or zinc-infiltrated tungsten) provide cooling as the infiltrant vaporizes (ref. 57). The infiltrants also reduce thermal-shock sensitivity by increasing thermal conductivity. Pressed-and-sintered tungsten without an infiltrant has had mixed success but its use is not common. Flame spraying has been used in a limited way to form small tungsten throat inserts and to coat a throat extension (ref. 36).

In the pressed-and-sintered method of fabricating tungsten components, the pressing practice, raw material purity, and particle-size distribution influence erosion behavior (ref. 58); a low-density tungsten component results in greater erosion and less resistance to thermal shock. Large grain sizes generally have contributed to brittleness. The probability of fracture of tungsten by thermally induced stress is related to the brittle-to-ductile transition temperature; processing conditions therefore are controlled to lower this transition temperature so that fracture strength is increased.

For the successful use of tungsten inserts, axial expansion gaps and radial expansion gaps (or a growth ramp) are necessary. Polycrystalline-graphite backup rings and fore and aft adjacent rings are commonly used for the same reasons that they are used with pyrolytic-graphite washer packs: heat sink, support, retention, and erosion-step mitigation. The interfaces between tungsten and graphite may be coated (tantalum or thoria coatings have proven satisfactory) to prevent formation of a low-melting-point tungsten-carbon eutectic that can substantially degrade tungsten performance (ref. 59). Uncoated tungsten has been used successfully, however, in Minuteman Stage I.

Heat treating of finished tungsten inserts in a circulating air atmosphere, a process that produces a tungsten oxide coating on the insert surfaces, has proved beneficial in reducing or eliminating thermal-shock and thermal-stress cracking. In this process, residual machining stresses are relieved, and oxide formation chemically removes the minute machine-tool grooves and ridges, which are natural stress risers. The oxides also provide some reduction in thermal diffusivity for a short period of time. If desired, the oxides can be removed by treating in a hot sodium hydroxide bath without affecting the first two benefits listed above.

Carbon/carbon composites. — Carbon/carbon composites are a class of very promising but relatively new nozzle materials. In the term "carbon/carbon", the first "carbon" identifies the reinforcement material; and the second "carbon" identifies the matrix that binds the reinforcements together. This terminology is consistent with that for other composites; for example, in the term "carbon-cloth/phenolic" the first part of the term identifies the reinforcement material as carbon cloth, and the second part identifies the matrix as phenolic resin. Carbon/carbon, therefore, indicates a composite consisting of a carbon reinforcement (fabric, fibers, or felt) in a carbon matrix. Usage of the term, however, has grown to include graphitic reinforcement and a graphitic matrix, or carbon reinforcement partially converted to graphite bound together with a carbon matrix that is also partially converted to graphite. The latter carbon/carbon composite represents the majority of these materials and is the type of carbon/carbon referred to throughout this document. Other names for carbon/carbon include graphite/graphite, fibrous graphite, prechars, graphitized composites, carbon composites, and prepyrolyzed materials.

The material is fabricated by depositing a carbon or graphite matrix into the carbon or graphite reinforcement structure. The reinforcing structure is most frequently made by pyrolyzing graphite-cloth/phenolic structures in an inert atmosphere. Two methods are in use for deposition of the matrix: chemical vapor deposition (CVD), and liquid impregnation followed by further pyrolyzation. In the CVD method, pyrolytic carbon is deposited from a

vapor into the reinforcement structure. In the liquid-impregnation method, resin or pitch under pressure is forced into the reinforcement structure and is then charred to form a carbonaceous matrix; the impregnation/charring cycle is repeated two or more times to build up to the desired density. The final step in either process is partial graphitization at a temperature of 4500° to 5000° F, a step that yields a composite with carbon reinforcements – partially converted to graphite – bound together with a carbon matrix – also partially converted to graphite.

Carbon/carbons possess erosion resistance approaching that of polycrystalline graphites but have better strength and are much less sensitive to thermal or mechanical shock. Carbon/carbons therefore can be used without the complex retention and support required for polycrystalline graphites. Carbon/carbon construction helps explain these superior properties.

Rings of carbon/carbon have proven to be more reliable than those of polycrystalline graphite when used fore and aft of pyrolytic-graphite washer throats. Such carbon/carbon rings are operational in the SRAM nozzle and currently are planned for the nozzles in the Trident I C4. The greater promise of carbon/carbon, however, is in nozzles constructed primarily of carbon/carbon, with these materials forming the exit cone, entrance, and, in some cases, the throat as well. References 31, 60, and 61 present results of test firing of nozzles constructed chiefly of carbon/carbon.

The carbon/carbon class of materials is attractive because of both potential advantages in weight (refs. 60 and 61) and potential improvements in nozzle efficiency (ref. 31). Weight likely can be reduced 35% (movable nozzle) to 60% (fixed nozzle), and nozzle efficiency increased by 1% or more. These improvements are possible because carbon/carbons are both excellent liner materials and excellent structural materials. Carbon/carbon structural properties (like those of pyrolytic and polycrystalline graphites) improve with temperature (up to the 3500 – 4500° F range). Insulation of carbon/carbon therefore is not required and a single layer of carbon/carbon can replace the three separate layers of liner, insulator, and structure necessary in previous nozzles.

The carbon/carbon composites of interest are those with a density of 1.40 gm/cm³ or greater. Earlier, lower density materials performed poorly (ref. 62). Carbon/carbons with density of 1.40 to 1.50 gm/cm³ exhibit erosion rates about one-third to one-half those of graphite/phenolic and carbon/phenolic. Carbon/carbons with densities as high as 2.0 gm/cm³ are now available and are expected to exhibit even better erosion resistance, such as that desirable for the throat region.

2.2.2.2 THERMAL LINER AND INSULATOR

Liner and insulator thicknesses are sized by estimating the depth of expected erosion, adding a margin of safety*, adding the estimated thickness of char, and adding sufficient

* As used herein, the margin of safety on erosion depth is $(t_a - t_e)/t_e$ where t_a = thickness allowed for erosion and t_e = expected erosion depth.

thickness of virgin material to drop the temperature to that for which the structure will be designed. If the liner is a low-erosion throat-insert material (refractory), a thickness usually is added in the liner to provide sufficient structural integrity, since thin sections of these materials tend to be structurally inadequate. If the liner is reinforced plastic, the liner thickness in conservative demonstration-test designs and in motor-test nozzles usually is sized to confine char to the liner, whereas in flightweight designs the char surface is allowed to penetrate into the insulator.

At this stage in design, erosion is estimated by extrapolation of erosion data, material by material, from the most nearly similar test for which data are available to the conditions of the new design. The erosion rates usually are scaled by the method of Bartz (ref. 63):

$$\text{Erosion rate} = \text{Measured rate} \times \left(\frac{P_c}{P_{cm}} \right)^{0.8} \left(\frac{D_{tm}}{D_t} \right)^{0.2} \quad (3)$$

where P_c and D_t are the chamber pressure and throat diameter of the motor being designed and P_{cm} and D_{tm} are pressure and throat diameter of the motor in which the measured rate was obtained. If the material is carbonaceous, an additional correction is made for propellant corrosivity (as measured by oxidation ratio or blowing coefficient (ref. 64)).

Char depth is estimated by extrapolation of measured data, corrections being made for time and temperature, or is estimated by the corrosion analogy (ref. 65):

$$X = A \theta^m \exp(-B/Q) \quad (4)$$

where

X = char depth, in.

A = empirical constant

θ = firing duration, sec

m = empirical constant

B = empirical constant

Q = cold-wall heat flux, Btu/(ft² - sec)

The values of the constants A, m, and B are determined experimentally for given materials and conditions. For example, as reported in reference 65, for graphite-cloth/phenolic

$$X = 0.036 \theta^{0.68} \exp(-66.5/Q) \quad (5)$$

and for silica-reinforced phenolic

$$X = 0.031 \theta^{0.68} \exp(-90.4/Q) \quad (6)$$

The margin of safety applied to erosion depth varies from 0.2 to 0.5 in throat and entrance, and from 0.1 to 0.5 in the exit for nozzles on motors not man-rated; for nozzles on man-rated motors, the margin is 1.0 in all areas. Most designers apply a zero margin of safety to char; those few designers who do apply a positive margin of safety to char apply smaller margins to erosion. However, for man-rated nozzles, a margin of safety of 0.25 on char in addition to the margin of safety on erosion is specified.

The outside envelope of the thermal components that results from summing these thicknesses at several locations is nonlinear. A straight line or series of straight lines encompassing the envelope usually is used for the back contours to simplify the design and thereby reduce fabrication cost of both the thermal components and the supporting structure.

The allowable throat-area change is a consideration based on internal ballistics and system tradeoffs and is not purely a nozzle design decision. If little or no throat-area change is desirable, the designer uses an erosion-resistant throat insert. If moderate erosion is tolerable, a graphite-cloth/phenolic or carbon-cloth/phenolic throat can be used to simplify the design. In a few cases, a large throat-area change is desirable, and an insulator-type material such as silica/phenolic or asbestos/phenolic may be used as the throat.

In most nozzle designs, graphite-cloth/phenolic or carbon-cloth/phenolic is selected as the liner immediately upstream and downstream of the throat, usually out to an expansion ratio of at least 2 to 4. Upstream and downstream of this ratio, where conditions are less erosive, insulator-type materials are used as the liner unless the inlet or exit is so short that it is uneconomical to change.

Figure 32 illustrates various interface configurations for thermal materials. The interface between different types of materials usually is parallel to the ply angle of one or the other material (fig. 32(a)); this condition provides economy in machining and avoids partial ply lengths on one side of the interface. The interface normally is stepped at the boundary between one liner and its insulator. The step in the interface preferably is cylindrical about the nozzle axis, both to obtain economy in machining and to make it less likely that a gas path through to the structure will open up as a result of relative motion of parts or

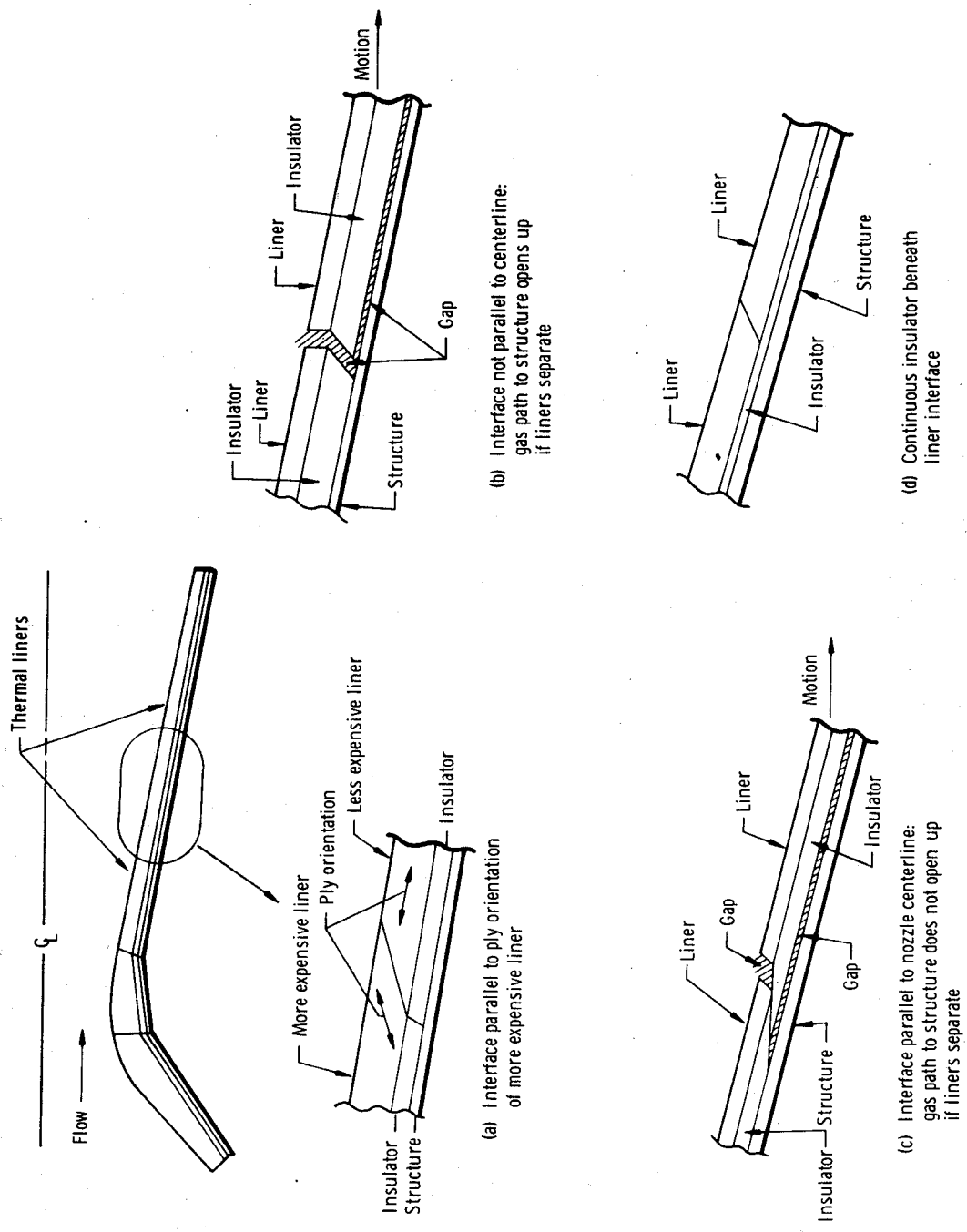


Figure 32. - Cross-section drawings of nozzle exit showing interface configurations for thermal materials.

distortion of the parts when loaded (cf. figs. 32(b) and (c)). Failure to step these interfaces has been a recurrent cause of failure in nozzles. An alternative and perhaps better method of preventing gas flow to the structure, if a path should open between two adjacent liners, is to use a single, continuous insulator behind both liners, as in figure 32(d).

Use of sealants in the interfaces is discussed in section 2.2.3.3.

Vent holes usually are provided for nozzle-exit thermal designs when the exit liner is a die-molded material and also when the insulator is asbestos-felt/phenolic. The vent holes provide gas paths that allow pyrolyzed gases to reach the surface. Without these vent holes, the pressure buildup from the formation of the gases causes spalling of die-molded liners. In general, vent holes are not provided in tape-wrapped liners, since the path between plies provides a natural escape path for gas. Vent holes are necessary with tape-wrapped liners, however, if the ply angle is parallel to the flow or if the insulator beneath the liner is asbestos/phenolic. Asbestos/phenolic contains a large amount of water of crystallization and therefore outgasses copiously as it chars. The swelling and shrinking of asbestos/phenolic as it absorbs and loses moisture also produces high stresses in adhesive bond layers adjacent to it. The resultant loss of bond strength has led to nozzle failure due to ejection of the exit cone when the asbestos/phenolic was not mechanically restrained in addition to being bonded.

In a typical vent-hole design, holes 0.060 in. to 0.100 in. in diameter on 1-in. centers are drilled to the expected maximum char depth.

2.2.2.1 Liner Materials

Thermal liners, or flame barriers, are the materials that form the gas-side contour of the nozzle. As noted, throat inserts are either highly-erosion-resistant materials (refractories) or reinforced plastic. The liners in the remainder of the nozzle usually are reinforced plastics, although, as previously noted, polycrystalline graphites have been used as blast-tube and throat-extension liners.

Elastomers are another group of materials that have also served as liners in some nozzle designs. Elastomeric liners in general have been used only in very-low-Mach-number regimes ($Mach < 0.2$) such as the large end of convergent-divergent nozzle inlets or the chamber side of a submerged nozzle (figs. 18 and 20).

Standard Reinforced-Plastic Liners

Phenolic resin combined with reinforcing material has been used so extensively and successfully as a nozzle liner that the phenolic composites can be regarded as standard liner materials. Typical properties of the common phenolic composites are presented in table III.

Table III. – Typical Properties of Phenolic Resin with Various Reinforcement Materials⁽¹⁾

Property	Reinforcement material				
	Carbon cloth	Graphite cloth	Silica cloth	Asbestos felt	Glass cloth
Density, gm/cm ³	1.43	1.45	1.75	1.73	1.94
Specific heat, Btu/(lbm·°F)	0.20 (0.36) 0.0108 (0.0125)	0.24 (0.39) 0.0126 (0.0128)	0.24 (0.30) 0.0080	0.19 0.0042	0.22 0.0069
Thermal diffusivity, ft ² /hr					
Thermal conductivity, Btu·ft/(hr·ft ² ·°F)	0.83 (0.93) 0.48 (0.58)	2.29 (2.90) 0.69 (0.92)	0.35 (0.38) 0.30 (0.32)	0.20 NA	0.16 NA
Thermal expansion, μ in./(in.·°F)					
with grain or ply (warp) across grain or ply	3.8 5.3 (31.0)	5.3 17.6	3.9 16.5	7.0 25.0	4.6 21.0
Ultimate tensile strength, ksi					
with grain or ply (warp) across grain or ply	18.0 (10.5) 0.90 (0.30)	10.5 (7.6) 0.74 (0.33)	12.0 (7.6) 0.72 (0.39)	36 NA	60 NA
Tensile modulus, 10 ³ ksi					
with grain or ply (warp) across grain or ply	2.64 (1.60) 1.80 (0.05)	1.57 (1.23) 0.44 (0.08)	2.62 (1.99) 0.48 (0.06)	3.0 NA	4.6 NA
Compressive strength, ksi					
with grain or ply (warp) across grain or ply	36.1 (13.5) 62.9 (42.5)	13.0 (3.98) 33.0 (2.16)	16.2 (8.13) 49.1 (21.3)	20 NA	50.6 NA
Compressive modulus, 10 ³ ksi					
with grain or ply (warp) across grain or ply	2.34 (1.73) 1.85 (0.75)	1.50 (0.89) 1.05 (0.37)	3.50 (1.95) 2.07 (0.78)	2.3 NA	3.7 NA

⁽¹⁾ All values shown are for room-temperature properties except that the values in parentheses refer to properties at 750°F.

NA = not available.

Graphite-cloth/phenolic and carbon-cloth/phenolic are the liner materials most often used in blast tubes, throat approaches, and throat extensions in all sizes of nozzles and in the throats of large nozzles. One or the other of these two materials has formed the throat of nearly all nozzles with throat diameters in excess of 10 in. These two materials are used almost exclusively as liners. The erosion performance of graphite-cloth/phenolic generally is reported to be better than that of carbon-cloth/phenolic. The apparent spread in erosion rates is less than 25 percent. Carbon-cloth material exhibits a greater tendency to delaminate and is a little less stable thermally. On the other hand, carbon-cloth is less expensive (by 1/4 to 1/3) and is somewhat stronger; furthermore, carbon-cloth/phenolic has a significantly lower thermal diffusivity (table III), a characteristic that allows the use of thinner sections or the elimination of a separate backup insulator.

Silica-cloth/phenolic, and to a lesser extent, glass-cloth/phenolic and asbestos-felt/phenolic, primarily used as insulators, have, because their cost is one-sixth to one-third that of carbon-cloth/and graphite-cloth/phenolic, been used as liners as well as insulators in regions of the nozzle where a severe erosion environment does not exist (e.g., in the aft exit cone). The optimum point in the exit for a switch from a relatively expensive graphite- or carbon-cloth/phenolic liner to a lower cost liner is determined by specific cost and weight trades for each nozzle; in general, the optimum point for a switch to silica-cloth/phenolic has been at an expansion ratio between 2 and 4. An erosion step will, of course, develop downstream of the interface. Erosion depth in the less-erosion-resistant material immediately downstream of the interface will be as much as twice that which would be predicted without the more-erosion-resistant material upstream and with all else equal. Severe steps formed at interfaces as the nozzle erodes greatly distort the original aerodynamic contour and may reduce performance, so interfaces are located to help minimize these steps. These insulator-type materials (silica/, glass/, and asbestos/phenolics) have even been used as the throat liner for nozzles under certain conditions: very low pressure (100 psi), very short firing duration (1 to 10 sec), low-temperature propellant (below 5000° F chamber temperature), or highly oxidizing propellant.

Another design and material consideration is the possibility of "slagging" (condensation and deposition of exhaust products on the nozzle thermal liner surfaces). Slagging occurs to some extent in most nozzles shortly after ignition when the liner surfaces are cool enough to cause some exhaust product to precipitate out of the gas stream, and during tailoff when the low pressure and low velocity of the exhaust stream encourage precipitation. In a few motors with unusual propellants, slagging can occur throughout the firing duration. Slagging during tailoff is of little concern; however, slagging during the major portion of the firing can affect the nozzle performance by (1) changing the aerodynamic contour, (2) changing the heat transfer into the liner, and (3) causing irregularities in the thrust trace as slag is expelled. In movable nozzles that incorporated a ball-and-socket design, slag buildup on the ball-and-socket surfaces has increased nozzle torque by as much as 300 percent by the end of firing.

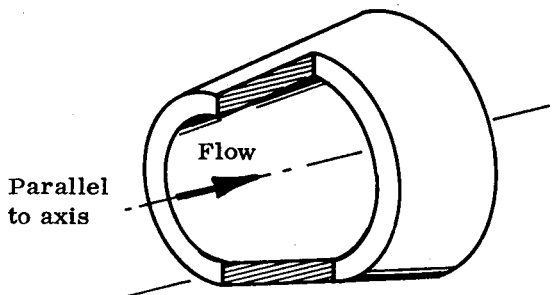
The possibility of slagging is a consideration in liner-material selection. Carbonaceous materials such as carbon and graphite phenolics are less prone to slag buildup than the silica-, glass-, and asbestos-base materials, probably because the surface of the carbon-base materials is maintained at a higher temperature. The carbonaceous materials therefore are specified where slag buildup is a potential problem (e.g., for ball-and-socket surfaces of movable nozzles).

The term "reinforced plastic" is applicable to several variations of the basic reinforced plastics: tape wraps, layups, and die moldings. The tape and layup forms are illustrated in figure 33. Tape and layup reinforcements allow the fibers to be oriented to advantage in the design because the composite properties vary with the orientation (refs. 66 and 67). Edge orientation to the flow (plies perpendicular to surface) is the most-erosion-resistant orientation: erosion rates are reduced 25 to 50 percent as compared with a low but practical angle to the flow such as 10°. (Orientation exactly parallel to the flow normally is avoided, because the plies tend to peel and thereby produce unacceptably high surface recession.) Edge orientation, on the other hand, produces the greatest depth of heat penetration measured from the eroded surface: the heat-affected depth is 25 to 50 percent greater than that occurring with low angles to the surface.

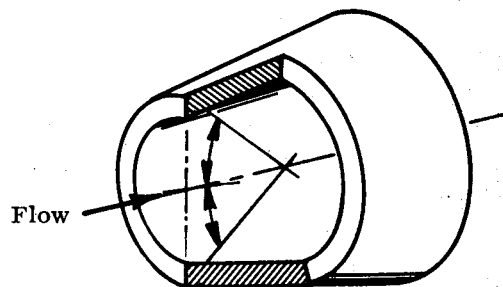
Reinforcement materials commonly used are "pre-preg", i.e., the reinforcement, cloth or fiber, is already impregnated with resin when purchased, so that after forming only heat and pressure are necessary to produce a cured reinforced-plastic part.

Tape wraps. — Tape wrap is the most economical use of fabric when the desired orientation can be obtained, because both scrap and labor are minimized. Tape is used in two forms, straight (warp) and bias, the designation referring to tape cut parallel to the weave and at an angle to the weave, respectively. Straight tape is lower in cost, as less splicing is required to obtain workable lengths; furthermore, straight tape exhibits greater strength in hoop tension than bias tape. The advantage of bias tape is that it will lie flat when laid up with the plies at a high angle to the part centerline. Since straight tape cannot take great amounts of distortion and remain planar, its use is limited to ply angles within $\pm 2^\circ$ of parallel to the part centerline. Straight tape has been used extensively for exit cones because the lower cost and high hoop strength are desirable while the relatively low ply angle to the surface (equal to the exit half-angle) keeps heat penetration near minimum. Maximum erosion-resistant orientation is not needed in the exit, where conditions are less erosive than those in the throat region.

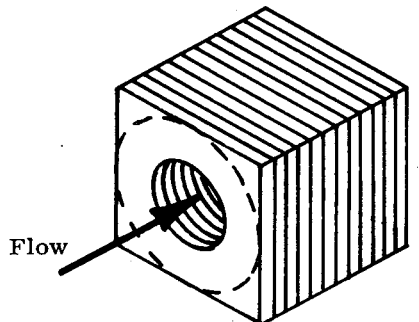
Bias tape, though able to remain planar even when distorted considerably, is limited in usefulness. As the part diameter becomes smaller, the part thickness greater, and the angle to part centerline steeper, bias tape is less and less capable of distorting without wrinkling. Tape-wrap capabilities are measured by the parameter ξ :



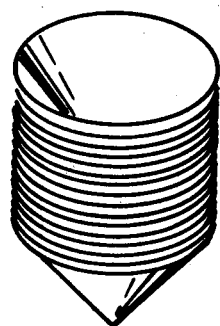
(a) Tape wrap parallel to axis
(straight tape)



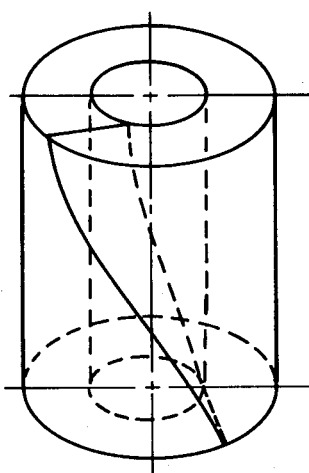
(b) Tape wrap angled to axis
(bias tape)



(c) Flat laminate
(thickness of plies exaggerated)



(d) Stacked cone



(e) Rosette

Figure 33. - Various methods for tape wrap and layup of reinforced-plastic parts.

$$\xi = \frac{D}{W \sin A} \quad (7)$$

where

ξ = tape-wrapping capability index

D = inside diameter of part, in.

W = tape width, in.

A = wrap angle (0° is parallel to axis of part), deg

Values for ξ of 5 and greater indicate no wrapping problem; when values for ξ fall below 1.6, wrapping approaches the impossible. Between 1.6 and 6, tape wrapping may or may not be possible, depending on the equipment and experience of the fabricator (ref. 68).

In general, processing of reinforced-plastic parts involves a debulk operation prior to final cure. To maximize as-wrapped density in tape-wrapped parts, tape is heated and pressed with rollers as it is applied. High as-wrapped density helps eliminate voids and wrinkles in the cured part that locally accelerate delamination and erosion.

The reinforced-phenolic part is then sealed in an evacuated bag and cured under heat and pressure. Hydroclave* cure in rubber bags (typically at 1000 psia and 310° F for 2 hours) is used for most parts, particularly for critical liners such as throat approach, throat, and throat extension. Autoclave** cure in plastic bags (typically at 250 psia and 310° F for 2 hours) is less expensive than hydroclaving and has been used extensively for less critical parts such as aft exit liner, insulators, and structural overwraps on previously cured parts. The difference in properties between hydroclave- and autoclave-cured layups has narrowed considerably in recent years as laidup densities have improved to 90 percent or better of final cured density.

Most reinforced-phenolic parts are subjected to a postcure cycle. Two examples of cycles in use are 350° F for 12 hours, and 300° F for 24 hours. Industry experience and experimental studies have indicated that postcure relieves residual stresses that contribute to distortion of the part and increased erosion. One facility specifies postcure to reduce volatiles in the part;

* High pressure (1000 psi) curing fixture with water as the pressurant.

** Medium pressure (300 psi) curing fixture with superheated steam as the pressurant.

otherwise, the volatiles escape during lengthy storage periods and react chemically with the propellant. The resin glaze on the surface of the part is removed prior to postcure because (1) the glaze seals the surface and thereby reduces the effectiveness of the postcure, and (2) the glaze has no reinforcement within it and therefore has little erosion resistance. Some facilities, however, have observed no benefit from postcure and do not specify it.

Layups. — A desired orientation that is outside the limits of tape capability can be obtained with flat laminate, stacked-cone, or rosette (helical) layups (fig. 32(c), (d), and (e)). A flat laminate is formed by stacking layers of fabric. The gas path later is cut through the stack with the axis perpendicular to the plies, resulting in ply orientation to the axis of 90° and angles to the flow approaching 90°.

The stacked-cone layup is formed by stacking conically shaped individual patterns cut from broadgoods. Any desired angle greater than 15° to the axis can be obtained with proper shaping of the patterns; angles less than 15° are very difficult to fabricate.

Rosette or helical layups are formed by interleaving patterns as rose petals are interleaved. The rosette has the advantages that edge orientation can be presented to the flow even with severe contours on the surface of the part, and each individual ply runs from the surface to the back contour of the part so that part of each ply remains virgin during firing.

Laidup parts are debulked, cured, and postcured with procedures similar to those used for tape-wrapped parts.

Die moldings. — Die-molded reinforced-plastic parts are less expensive in large quantities than tape-wrapped or laidup parts for nozzles up to about 20-in. throat diameter. The cost of matched metal dies is substantially greater than that of wrap mandrels; therefore, unless existing dies can be used or modified inexpensively, tape-wrapped or laidup parts (which require less expensive tooling) are less expensive for small quantities. Die molding is impractical for very large nozzle parts because of the expense of the die and the lack of presses with the capacity to apply the desired molding pressure (2000 psi is typical); however, a few nozzles in which die-molded segments were joined together to form a larger cone have been demonstrated successfully (ref. 69). Die-molded parts exhibit lower erosion resistance, lower strengths, and a greater tendency for surface spalling and chunking than do tape-wrapped or laidup parts. Tape-wrapped or laidup parts therefore are more common in critical areas (e.g., the throat region) and in designs where weight minimization is primary.

Nonstandard Reinforced-Plastic Liners

Reinforcements other than carbon, graphite, silica, asbestos, and glass and resins other than phenolics are not commonly used for liners; however, glass-reinforced epoxy has been used extensively for insulators and structural components. Recent programs have investigated the potential of lower cost reinforcements, resins, and fabrication methods (refs. 69 and 70),

and several of these newer combinations are approaching state-of-the-art status. Results with canvas-cloth/phenolic (one-half to one-fourth the cost of silica-, asbestos-, or glass-cloth/phenolic) have been good; so have results with "double thick" but otherwise standard reinforced-phenolic materials. In the latter case, reduced fabrication time reduces cost. A new lower cost carbon/phenolic material (one-fourth the cost of standard carbon/phenolic) made from pitch-based carbon is under development and appears promising. Oven cure of standard reinforced-phenolic material with pressure (30 to 300 psia) applied by an overwrap or a tape that shrinks when heated has produced satisfactory parts (ref. 71).

Ambient-pressure-curing resin systems such as epoxy have been successfully demonstrated (refs. 72 and 73) and are used throughout one nozzle design that is in advanced development. Castable or trowelable liner materials also have been successfully demonstrated (refs. 74 and 75).

2.2.2.2 Insulator Materials

Glass-, silica-, and asbestos-reinforced phenolic or epoxy resins are one of two groups of materials commonly used for insulators; the other group is the filled elastomers. Much of the preceding discussion of graphite-cloth/phenolic and carbon-cloth/phenolic fabrication applies to silica/, glass/, and asbestos/phenolic as well.

Reinforced plastics. — In many designs the use of a separate insulator material between the liner and the structure is desirable for one or more of the following reasons:

- (1) The lower thermal diffusivity of the insulator material reduces the overall thickness necessary when thickened liner material serves the dual function of liner and insulator. Envelope and often weight can therefore be reduced.
- (2) Insulator raw materials costs are one-fourth to one-third those of carbon-cloth/phenolic or graphite-cloth/phenolic.
- (3) Some insulator materials have structural properties superior to carbon-cloth/phenolic or graphite-cloth/phenolic and so may be usable for the dual function of insulator and structure, thus simplifying the design.
- (4) A separate insulator provides an added safety feature in that, if a delamination opens up in the liner, no gas path through to the structure is provided, as would be the case if the liner were also serving as insulator.

The disadvantages of separate insulators are a more complex design and increased fabrication cost. To minimize the increase in fabrication cost, composite cure of liners

overwrapped with insulators has been used extensively. In this technique, the insulator is wrapped over the debulked liner and the composite is bagged and cured as a unit. In some cases, the liner is partially cured (staged) and the outer surface is machined before the insulator is overwrapped.

Maximum insulation properties in layup insulators are achieved if the ply orientation is parallel to the gas flow (perpendicular to the heat-transfer path), since the thermal diffusivity is minimum perpendicular to the plane of the plies. This optimum orientation frequently is compromised slightly so that the insulator can be wrapped parallel to the liner back surface to simplify fabrication, or parallel to the centerline to allow use of less expensive straight tape.

As noted previously, die molding is used more extensively for insulators than for liners because close attention to orientation in order to obtain increased erosion resistance is not necessary. The choice between layup and die molding of insulators usually is a purely economic one. In some instances, however, the superior strength of a tape-wrapped part may be desirable (e.g., when the insulator also serves as structure).

Filled elastomers. — As noted, the use of filled elastomers has been limited to low-Mach-number regimes ($Mach < 0.2$), where the material has served as both liner and insulator. (Since erosion is not a severe problem at low Mach numbers, the material functions primarily as an insulator and therefore is discussed in this section.) In flight-type designs, only heat-and-pressure-cured elastomers are common. Trowelable, ambient-curing elastomers (mastics) have been used in the large end of test-weight nozzle inlets.

The fillers in the common elastomeric insulations are carbon, silica, and asbestos, alone or in combination, in the form of either powder or chopped fibers. The usual base material in the heat-and-pressure-cured filled elastomers is butadiene-acrylonitrile; a typical base material in ambient-cured elastomers is polysulfide epoxy. Many elastomers are not suitable for use in low-temperature ambient storage and operating environments, because they become brittle.

Three fabrication methods are common for elastomeric insulations: die molding under heat and pressure; layup followed by autoclave cure; and trowel-in-place followed by cure at room or slightly elevated temperature. The first two methods produce essentially equivalent parts, so the choice is economic. The trowelable material, as previously noted, is not used in flight designs.

2.2.3 Structural and Mechanical Design

The structural and mechanical design phase consists of (1) configuring the basic structural framework that will support the insulators and liners and will carry the nozzle loads and (2) developing the mechanical components that provide for movement if the design is to

incorporate movable-nozzle TVC. In the first iteration of design, each structural ring and shell generally is sized on the assumption that it is acting independently of adjacent structure. Furthermore, the load-carrying capability of the thermal components usually is disregarded, and the structural frame is designed to react all the loads and prevent excessive deflections without benefit from the thermal components.

2.2.3.1 BASIC NOZZLE STRUCTURE

The basic structure of both external and submerged nozzles (fig. 1) is subjected to internal pressure loads and flight loads. The internal pressure load is divided into an axial ejection (blowout) load and an opposing axial thrust load; the flight loads include aerodynamic loads, inertial loads, and vibration loads. In addition to these loads, the submerged structure of a submerged nozzle is subjected to chamber pressure loads. If the nozzle is used with an attached TVC system, the nozzle structure must support the attached system and react the localized loading produced by TVC.

The configuration of the structural components depends primarily on the most critical design requirement imposed. The governing design requirement generally will fall into one or more of the following four categories:

- (1) Strength limitations. — The configuration is determined by the ability of the component to withstand the imposed stresses without exceeding the material design strength.
- (2) Deflection limitations. — The configuration is designed to limit a particular displacement to a predetermined critical value in order to limit strain in the liner and insulator components supported by the structure.
- (3) Stability limitations. — The configuration is designed to prevent buckling.
- (4) Economic limitations. — Program expense limitations prohibit the use of the optimum design.

To a varying extent, economic limitations enter into all designs. For example, in the exit shell of a small nozzle for a low-pressure motor, a shell thickness of 0.001 in. may satisfy stress, deflection, and buckling; but the expense of fabricating so thin a shell likely would be prohibitive even if fabrication were technically feasible.

The first step in design of a nozzle structure is to determine the loads and subsequent load combinations that will be applied. The primary sources of internal loads on a nozzle structure are the internal pressure of the gas and the tendency of the liner materials to expand when heated. Thermal loads generated by such expansion often are the major factor

in structural design. These loads produce a complex state of stress in the structural shell, the insulator, and the erosion-resistant liner. Pressure distributions are determined with a high level of confidence by reasonably-well-defined laws for compressible flow; however, the thermal loading is predicated on material property data that can be reliable or uncertain, the validity depending on the particular material. Other internal loads that must be considered when they exist include the higher-than-normal pressure distribution that can exist in the nozzle exit section during aft-end ignition and the high-frequency flow oscillation sometimes occurring in high-area-ratio nozzles during ignition transient. In some cases, dynamic excitation of the exit-cone section can induce excessive loading and therefore must be considered. During motor tailoff, the internal pressure on the exit of an overexpanded nozzle may be lower than atmospheric pressure, and the exit cone may collapse.

Additional possible sources of loads are listed below:

(1) Operational external loads

(a) TVC system

- Asymmetrical internal pressure distribution
- Mechanical support and attachment

(b) Flight trajectory environment

- Dynamic pressure
- Wind
- External heating
- Gravitation
- Acceleration
- Vibration

(2) Nonoperational external loads

(a) Handling, storage, and shipping

- Gravitation
- Acceleration

- Vibration
- Environmental heating
- Mechanical support and attachment
- Environmental seals

(b) Hydrostatic proof and bench testing

- Proof-test pressure
- Test-rig actuator loads
- Attachment and support

Nonoperational loads can be more severe than the operational loads; e.g., in a hydrostatic test of a nozzle at full chamber pressure with the throat stopped with a plug. The nozzle sees a higher load during this test than during firing since (1) full pressure is applied throughout the inlet, whereas if the gas were flowing the static pressure would drop near the throat; (2) the load on the plug is carried into the nozzle; and (3) the thrust developed in the exit in firing would reduce the net load on the nozzle inlet.

The next step in structural design is to size each ring and shell for one of the design requirements previously stated: stress, deflection, or stability. Experience often indicates which requirement will be most critical in any specific area of the nozzle; for example, the convergent or inlet section and throat backup shells of an external nozzle generally are stress limited, whereas submerged portions of nozzles frequently are critical from the standpoint of buckling stability.

When loading is well defined and strength is the design requirement, relatively low factors of safety (1.15 to 1.25) are used. As a general rule, stability and displacement are less easily analyzed, and therefore a higher factor of safety (1.25 to 1.50) is used on components that are critical under these requirements.

2.2.3.2 STRUCTURAL MATERIALS

The most common materials for the structural components in nozzles are metals and composite materials. The metals include steel, aluminum, and titanium. Occasionally, relatively high operating temperatures dictate the use of tungsten, molybdenum, columbium, or a Haynes alloy. Typical properties of the most common metals for nozzles are shown in table IV.

Table IV. — Typical Room-Temperature Properties of Nozzle Structural Metals

Property	Aluminum (7075-T6)	Titanium (Ti-6Al-4V)	4130 Steel		18%-Ni steel (200 Class)
			Normalized	Heat treated	
Density, gm/cm ³	2.80	4.47	7.83	7.83	8.00
Ultimate tensile strength, ksi	82	178	90	180	210
Yield strength, 0.2% offset, ksi	72	160	70	179	200
Yield strength/density	25.7	35.8	8.9	22.9	25.0
Modulus of elasticity, 10 ³ ksi	10.4	16.0	29.0	29.0	27.5
Shear strength, ksi	46	90	55	109	—
Elongation, %	11.0	8.0	10 to 20	15	9 to 10
Poisson's ratio	0.33	0.31	0.30	0.30	0.31

The composite materials consist of some type of fibrous roving, tape, or cloth bonded together in a phenolic or epoxy resin system. The elastic and strength properties of these composite materials vary widely with respect to type and orientation of the reinforcement system and the binder system used.

Ultra-efficient designs often incorporate honeycomb materials in the areas where elastic stability is a problem. Both metal and fiberglass are used for the facings, and the core material is usually aluminum or fiberglass. If the mechanical properties of the materials of which the honeycomb structure is composed are known, the critical stress and the strength of the structure can be determined as discussed in reference 76.

At present, steel, aluminum, and fiberglass are the popular choices for inlet and throat shells; development of a composite shell of high-strength graphite filament in an epoxy matrix is underway. Steel or aluminum is the usual selection for the attachment flange. Protection against galvanic corrosion is provided if dissimilar metals are joined.

Fiberglass is the most popular structural material for exit cones. A combination of forms of glass/phenolic has commonly been used. For exit structures, gore strips (more-or-less triangular patterns as long as the cone and shaped to lie flat on a conical surface) are usually

laid up over the liner-insulator combination and secured with filament-wound glass/phenolic or glass/epoxy roving at each end (figs. 16 and 20). In other designs, helical-wound glass filament has formed the exit structure. In submerged structure, axially oriented gore strips (for axial strength) have been overwrapped with glass tape (for hoop strength) (ref. 77; figs. 14 and 34). Exit-cone structures of high-strength graphite filament in an epoxy matrix can provide the strength of fiberglass composites at less weight; however, these structures are not operational.

Honeycomb exit structures have been used in several large nozzles (refs. 71 and 77; fig. 34). Firm guidelines for the use of honeycomb structures have not been developed; however, the practical use appears to be limited to the exits of large nozzles (exit diameter > 100 in.).

Actuation brackets, gimbal rings, and almost all components of the actuation system are fabricated from steel or aluminum with an occasional titanium application. Titanium is considerably more expensive to buy and more costly to fabricate than either steel or aluminum, but it has a higher strength-to-weight ratio and retains its strength better at elevated temperature than either of the other two. Because of the high cost of finished parts, the use of titanium is justified only when weight is extremely critical or when the structure is designed to operate at elevated temperature.

When metals are selected as the structural material, protection against corrosion may be required. Steel usually is painted for protection, whereas aluminum is anodized.

2.2.3.3 ADHESIVES, SEALANTS, AND SEALS

Adhesives are materials applied between components to bond the components together structurally. Sealants are liquid-solid mixtures installed between components to prevent gas flow. Seals are shaped materials (e.g., O-rings) installed between components to prevent gas flow.

In most nozzle designs, epoxy adhesive is used for both adhesive and sealant functions. Epoxy adhesives that cure at room temperature are most common; however, adhesives that cure at elevated temperatures are used for some applications, particularly if the adhesive must function in the design at elevated temperature. The disadvantage of curing at elevated temperature is that differences in thermal expansion among the adhesive and the components may produce significant residual stresses when the assembly cools to ambient temperature. Gaps between components for adhesive or sealant normally range from 0.005 in. to 0.030 in.

Adhesive bonds alone rarely are depended on for retaining liner and insulator components. Mechanical retainers such as pins through the structure into the insulator (figs. 5, 17, 24, 26, and 30) or retaining lips at the exit plane (figs. 7, 8, and 11) normally provide the primary

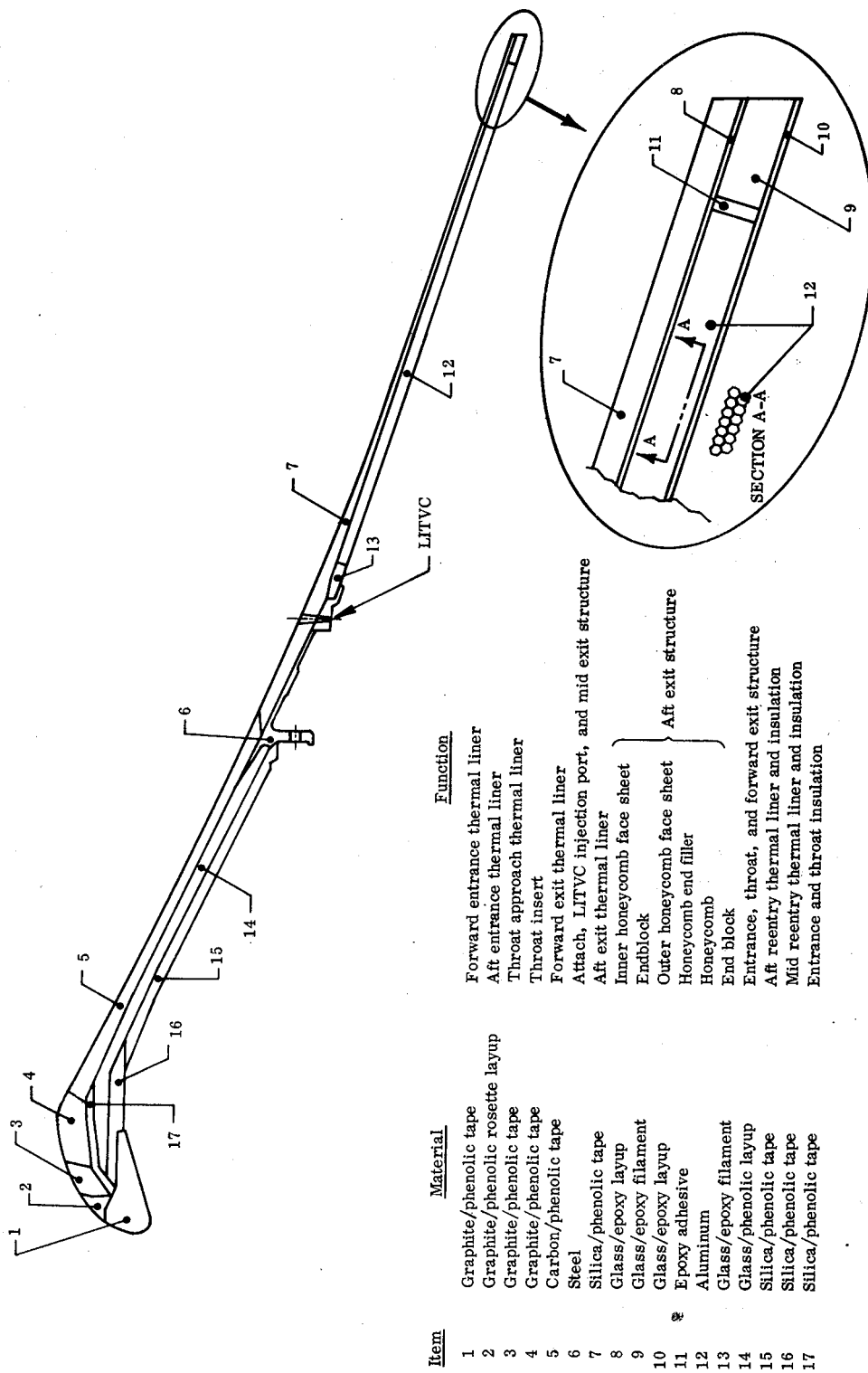


Figure 34. - Large submerged nozzle with honeycomb exit structure.

means of retaining exit and throat liner and insulator components against ejection loads. Adhesive bonds are not dependable retainers because (1) bond strengths vary greatly from nozzle to nozzle and (2) nondestructive testing methods are not capable of accurately evaluating bond strength or the degree of structural bonding between components. In the few nozzles wherein adhesives are used as the only retention method, very large factors of safety (5 or greater is typical) are imposed on the bond strengths obtained with laboratory samples of similar materials.

Surface preparation, particularly the preparation of aluminum, is critical in achieving an adequate bond. An anodized aluminum surface does not bond well, so aluminum surfaces to be bonded are sealed off during anodizing or the anodized layer is grit blasted off prior to bonding. The best bonds to aluminum are achieved if the surface is acid etched just prior to bonding, either in an acid bath or with an acidic paste cleaner.

Since large areas of unbond are common in nozzles, O-ring seals normally are included in the design for two reasons: (1) to prevent gas leakage between components, and (2) to prevent pressurization of the unbond area, which would result in an undesirable load on components. One of the major problems in O-ring groove design in nozzles has been to keep adhesive from flowing into the O-ring groove. To function properly, the O-ring must be free to extrude into a gap to seal it. O-rings often are coated lightly with a lubricant both to allow them to move more freely and to keep adhesive from bonding to the O-ring. Other methods of keeping the O-ring free of adhesive are to (1) install a second O-ring to keep adhesive from flowing to the first, or (2) bond the components first and then cut the O-ring groove after the adhesive has cured.

O-rings usually are designed with a diametral squeeze rather than an axial squeeze so that relative axial movement between components does not break the seal, as would be the case with a face seal. For best results, the recommendations of the O-ring manufacturer with respect to correct compression as installed are rigidly adhered to. Failure to follow such recommendations was regarded as a possible cause of a series of failures during testing of an early design of the Poseidon C-3 second-stage nozzle.

2.2.3.4 ATTACHED TVC SYSTEM

As noted, of the various attached TVC systems, only liquid injection (LITVC) is operational with high-energy solid rockets. The following discussion therefore is limited to LITVC.

Mating an LITVC system with a nozzle requires (1) mounting pads for injector attachment; (2) nozzle reinforcement to react side loads and limit distortion due to asymmetric loading; (3) injection ports through the nozzle wall; (4) thickening of the liner and possibly changing of liner material to accommodate reaction of the injectant with the liner and the added erosion due to increases in local pressure and heat transfer downstream of the shock front;

and (5) possible mounting of injectant tanks and the injectant pressurization system (ref. 78).

A circumferential ring, rather than individual pads, usually is provided for injector mounting, because a ring also serves to reinforce the nozzle. A limitation of ring deflection under point loading usually is applied for ring sizing. The required injection ports are relatively small and present no significant design problem. Each port usually is lined with an individual die-molded or tape-wrapped insert. Of the three injectants in common use – Freon 114-B2, nitrogen tetroxide, and aqueous strontium perchlorate – the latter two react adversely with particular nozzle materials. Nitrogen tetroxide reacts strongly with carbonaceous materials; therefore, silica-cloth/phenolic is used to line the injection port and the nozzle in the injection region. Strontium perchlorate, on the other hand, attacks carbonaceous materials less severely than siliceous materials, so carbon-cloth/phenolic is used in the injection region. The compatibility of nozzle materials and injectants is discussed in detail in reference 79.

Mounting provisions for injectant and injectant pressurization systems have been incorporated in some nozzle designs. The effect of the additional and asymmetrical loading thereby imposed must be considered in design analysis (ref. 2).

2.2.3.5 MOVABLE-NOZZLE TVC SYSTEM

Single-nozzle systems, in comparison with four-nozzle systems, significantly increase the performance of a solid rocket motor and lower the costs. (The losses from flow splitting and turning are eliminated, and the larger single throat is more efficient (ref. 20).) For these reasons, new solid rocket motor designs in recent years have incorporated only single-nozzle systems. The following discussion therefore excludes the movable-nozzle concepts peculiar to four-nozzle systems (e.g., rotatable canted nozzles and hinged ball-and-socket nozzles).

A movable-nozzle design, as compared with a fixed-nozzle design, requires three additional design features: (1) provision for motion between the fixed and movable parts of the nozzle; (2) provision for a gas seal between the fixed and movable parts; and (3) provision for a load path between the fixed and movable parts. In addition, it is often desirable to build mechanical stops into the design capable of allowing the movable portion to slam into the fixed portion without damage during actuation checkout. These stops are usually set $1/4^\circ$ to $1/2^\circ$ greater than the planned maximum vector angle.

As noted, of the various movable-nozzle concepts, the flexible-joint design currently is of most interest. The following discussion is limited to flexible-joint movable nozzles, although the special considerations are typical of movable-nozzle systems in general.

The flexible joint (also known as flexible seal, flexible bearing, and elastometallic joint) serves all three functions required of a movable nozzle: motion, sealing, and load path. The

flexible joint consists of alternating layers of elastomeric material and rigid material, each a segment of different spheres about a single point. Both metals and reinforced plastics have been used for the rigid material (the reinforcing rings). The elastomers used characteristically can deform in shear under a relatively small load while carrying large loads in compression. Motion is produced by applying a torque that results in shear strain of the elastomer in each layer about the spherical center.

Since the reinforcing rings and elastomer layers are vulcanized or bonded together, the flexible joint forms a gas-tight seal between the fixed and movable parts of the nozzle. The flexible joint is so placed within the design that the nozzle ejection load and vectoring side loads are transmitted from movable to fixed parts by means of compression in the flexible seal. The reinforcing rings limit the elastomer stress and deflection to acceptable levels.

The flexible joint has been demonstrated chiefly in submerged integral-nozzle designs. Flexible-joint TVC influences nozzle design as follows: (1) thermal protection must be provided for the flexible joint; (2) attachment and mounting must be provided for the actuation system; and (3) the nozzle must be reinforced to react TVC side loads and limit nozzle distortion.

Methods for thermal protection of the joint are illustrated in figure 35. On small nozzles where the expansion ratio at the exposed side of the flexible joint is large (> 10), a folding elastomeric boot alone (fig. 35(a)) has offered sufficient protection against convective and radiative heating. In designs where the expansion ratio at the exposed side of the flexible joint is small (and the flow velocity therefore is likely to be great), the boot is augmented by a protective cowl and splitline of insulator-type plastics (fig. 35(b); ref. 80). The latest and lightest weight thermal protection system, developed in the Trident I C-4 program, is illustrated in figure 35(c). The composite reinforcements (but not the elastomer layers) extend beyond the dimensions required for the operation of the joint. The slots between the extensions act as a labyrinth to stagnate the hot exhaust gases and thus protect the joint.

A circumferential metal ring usually is added to the exit cone for attachment of linear hydraulic actuators (the most common means of actuation). The ring may also serve to react actuation loads, limit strain of exit materials, or provide sufficient structural stiffness to ensure stability of the TVC control system. In small nozzles, the metal structure usually is continuous from the throat structure to the exit rings; in large nozzles, separate metal structures with composite structure between them may be employed.

2.2.3.6 NOZZLE-TO-CHAMBER ATTACHMENT

Four methods for attaching the nozzle to the chamber are in common use for flightweight production design (fig. 36). A bolted joint is most common because it is positive and rigid, provides means for accurate thrust alignment, disassembles freely, and is not size limited.

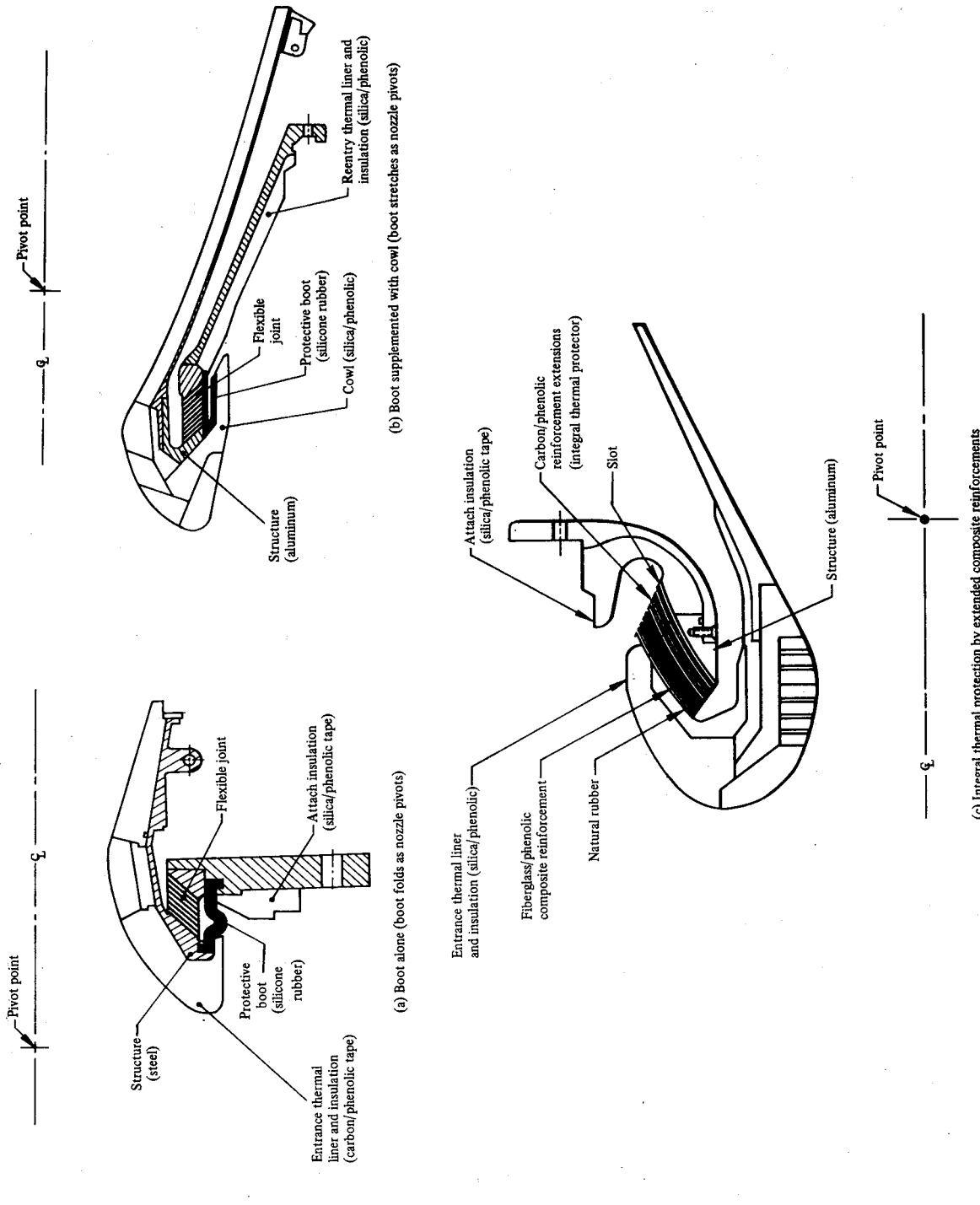


Figure 35. - Three methods for thermal protection of a flexible joint.

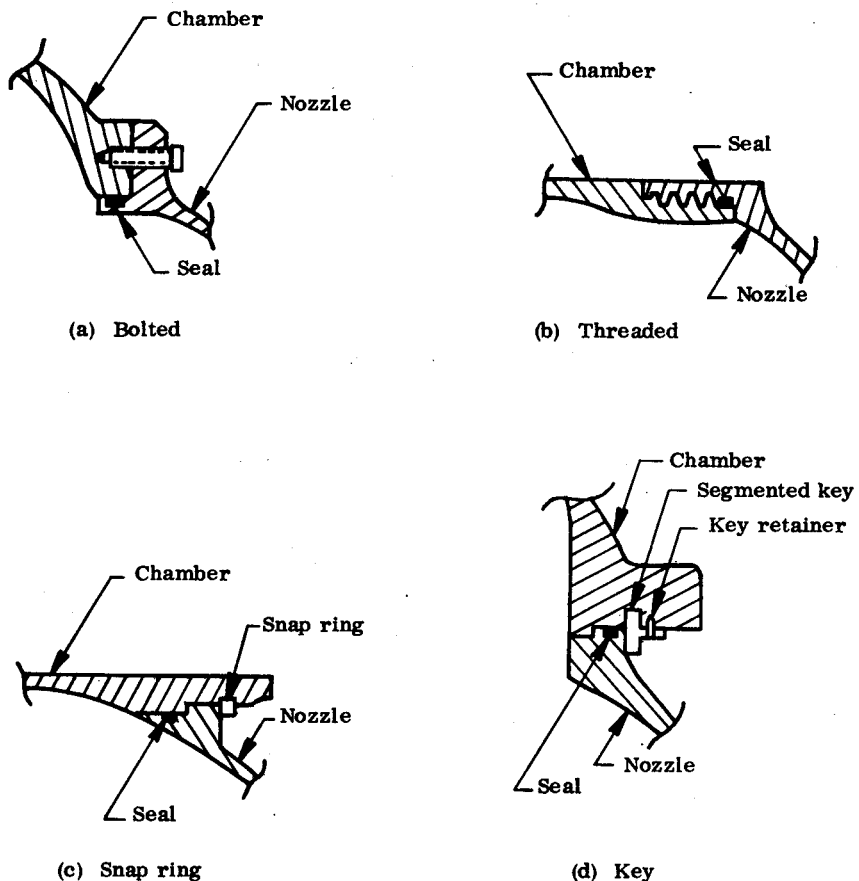


Figure 36. - Basic methods for attaching nozzle to chamber.

Disadvantages are weight (for interface diameters below about 14 in.), number of parts, and amount of labor required to assemble and disassemble.

The threaded attachment provides light weight, simplicity, and positive alignment, but at the cost of precision machining. Alignment cannot be adjusted to compensate for inaccurate machining, whereas a bolted connection can be shimmed. Accurate circumferential location of attached components is difficult at assembly. The cost of maintaining the tolerances required becomes prohibitive at diameters above about 14 in. (ref. 81).

The snap ring provides rapid assembly and disassembly, light weight, simplicity, and relatively low cost for small sizes. The disadvantages are those of the threaded joint plus the

difficulty of predicting deflection. Excessive deflection has resulted in motor failures. The cost of precise tolerance control makes the snap ring prohibitive at diameters above about 10 in. (ref. 81).

The key joint exhibits advantages, disadvantages, and size restrictions similar to those of the snap-ring joint. An added disadvantage is difficulty of disassembly.

Lockwire joints are in limited use. The advantages and disadvantages are similar to those of the snap ring but with the further disadvantage of higher cost.

In addition to the above joints, a variety of other joints are in use for test and concept-demonstration motors including band clamps, segmented or split rings, retaining collars, and shear plates. All of these joints reduce cost and speed up assembly and disassembly.

2.2.3.7 NOZZLE CLOSURE

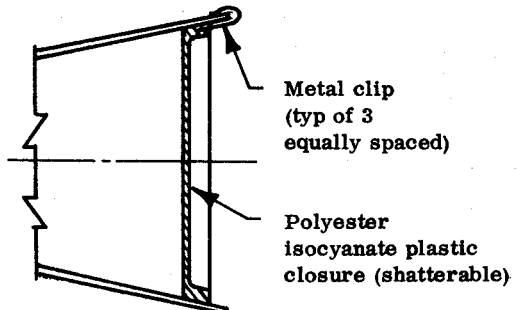
A seal, plug, or cover, commonly referred to as a nozzle closure, is often a part of a nozzle design. Nozzle closures are provided to achieve one or more of the following objectives: (1) an environmental seal to keep dust and moisture out of the motor, (2) a mounting platform on which the motor igniter can be mounted, and (3) a temporary flow restrictor to improve motor ignition characteristics. Figure 37 illustrates each type of closure.

Environmental seals are the simplest of the three types and require little special design consideration. A rubber snap-on cover (fig. 37(a)) is the most common environmental seal. Another common seal is a plastic or rubber disk bonded to the nozzle thermal liner at or just aft of the throat. A variation of the latter design is a disk located between the aft throat thermal liner and the forward exit thermal liner, as in figure 37(b).

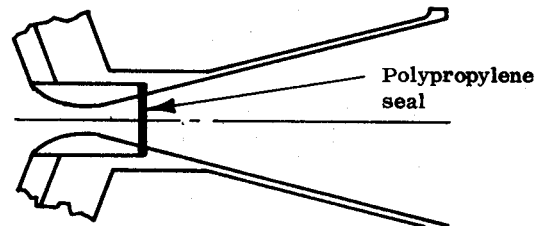
The igniter-platform closure (fig. 37(c)) places concentrated loads on the nozzle where it is attached. These additional loads must be considered in the design of the nozzle structure.

The flow-restrictor closure (fig. 37(d)) has the greatest effect on nozzle design and requires the most care in design. This closure is designed to restrict the flow during ignition to cause more rapid buildup of motor pressure, and then be ejected cleanly after serving its purpose. The pressure within the nozzle prior to ejection of the closure — and the loads thereby created — are in some designs the highest loads to which the nozzle is subjected during firing. Thus the loads imparted by the closure may be the critical design requirement for the nozzle structures.

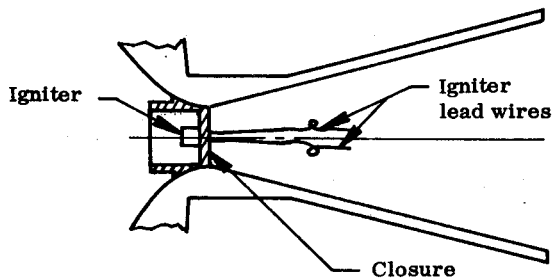
Design of the closure release mechanism often is a difficult task, since premature release can prevent proper ignition and late release can result in motor overpressurization and failure.



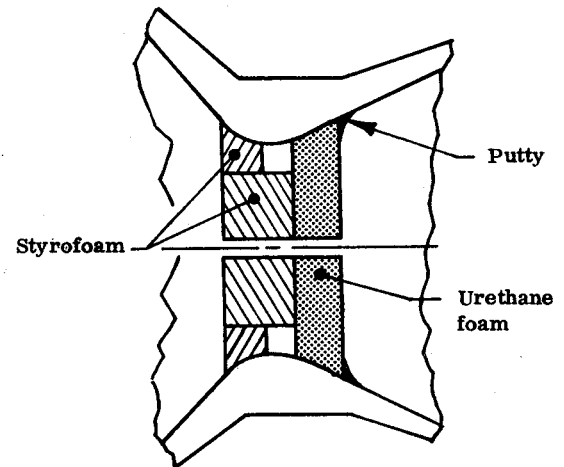
(a) Snap-on cover environmental seal



(b) Integral environmental seal



(c) Igniter platform



(d) Flow restrictor

Figure 37. - Types of nozzle closures.

2.3 NOZZLE ANALYSIS

Analysis of the nozzle is comprised of both aerothermal and structural analyses. Aerothermal analysis encompasses definition of combustion-product thermodynamic properties and composition, transport-properties determination, aerodynamic analysis (both theoretical and experimental), heat-transfer analysis, and material-response analysis. Structural analysis encompasses prediction of stress distribution, calculation of structural deflection, and prediction of thermal-mechanical effects.

2.3.1 Aerothermal Analysis

The techniques generally employed in the aerothermal analysis of solid rocket nozzles are illustrated in figure 38. First, a thermochemical analysis provides (1) input needed for flow-field and subsequent material-response analysis and (2) transport properties for later use in thermal analysis. Next, an inviscid-flow-field analysis is performed to provide input needed for the viscous-flow-field analysis that yields the boundary-layer properties. Flow-field theoretical analysis may be supplemented with experimental analysis such as water-table or cold-flow simulation. The values obtained in these analyses are then applied in thermal analysis, which consists of heat-transfer and material-response analyses. The theoretical analyses are often supplemented with experimental thermal analysis, preferably test firing of the nozzle.

The type of nozzle, the complexity of the design, the design philosophy, and the similarity to previous designs dictate how rigorous the analysis need be. Each step of the analysis is discussed in some detail in the following sections.

2.3.1.1 THERMOCHEMICAL ANALYSIS

A thermochemical analysis of the propellant exhaust products is necessary to determine the thermodynamic properties and composition. From the basic propellant formulations and chamber pressure, these parameters can readily be determined for equilibrium- or frozen-composition gas expansion by the method of Zeleznik and Gordon (ref. 82) or by the methods of references 83 through 86. These techniques are based on conservation of mass, Dalton's Law of Partial Pressures, adiabatic combustion, and an isentropic combustion process. The enthalpy, heat of formation, and free-energy data can be obtained from a current file of JANAF data (ref. 87). The species system usually is set to allow every gaseous species to be in the system of products selected from the thermodynamic file. Gaseous or liquid species are allowed to change phase at equilibrium temperature. Further discussion of the analysis is contained in reference 9.

The thermodynamic properties and chemical composition thus obtained are used in the aerodynamic and material-response calculations.

2.3.1.2 TRANSPORT-PROPERTY ANALYSIS

From kinetic theory (ref. 88), the viscosity, thermal conductivity, and self-diffusion coefficients for the pure components of the gas mixture can be calculated. In addition, the viscosity, thermal conductivity, binary diffusion coefficients, and Prandtl number of the gas mixture can readily be determined (refs. 89 through 92). For the most common propellants these properties have been determined and are documented; therefore, it is necessary to determine properties only when new propellant formulations are being considered.

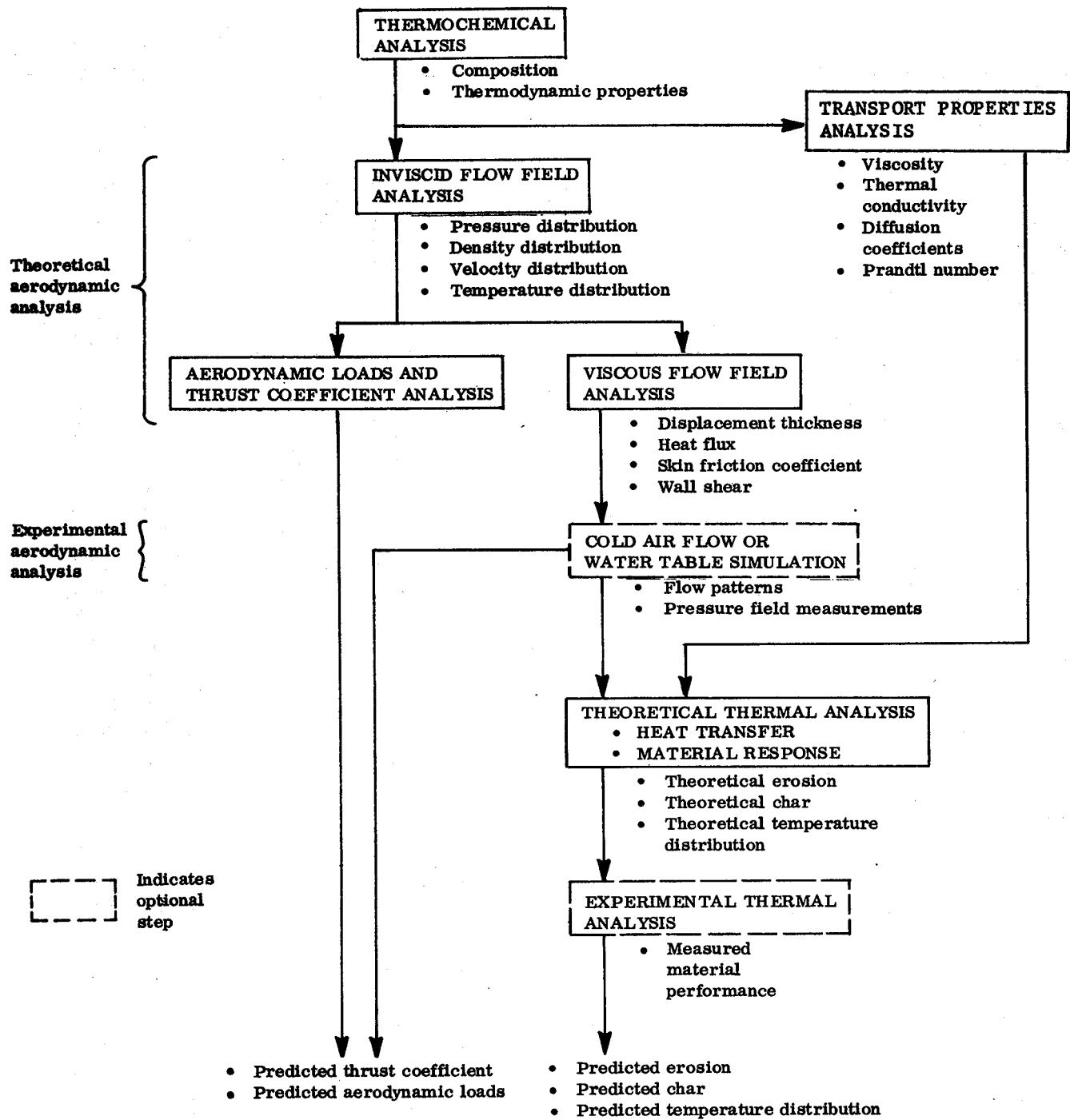


Figure 38. - Steps in aerothermal analysis of a nozzle.

Three programs – EST3, GASKET, and ACE (refs. 93, 94, and 95) – currently are widely used for this analysis. EST3 considers only diffusion-controlled reactions; GASKET, only kinetic-controlled. ACE incorporates subroutines from both EST3 and GASKET and therefore considers both types of reactions. In addition, ACE considers melt-layer reactions (e.g., those with silica/phenolic) and has the capability to perform thermochemical calculations as described in section 2.3.1.1.

2.3.1.3 THEORETICAL AERODYNAMIC ANALYSIS

Aerodynamic analysis of rocket nozzles involves calculation of the inviscid flow properties. These properties are then used to calculate the viscous flow field from which the convective heat-transfer coefficient is determined. These properties are also needed to calculate the nozzle thrust coefficient and the aerodynamic loads.

2.3.1.3.1 Inviscid Flow Field

The inviscid flow field normally is divided into three distinct regions that must be analyzed to determine flow velocities and pressures necessary for calculating aerodynamic loading as well as the viscous-flow properties. Nozzles having a smooth continuous inlet and exit contour and a small convergent half-angle ($< 45^\circ$) usually can be adequately analyzed with one-dimensional isentropic-flow theory (ref. 96). In other words, if the wall contour is such that nonuniform localized acceleration or deceleration of the flow or flow separation will not occur, one-dimensional theory yields reasonable results.

Nozzles that do not meet the above criteria (e.g., submerged nozzles, most movable nozzles, and supersonic-splitline nozzles) are analyzed more rigorously in one or more of the three flow regions: subsonic flow, transonic flow, and supersonic flow.

Subsonic flow. – The subsonic-flow region of more complicated nozzle inlets can readily be analyzed by potential-flow theory. Computer programs for calculating the inviscid, steady-state flow field use a relaxation solution of the finite-difference equations in terms of the stream function (ref. 97). Compressibility effects are considered by providing a density correction at each mesh point in the flow field.

Arbitrary boundaries can be set with very few restrictions. Mass addition (from burning or ablation) can also be considered along any boundary as a gradient in the stream function. This capability is particularly useful where the propellant surface is close to the nozzle inlet. Flow properties such as flow velocity, flow angle, pressure ratio, and Mach number can be determined along any specified streamline. The inviscid flow field at the edge of the boundary layer can thus be defined such that the viscous flow field can be calculated.

Transonic flow. — The transonic-flow region (Mach 0.8 to 1.2) cannot be analyzed by potential-flow theory. However, with entrance contours that accelerate the flow uniformly, extrapolation in the transonic range yields adequate results. If the flow, as indicated by potential-flow analyses, is accelerated to sonic velocity an appreciable distance upstream of the geometric throat (more than 0.15 throat diameters), extrapolation becomes unreliable, and a transonic-flow analysis is necessary.

An analysis technique developed by Hopkins and Hill (ref. 98) develops the transonic flow field for a prescribed velocity distribution along the centerline. Steady, isentropic, irrotational flow and constant specific-heat ratio are assumed. An iteration on wall geometry and centerline velocity distribution is performed until the desired wall geometry is obtained. This technique yields the inviscid flow properties at the wall that are required for calculation of the viscous flow field. In addition, a sonic line that can be used to initiate the analysis of the supersonic-flow regime is established.

Supersonic flow. — For thermal-analysis purposes, one-dimensional theory is often adequate for defining wall conditions in the supersonic-flow field. However, for accurate performance prediction, more accurate definition of the inviscid flow field is required. Numerous computer programs for supersonic-flow analysis have been developed and are available throughout government and industry (refs. 99 and 100). Most of these programs rely on the method of characteristics for solution.

Nozzle systems that control the thrust vector by creating a flow disturbance in the supersonic region (e.g., secondary injection, supersonic splitline) also are difficult to analyze adequately with one-dimensional theory. If a more sophisticated performance calculation is required, an axisymmetric, two-phase, perfect-gas performance program (ref. 100) and a one-dimensional, two-phase, reacting-gas nonequilibrium performance program (ref. 101) are available. These programs require specification of the propellant, relaxation rates, and nozzle geometry.

Analysis of the flow field in supersonic-splitline or secondary-injection nozzles requires handling of the shock waves generated by the TVC system. A method-of-characteristics program presented in reference 99 provides a shock-wave solution from which the flow properties along the wall in the plane of the disturbance can be calculated. For supersonic-splitline nozzles, flow properties on each side of the nozzle can be determined by analyzing each side separately. Assuming a pressure variation between corresponding points on either side of the nozzle and performing a pressure area integration yields a reasonable prediction of aerodynamic loads.

The flow field in a secondary injection nozzle can be analyzed in a similar manner. However, it is first necessary to define the injection plume under the influence of the motor exhaust gases. This definition can be accomplished with the method-of-characteristics program mentioned previously (ref. 99). The plume shape is then handled as a solid wall and a characteristics solution is obtained for the supersonic flow field.

2.3.1.3.2 Viscous Flow Field

In a solid rocket nozzle, the boundary layer generally is turbulent in the critical areas for analysis. It is, however, common practice to check the Reynolds number to verify turbulent flow.

A boundary-layer solution developed by Elliott, Bartz, and Silver (ref. 102) is widely accepted in the solid rocket industry. This method provides for simultaneous solution of the integral momentum and energy equations. The displacement thickness, convective and radiant heat flux, skin friction coefficient, and the wall shear can be determined by this method. Another widely used boundary-layer solution is the ARGIEBL program presented in reference 103.

Solutions for a turbulent boundary layer have also been developed by D. R. Bartz (ref. 63). The simplified Bartz solution is adequate for rough sizing calculations, but should not be used when more exacting analysis is desired.

Reference 104 compares various boundary-layer solutions. In most cases, the results were similar, and selection of a particular solution is left to the analyst.

The viscous flow properties can thus be defined throughout the subsonic, transonic, and supersonic portions of the nozzle. However, if separation and reattachment occur (e.g., on the backside of deeply submerged nozzles or in the splitline region of supersonic-splitline nozzles), it is necessary to restart the boundary layer at the reattachment point, and conditions must be modified to account for reattachment heating in this region.

Purely analytical techniques for describing the flow in the separated region are not adequately developed. A semi-empirical technique (ref. 97) yields reasonable results for separation occurring in the aft case region of the motor and reattaching on the backside of the nozzle. Techniques for analysis of a separated region in the supersonic flow field also are not yet developed. However, in most cases, interpolation between the separation and reattachment points yields reasonable results.

2.3.1.4 EXPERIMENTAL AERODYNAMIC ANALYSIS

Two methods of flow simulation are used extensively in the rocket industry: water tables and cold-gas flow. Water tables have the advantage of low cost and are particularly valuable for investigating separated-flow regions. Data obtained with water tables are chiefly qualitative; however, some users have developed techniques for obtaining quantitative velocity and pressure distributions. Water tables are particularly useful for obtaining insight into complex flow patterns (refs. 105 through 110).

Cold-gas simulation testing has been used to approximate the flow characteristics of solid propellant exhaust gases in the aft case and nozzle region. The cold-flow model can be designed to provide simulation of the nozzle, propellant, and aft case geometry. The effluxing propellant surface can be simulated by using a perforated metal to simulate the grain; perforations are located to match the percentage distribution of the propellant mass flow. Examples of cold-flow test programs are described in references 11, 12, 111, and 112.

Subsonic, transonic, and supersonic flow regimes – all can be analyzed by cold-flow simulation. However, in the transonic and supersonic regimes, the Mach-number probes cannot be utilized. A good approximation of the Mach number can be calculated from the measured pressure ratio.

Cold-flow simulation requires that the cold-flow model simulate the geometry, Mach number, and Reynolds number of the actual nozzle. However, in supersonic flow the variation in specific heat ratio becomes significant, and more careful analysis is required. For subsonic flow, geometrical and Mach-number similitude can be achieved by direct scaling. It is common practice to match the Reynolds number at either the propellant port or the nozzle throat by varying the total pressure of the test runs. Mach-number probes installed in critical areas can yield the flow direction as well as the Mach number. In addition, static-pressure taps and flow-visualization smears can be used to define the flow characteristics.

Measured data obtained in cold-flow simulation can be used to calculate the viscous flow properties for input to the thermal analysis. By varying the grain configuration to simulate grain burnout, flow characteristics can be determined at various burn times such that interpolation can be achieved. This allows for description of flow conditions, heating rates, and erosion patterns throughout the firing.

Because of difficulty in scaling particle size and distribution, two-phase flow generally is not simulated in cold-flow tests.

2.3.1.5 THEORETICAL THERMAL ANALYSIS

Thermal analysis of a solid rocket nozzle requires (1) defining the heat transfer between the exhaust gases and the nozzle liner materials, and (2) calculating the thermal response of these materials.

2.3.1.5.1 Heat Transfer

Heat transfer between the exhaust gases and the nozzle wall occurs through convection, radiation, and particle impingement. In the supersonic flow regime, heat transfer is primarily

convective. Calculation of the convective heat-transfer coefficient was discussed previously (sec. 2.3.1.3.2) and is considered further below.

The effective values of emissivity and source temperature are somewhat uncertain. The radiation effect of aluminum oxide in two-phase flow generally is evaluated by extending the method of analysis for isothermal particle clouds (ref. 113). The method predicts unit emissivity for most of the solid propellants that contain an appreciable amount (5 percent) of aluminum; however, the predicted value can be less than unity for small motors or for very low pressures, so the assumption of unit emissivity is not uniformly valid (ref. 114). It was found by direct measurement that the total heat flux at the nozzle throat is correlated by the same empirical relationship for both aluminized and nonaluminized propellants (ref. 115). At lower Mach numbers (Mach < 0.8), the convective heating is reduced, and it is necessary to consider radiative heating to obtain agreement with empirical results. In the subsonic flow regime, however, the assumption of unit emissivity does yield reasonable results.

Particle-impingement heating also is significant in the subsonic range but need not be considered in most applications in the transonic and supersonic flow regimes. Particle-impingement calculations require definition of the gas flow field by aerodynamic analysis. The velocity and direction of individual particles are then traced through the nozzle by use of the second law of motion and an approximate drag law for various-size particles (ref. 116). The mechanism that causes an accelerated removal of nozzle material in areas of particle impingement is not well understood. The analytical solution of this problem is presently inadequate, so allowances for this effect are made on the basis of measured data from previous firings.

Convective heat-transfer coefficients normally are calculated by the methods discussed in section 2.3.1.3.2. These techniques pertain to a nondegrading surface. In cases where mass is injected into the boundary layer by decomposing ablating walls, the heat-transfer coefficients are modified by a "blowing constant" that is determined experimentally by a correlation between predicted and measured data:

$$\frac{St}{St_D} = 1 - a B' \quad (8)$$

where

St = local Stanton number

St_D = Stanton number for zero blowing

a = blowing-rate constant

B' = blowing-rate parameter, a quantitative measure of the species that can react with carbon.

Values for the blowing-rate constant a normally lie in the range from 0.2 to 0.4 (refs. 117 and 118).

The variation in flow distribution induced by the geometry of the propellant grain perforation can result in a substantial difference in the convective heat-transfer coefficient, and this difference will be reflected in the predicted erosion.

2.3.1.5.2 Material Response

Effective design of solid rocket nozzles that are cooled by heat sink or ablative techniques requires prediction of the effects of high-temperature combustion products on candidate nozzle materials. When subjected to exhaust gases, these materials may respond through a number of mechanisms, including mechanical erosion, chemical erosion, vaporization, melting, and charring. In common usage, however, the term "erosion" refers to all surface recession regardless of the mechanism.

Numerous techniques are available for predicting response of materials exposed to the severe environment of solid rocket exhaust gases; however, the CMA and ASTHMA computer programs (refs. 117 and 118) are the accepted industry standards. The CMA program for charring-material thermal response and ablation (ref. 117) is used to analyze portions of the nozzle where axial temperature gradients are not significant; this condition exists with charring type materials, which have low conductivity. The low-erosion throat-insert materials have higher thermal conductivities and significant axial heat fluxes and therefore require more accurate analysis.

The two-dimensional axisymmetric ASTHMA program for predicting transient temperature response (ref. 118) provides more accurate analysis. With ablative materials, the heat of ablation must be included; this can be accomplished by increasing the specific heat of the material over the charring-temperature range. This technique is extremely useful for preliminary design analysis in programs that are severely limited in time and allowable cost.

The program in reference 119 also provides sophisticated analysis of ablating nozzle materials. This program considers all of the thermal-response mechanisms mentioned above. Surface recession either by melting and vaporization (the predominant recession mode with siliceous materials) or by surface chemical reaction and vaporization (the predominant recession mode with carbonaceous materials) is permitted. Melt flow is governed by the surface shear-stress gradient. The vaporization mode includes thermochemical

decomposition to gaseous products. The heterogeneous chemical reaction rates may be controlled by a combination of mass transfer and surface chemical kinetics. The output parameters calculated with this program are the char profile, the erosion profile, and the in-depth temperature profiles as a function of time. This "2-D ABLATE" program is considerably more difficult and costly to use than the 2-D axisymmetric transient-temperature (ASTHMA) program and does not lend itself to short-duration preliminary analysis.

Three-dimensional methods for analysis of axisymmetric nozzles are under development. These techniques are not yet adequate and, even when fully developed, may be impractical in most design applications because of the computer expense required.

2.3.1.6 EXPERIMENTAL THERMAL ANALYSIS

Nozzle firing tests, usually instrumented as discussed in reference 120, are often performed to verify a design and to provide material characteristics and property data for use in analytical prediction. Full-scale tests are always preferable to subscale tests, since possible inaccuracies in scaling data are precluded; however, the cost of full-scale tests may be prohibitive. Subscale tests to acquire the data at less expense are often suggested; however, very critical examination of the costs versus benefits of subscale testing is usually in order. When subscale tests are performed in support of a design, two designs must be produced and analyzed (subscale and full), two sets of drawings issued, two procurements conducted, two nozzle-fabrication learning processes paid for, and the cost of analytically scaling the data must be borne. Furthermore, it must be recognized that scaled data are always somewhat questionable. Subscale programs often have been more expensive than anticipated when problems that did not exist with the full-scale design developed with the subscale design; expenses thus were incurred to solve subscale problems not relevant to the full-scale design. In other cases, conditions in the full-scale nozzle not predictable from subscale tests led to nozzle failure (ref. 121).

It is likely that up to a throat diameter of 18 in., development test firing of the full-scale nozzle is more cost effective than subscale development firings, because the duplication of effort discussed above is eliminated. In designs with very small margins of safety, failure is somewhat probable on the first full-scale tests. To avoid such a failure (which would involve loss of most of the data), testing with a reduced propellant charge has been used in such a manner that only the duration of the firing is reduced while pressure and flowrate are kept at full-scale values. The reasoning is that reliable data can be obtained (only duration must be extrapolated) and incipient failure (if the nozzle is underdesigned) determined from data analysis, with risk of failure virtually eliminated. In very large nozzles, full-scale tests are prohibitively expensive, and designers must resort to subscale tests.

When subscale tests are conducted, the nozzle configuration and material system of the full-scale nozzle are simulated as closely as practical in the subscale design. Additionally, the

propellant composition and grain design are selected to obtain similar flow characteristics in the subscale and full-scale nozzle approach region. From the subscale-nozzle test data for surface erosion and char depths, analytical techniques are used to predict the performance of the full-scale nozzle. When temperature-measuring instrumentation is used in the subscale test, the data enable prediction of the temperature gradient in the liner of the full-scale nozzle.

Since material erosion in the regions of particle impingement and separated flow cannot be treated adequately theoretically, test results on subscale nozzles can provide correlation coefficients that supplement the analytical model in predicting material erosion and the temperature gradient of the full-scale nozzle. From the measured erosion of the subscale nozzle, correlation coefficients are derived for input into the ablation computer program to predict the material erosion of the full-scale nozzle. The correlation coefficients take into account thermal-transient and size effects.

The most common methods currently used to predict material erosion are the program in reference 117, and, to a lesser extent, programs (the chief use of which is to predict pyrolytic graphite erosion) based on kinetically controlled reactions.

The program of reference 117 often overpredicts material erosion, so empirical adjustments are necessary. Two adjustments (refs. 122 and 123) are based on the results of firing subscale test nozzles and on the calculated surface heat flux. Another method (ref. 71) adjusts predicted and measured subscale data on the basis of comparative mass-transfer coefficients and surface temperatures.

As discussed (sec. 2.2.2.2), for preliminary design purposes a simplified method is available for calculating instantaneous erosion rate experienced by the same material in two nozzles different in size. Approximation methods are used to account for different propellant composition, density, pressure, and diameter or size. For different propellant compositions, the mass fraction of the total oxidizing species is determined for each propellant. The erosion rate for carbonaceous material is then adjusted by the direct ratio of the mass fraction, while no correction for chemical composition is necessary for silica material. For the same material with different densities, the erosion rate is taken as inversely proportional to the density. Bartz's approach (ref. 63) is used to adjust heat-transfer and mass-transfer coefficients for differences in pressure and diameter, on the assumption that the heat of ablation is independent of heat flux. This simplified method, however, does not account for the starting transient. Since this method calculates the instantaneous erosion for a constant pressure and diameter, inaccuracies can be introduced when the method is applied over a long duration and either pressure or diameter changes significantly.

2.3.2 Structural Analysis

Relatively recent advancements in structural analytical techniques in conjunction with the electronic computer have provided means by which very detailed predictions of the structural behavior and integrity of complex nozzle components can be made.

In general, there are three major areas of concern in a typical solid rocket motor nozzle:

- (1) The stress distributions in the basic structural shell of the nozzle induced primarily by internal pressure, ejection (blowout), TVC side loads, and differential thermal expansion of components in contact with the shell.
- (2) The deflections of the structure in the area of the splitline of movable nozzles produced by movement of the flexible joint or other movable-nozzle element.
- (3) The mechanical stresses and strains induced in liner and insulation materials by the thermal gradients normally associated with hot-gas flow.

Analysis of nozzle structures is accomplished almost universally with computerized finite-element methods supplemented by computerized finite-difference methods for shell structures. A great number of computer programs are available; reference 124 is an excellent guide to the capability and availability of the various structural-mechanics computer programs. Two groups of programs are considered to be industry standards: (1) the series AMG-032, -033, and -045 covered in references 125 and 126, and (2) the SAAS III program of reference 127 and its modifications. Both groups of programs are in extensive use under other computer program names, since many analysts have modified these basic programs to fit particular needs.

The AMG-032 program has the capability to consider an axisymmetric isotropic continuum and orthotropic shells. AMG-033 has the capability to consider a planar isotropic continuum and orthotropic shells perpendicular to the plane of analysis. AMG-045 has the capability to consider an axisymmetric isotropic continuum and orthotropic shells; also, it considers nonsymmetric loads, whereas AMG-032 and -033 are limited to symmetric loads. Post-yield analysis commonly is performed with these programs by an iteration process in which the moduli of the elements are modified.

SAAS III has the capability to consider an axisymmetric isotropic continuum, orthotropic shells, and, unlike the AMG programs, can handle post-yield analysis (sometimes called elastic-plastic analysis) automatically.

Other finite-element programs in common use for nozzles are DOASIS (ref. 128), which has capabilities similar to SAAS III but uses a different post-yield theory, and NASTRAN (ref. 129), which is more general than the structural analysis programs discussed above in that it can handle 3-D problems, dynamic problems, and a variety of other types of structures.

The two most widely accepted finite-difference programs are BOSOR 3 (ref. 130) and STAGS (ref. 131). Both programs are capable of the analysis of orthotropic layered shells under nonuniform loading, and both have stability-analysis capability not found in the finite-element programs discussed above. In addition, BOSOR 3 has capability for dynamic-response analysis, and STAGS can handle 3-D problems in nonlinear geometric response.

Finite-element analytical techniques repeatedly have demonstrated that they provide accurate prediction of mechanical stresses in a pressure vessel. Predicted stress has been correlated with strain-gage data obtained from hydrostatic proof test of the pressure vessel. As an example, in reference 132 the measured and predicted stresses throughout the motor case and nozzle shell generally agreed within 10 percent except in areas of high discontinuity stresses.

The correlation of calculated thermally induced stress with measured stress is less impressive, mainly as a result of a lack of reliable thermal and mechanical values for materials at elevated temperature. Analytical procedures to determine the thermal stress accurately are available, but the reliability of the input elastic properties presently is not consistent with the method of analysis. The analytical results, however, can be used to identify critical areas and to guide the designer to corrective action in the event of a problem. An example is contained in reference 133, where the analysis indicated a high maximum strain in the exit-cone liner near the material changeover location, the result being a negative margin of safety. As a consequence of this high strain, interlaminar separation at the interface of the two different materials was deemed probable. Test results of nozzles with similar designs showed delamination at the interface but with no apparent detriment to the nozzle performance. These test results lend validity to the analytical technique.

2.4 NOZZLE QUALITY ASSURANCE

Nozzle quality is assured by good process controls, nondestructive testing, destructive sample testing of components, and leak testing of the nozzle assembly. In addition, movable nozzles are vectored while pressurized.

Nondestructive testing such as X-ray, alcohol wipe, ultrasonic, dye penetrant, and hardness testing generally is performed on all components. Reinforced-plastic composites usually are subjected to X-ray (tangential) and alcohol wipe; no cracks are allowed, and delaminations and voids are limited to specific sizes depending on part size and location of the defect. Graphites normally are subjected to 100-percent X-ray inspection and 100-percent dye-penetrant inspection; no cracks are allowed, foreign inclusions are limited to few in number with none penetrating the surface and none in a region that erosion might reach, and voids are limited to six times the average natural void size. Elastomeric materials are checked for hardness and subjected to X-ray; no voids, delaminations, or foreign inclusions are allowed. Metal components are normally subjected to dye penetrant, magnetic particle, X-ray, or ultrasonic test, with no cracks allowed. All critical welds are subjected to 100-percent X-ray inspection.

Destructive sample testing usually is accomplished by one of three methods: (1) random selection and destructive testing of one actual component of every so many produced (1 of 20 is typical); (2) destructive testing of an excess part of the component or "tag end"; or (3)

destructive testing of an extra test slab of component material that has been processed with a batch of components (e.g., hydroclaved with them or heat treated with them). Method (1) has the advantage that an actual part is tested; it has the disadvantages of expense and the statistical probability that a part not tested is bad. Method (2) has the advantage that a test is conducted for each part, but it is questionable that the tag end is truly representative of the part; end effects in processing may change the properties. Method (3) likewise is questionable as to whether the test slab is truly representative. Method (1) is practical only in production quantities; therefore, methods (2) and (3) normally are used in concept-demonstration programs. If factors of safety are large, destructive testing often is not included in test and development programs.

The destructive tests usually performed on plastics include density, volatile content, resin content, acetone-soluble content, tensile strength and modulus, compressive strength and modulus, interlaminar shear, hardness, flexure strength, and modulus. Tests for density, compressive strength, and tensile strength are performed on graphites. Metals are checked for density, hardness, tensile and compressive strength, modulus, percent elongation, and percent reduction of area. Metal quality assurance is covered in more detail in reference 81.

Leak testing of nozzle assemblies usually is conducted as part of a motor leak check at pressures typically in the range of 30 to 50 psia. The throat is plugged for this test. Nozzles sometimes are tested at full pressure prior to installation on the motor. Movable nozzles are vectored while at full pressure to ensure sealing by the dynamic O-ring and to measure dry torque to check for abnormal values (ref. 2).

Reference 134 reports tests of the effects of selected defects on nozzle performance.

3. DESIGN CRITERIA and Recommended Practices

3.1 DESIGN REQUIREMENTS AND CONSTRAINTS

The definition of design requirements and constraints shall be sufficiently accurate and complete to enable the nozzle design to proceed with a minimum number of iterations.

Each of the following parameters is required for nozzle design. The recommended practice for obtaining each value (when the choice is the designer's) follows each item.

Design pressure. — Use MEOP if known; if not, estimate it as 110 percent of the maximum pressure in the predicted trace if it is known, or as 120 percent of average pressure otherwise. Maximum and average pressure should be those corresponding to the maximum grain temperature during operation.

Predicted pressure-time trace. — Assume a constant pressure trace at the average pressure level for the duration of firing. Average pressure and duration must be provided to the designer.

Propellant properties. — Use properties specified; if none, assume the known chamber temperature, thermodynamic constants, and corrosion characteristics of a propellant used for a similar vehicle application.

Throat size. — Must be provided to the designer.

Acceptable change in throat size. — Limit throat area increase during firing to not more than 25 percent.

Envelope limits. — Must be provided to the designer.

Expansion ratio. — If the thrust coefficient is specified, choose the expansion ratio that corresponds to the thrust coefficient and the exit configuration as specified; otherwise, use the following guides: for test nozzles, the expansion ratio at which predicted exit-plane pressure equals ambient; for flight nozzles, an expansion ratio of 7 to 10 for first-stage and single-stage low-altitude vehicles, and 15 to 80 for upper-stage and high-altitude vehicles. With fixed nozzles, limit the exit-plane outside diameter to the case diameter; with movable nozzles, limit the exit-plane diameter to provide adequate clearance with the specified envelope when the nozzle is in the hard-over position, the motor being pressurized or unpressurized (whichever condition governs).

Exit configuration. — When motor length and performance are not critical, use a 15° half-angle cone if throat diameter is less than 10 in.; use a 17.5° cone otherwise. When motor length and performance are critical, use a contoured nozzle with a 25° initial angle and a 13° exit angle.

Nozzle submergence (submerged nozzle only). — Submerge to the extent that the throat plane is at the same axial location as the case-to-nozzle interface.

Design vector angle or TVC side-force requirements (movable nozzles only). — Use 4° to 6° for the first stage of a multistage vehicle, and 2° to 4° for upper stages. Select the vector angle for other applications on the basis of specific experience.

Diameter of interface with case. — Use the smallest opening compatible with the nozzle.

Weight, cost, reliability, and development-time guidelines. — Estimate by reference to the most nearly similar previous design. Minimize weight insofar as practical without use of exotic technologies or materials. Limit reinforced plastic and aluminum structures to 100° F temperature rise, steel to 300° F, and titanium to 1000° F.

Production quantity and rate. — Must be provided to the designer.

Storage and operating ambient environment. — Should be provided to designer. If not, assume an environment from knowledge of the motor application.

3.2 NOZZLE CONFIGURATION AND CONSTRUCTION

3.2.1 Aerodynamic Design

3.2.1.1 ENTRANCE

The entrance design shall suit the type of nozzle and satisfy the propulsion system requirements.

A submerged entrance should be selected if the propulsion system is length limited or if the nozzle is a movable, integral type. An external convergent-cone entrance should be selected if cost minimization is the primary consideration or if it is desirable to eliminate the possible specific impulse loss associated with a submerged entrance.

3.2.1.1.1 Submerged

The entrance geometry of a submerged nozzle shall induce approximately uniform acceleration and an acceptable erosive environment.

In general, the expansion ratio at the leading edge should be 3.0 or more, and the leading edge should be located at least one throat radius forward of the throat plane. The leading edge and throat should be joined by an ellipse, a hyperbolic spiral, or a series of tangent arcs that approximate the ellipse or spiral in order to obtain uniform flow acceleration and thereby achieve a more nearly uniform entrance erosion profile.

Entrances with expansion ratios as low as 1.5 and as short as 0.42 throat radius can probably be developed successfully if the performance penalty and increased erosion are acceptable; however, hardware development trial-and-error iterations should be expected.

3.2.1.1.2 External

The entrance geometry of an external nozzle shall balance length minimization and erosion control.

For most designs, a convergent-cone entrance with half-angle between 30° and 60° should be selected as a good compromise between length minimization and erosion minimization. Forty-five degrees is preferable; it is more-or-less standard and makes comparisons to other nozzles more tenable. Inlet angles of 45° and less are more amenable to analysis than larger ones. Erosion increases with the steepness of the angle, however, and since this effect is exaggerated at high pressures, shallow angles (< 30°) should be used for maximum erosion control and for all high-pressure designs.

3.2.1.1.3 Blast Tube

The blast tube geometry shall minimize the nozzle envelope and shall be consistent with an acceptable flow environment for the nozzle splitline where applicable.

For fixed nozzles, subsonic-splitline movable nozzles, and supersonic-splitline movable nozzles, the inside surface of the blast tube should generally be cylindrical in order to minimize weight and cost. For integral movable nozzles, the blast-tube diameter should be selected so that the one-dimensional Mach number at the nozzle splitline is not greater than 0.15.

Flow-straightening blast tubes for four-nozzle systems should be designed experimentally as described in references 18 and 19.

3.2.1.2 THROAT REGION

The throat region geometry shall provide smooth transition from subsonic to supersonic flow, predictable erosive conditions, and – when feasible without performance penalty – ease of fabrication and alignment.

The cross section of the upstream and downstream approaches to the throat should be arcs of no less than 0.5 throat radius. Larger radii (1 to 2 throat radii) should be used when the weight, cost, and length penalties incurred are acceptable. Even larger radii should be used when they can provide a smoother transition to entrance or exit sections designed for special requirements such as movable-nozzle TVC.

A short cylindrical section at the throat aids nozzle alignment and fabrication and should be incorporated if no penalties are incurred.

3.2.1.3 EXIT

The exit geometry shall maximize performance without violating length, weight, or cost constraints.

Conical exit. — Conical exits are recommended for designs in which the smaller cost of the cone is significant (as is often the case with high production rates), for concept-demonstration nozzles, and for motor-test nozzles.

For production nozzles, the half-angle selected should be optimum for the design altitude and throat-to-exit length as determined by the method described previously.

Conical exits with a standard half-angle (15° up to 10-in. throat diameter, and 17.5° beyond) are recommended for concept-demonstration and motor-test nozzles in which exit configuration is not a test variable; this practice will help isolate the effects of the variables under test and also reduce cost by simplifying design and by permitting possible reuse of existing fabrication tooling.

Contoured exit. — Contoured exits are recommended for lightweight production nozzle designs in which performance maximization is paramount, since a 0.5 to 1.0 percent improvement in delivered specific impulse likely can be realized over a conical exit of the same length. In addition, in length-limited systems, a contoured nozzle will minimize nozzle length for a given delivered specific impulse level; cost and weight difference usually are less important, unless the exit incorporates honeycomb structure. A contoured exit will experience greater erosion near the exit plane than will a conical exit, and this difference must be considered in the weight tradeoff.

Circular arcs, parabolas, and streamlines of method-of-characteristics flow-net contours — all have been shown to improve performance in comparison with conical exits of the same length. The benefit of the variation among these contours is not established; therefore, it is recommended that the choice of curve be the shape for which the designer has accumulated experimental data, so that performance can be predicted with confidence.

The initial divergence angle should be limited to a maximum of 32° . With propellants containing 15 to 20 percent aluminum, the difference between the initial and exit angles should be less than 12° , as experimental data indicates poor delivered specific impulse performance with greater curvature. With lower percentages of aluminum, greater curvature is allowable.

3.2.2 Thermal Design

3.2.2.1 THROAT INSERT

The throat insert shall possess adequate structural and thermal-structural properties and an erosion rate consistent with the desired thrust-time trace.

Polycrystalline graphite, pyrolytic graphite, and tungsten throat inserts should receive first consideration in smaller nozzles. Reinforced plastics, particularly graphite-cloth/phenolic and carbon-cloth/phenolic, have formed the throats of most nozzles with a throat diameter exceeding 10 in. and should receive first consideration for large nozzles. Carbon/carbon composites should be considered when erosion resistance approaching that of polycrystalline graphite is needed without the limitations of polycrystalline graphite. Ceramics and cooled throats should not be considered except for further exploratory development. In all cases, the nozzle designer and grain designer must work in coordination to establish a mutually agreeable erosion rate for the throat insert.

Polycrystalline graphite. — Polycrystalline graphite should be restricted to the throat, blast tube, throat approach, and throat extension of flight nozzles, and, in general, limited to nozzles of less than 8-in. throat diameter. Above this nozzle size, this material should be regarded as developmental, and the test budget increased accordingly. Graphite sections should be segmented into rings to reduce stresses and provide escape paths for pyrolysis gas. To allow for thermal growth, the design must incorporate an unfilled gap or a gap filled with a material that pyrolyzes at low temperature (600° F or less).

The imperfect capability to analyze graphite (for the reasons given previously) should be taken into account in budgeting a test program.

Because of its low cost, polycrystalline graphite should always be considered for test nozzles when the weight of thick sections is acceptable.

Pyrolytic graphite. — Pyrolytic graphite is recommended for the throat insert when greater erosion resistance and greater strength than can be obtained with polycrystalline graphite or carbon/carbon is required. Stacked washers are the recommended form. In general, for maximum resistance to delamination, individual washers should be not more than 3/8-in. thick. To effect economy in procurement of the washers, it is recommended that the overall height of the washer stack rather than the thickness of each washer be specified.

To provide for thermal growth in the axial direction, the design must incorporate an unfilled expansion gap or a gap filled with a material that pyrolyzes at low temperatures (600° F or less). Polycrystalline graphite or carbon/carbon is recommended fore and aft of the washer pack so that it may act as a heat sink and limit differential erosion, since formation of erosion steps contributes to delamination and reduces nozzle efficiency.

Use of pyrolytic graphite throat inserts should be treated as developmental when throat diameter exceeds 15 in.

Refractory metals. — Tungsten or tungsten alloys are recommended when minimum throat erosion is required. For propellants with flame temperature up to approximately 6000° F, pure or thoriated tungsten is recommended. For economy, use extruded stock up to the maximum diameter available (ca. 3 in.); above this diameter, forged stock is recommended. For flame temperatures in and above 6000° to 6500° F range, or for reduced sensitivity to thermal shock, silver- and copper-infiltrated tungsten should be considered.

The design must incorporate provisions for axial and radial thermal growth. The possibility of reduction of throat area due to possible inward thermal growth of the tungsten should be evaluated carefully, so that design provisions to prevent motor overpressurization can be made when necessary.

Tungsten surfaces that mate with carbonaceous materials should be coated with tantalum or thoria to prevent formation of a low-melting-point eutectic. Heat treating of finished tungsten components is recommended as a means to reduce sensitivity to thermal shock.

Use of tungsten in diameters larger than 7.5 in. must be treated as developmental.

Carbon/carbon composite. — Carbon/carbon materials should be selected in preference to polycrystalline graphites if the erosion rate of the carbon/carbon is acceptable. For throat diameters above 8 in., carbon/carbon should be selected over graphite/phenolic or carbon/phenolic for better erosion resistance if the higher cost is acceptable.

3.2.2.2 THERMAL LINER AND INSULATOR

The thermal liner and insulator shall, within weight, cost, and envelope constraints, adequately control erosion and limit structural temperatures to acceptable levels.

It is recommended that, for the initial design, erosion be estimated by scaling, material-by-material, from the most nearly similar tested nozzle; use the method of Bartz (sec. 2.2.2), with an additional correction made for propellant corrosivity if the liner is carbonaceous. A margin of safety on erosion depth of not less than 0.2 is recommended in the throat and entrance, and not less than 0.1 in the exit. Greater margins should be applied if the test parameters of the nozzle from which the erosion was scaled are significantly different from those of the new design, if the material is not well qualified, or if weight is not critical. A margin of 1.0 is recommended for nozzles for man-rated systems.

It is recommended that char depth be estimated with the corrosion analogy (sec. 2.2.2.2) or scaled from a similar firing. A separate margin of safety on char depth is not recommended, since erosion and char depth are somewhat compensatory. If the erosion depth is greater than predicted, char normally is less than predicted, because the erosion process absorbs heat and reduces the input to the charring process.

Bond gaps between cured thermal components should be 5 to 30 mils, the larger gaps in larger nozzles. Epoxy adhesive systems are recommended.

The interface between adjacent liner materials should parallel the ply angle of the more erosion-resistant material (which is, also, almost always the more expensive material). The interface should contain a step, preferably cylindrical, between the predicted char depth and the inner surface of the structure.

If the liner is backed with an asbestos/phenolic insulator, vent holes 0.060 in. to 0.100 in. in diameter on 3/4 to 1-in. centers should be drilled through the exit liners to the depth of the expected char line in the asbestos/phenolic insulator. Die-molded exit liners of all materials should be drilled to the expected char depth with a similar drill pattern.

3.2.2.2.1 Liner Materials

The liner material shall, within the weight, budget, and envelope constraints, control erosion within allowable limits.

Standard Reinforced-Plastic Liners

Graphite-cloth/phenolic, carbon-cloth/phenolic and carbon/carbon materials should be considered first for the throat insert of nozzles with throat diameters above 15 in. and traded against the more-erosion-resistant throat inserts for smaller sizes. These materials should be considered for the blast tubes, throat approaches, and throat extensions (forward exit liners) in nozzles of all sizes. In all cases, a trade study considering cost, reliability, vehicle performance, and similar parameters should be conducted to select the best materials.

Graphite-cloth/phenolic should be selected over carbon-cloth/phenolic if control and reproducibility of erosion is paramount; carbon-cloth/phenolic should be selected if cost or strength is paramount or if the liner material is also to serve as insulator. Carbon/carbon (free standing without insulator or structure) should be considered for reducing nozzle weight and/or improving strength-to-weight ratio.

Silica-cloth/phenolic should generally be selected as the thermal liner in the aft exit cone. In nozzles for low-pressure operation (800 psi or less), this relatively-low-cost material often provides adequate erosion resistance beyond an expansion ratio of about 2 to 4. At expansion ratios larger than 8, glass-cloth/phenolic may be acceptable; however, silica should be selected if erosion control is paramount, whereas glass should be selected if cost or strength is paramount. Allowance should be made for an erosion depth just downstream of the interface approximately double the depth that would be predicted in the silica or glass at this point if the entire exit liner were silica or glass.

If the erosive environment is relatively mild (e.g., on the chamber side of a submerged nozzle), asbestos-felt/phenolic as both liner and insulator should be considered rather than silica or glass. Currently, the asbestos felt/phenolic offers both economy and minimum weight, but increases in asbestos costs could reduce its economic advantage.

Tape-wrap, layup, and die-molding methods of fabrication should be traded off and selected on the basis of the property differences discussed below.

Tape wraps and layups. — Edge orientation to the flow should be specified when erosion resistance is paramount, and a small downstream angle to the flow specified when heat transfer through the material is to be minimized. To prevent peeling, liners generally should not be oriented exactly parallel to the flow.

Tape wrap should be selected if the desired orientation can be obtained. Straight tape should be given first consideration for economy if the ply angle to the flow that results from wrapping parallel to the centerline is acceptable. In many exit cones, parallel-to-centerline orientation represents an excellent compromise among economy, erosion resistance, and heat-transfer limitation and should always be considered. Bias tape should be considered next. The formula in section 2.2.2 serves as a guide to the limits of tape wrapping capability.

If the desired orientation is unobtainable with tape wrap, the flat-laminate, stacked-cone, and rosette layups should then be considered in that order. Stacked-cone layups should be greater than 15° to the axis.

Rosette orientation should be specified if the geometry of the part is such that some short tape or stacked cone plies would erode entirely away by the end of the firing. The rosette eliminates this problem.

In general, critical reinforced-plastic parts (throat, throat approach, throat extension, and all parts with very tight thermal, structural, performance, and weight design margins) should be hydroclave cured. For economy, less critical parts such as aft exit liners should be autoclave cured.

Post cure of reinforced-plastic parts is recommended as a means to reduce volatiles and relieve residual stresses. The surface resin glaze should be removed prior to post cure.

Die moldings. — Die molding of reinforced-plastic parts is recommended when economical quantity production of small and moderately sized parts is desired or when existing dies are suitable, if the required properties can be obtained. Tape wrapping is more economical for very large parts (16-in. diam. and up).

In comparison with tape-wrapped or layup parts, die-molded parts generally have lower strength, poorer erosion resistance, and poorer erosion reproducibility; these differences must be taken into account in the design. In general, die-molded parts are not recommended for the throat or for designs in which weight minimization is primary.

Nonstandard Reinforced-Plastic Liners

Use of plastics and fabrication methods different from those discussed previously must be treated as developmental for lightweight designs. These methods and materials should be considered, however, for concept-demonstration and test-motor nozzles. Canvas-cloth/phenolic in particular is worthy of consideration, as are the "double thick" standard materials. Oven cure of components, either at ambient pressure or with pressure applied by overwrap, merits consideration. Low-cost carbonaceous materials and castable and trowelable materials should be considered for test-motor nozzles.

3.2.2.2. Insulator Materials

The insulator material shall, within the weight, budget, and envelope constraints, limit the structural temperature to allowable levels.

As noted previously the liner and insulator may be a single material, the insulator and structure a single material, or all three a single material.

A separate insulator backing a thermal liner should be specified if the reduction in envelope obtainable with the superior insulation properties of the insulator is required, if the cost of a separate insulator is less than that of a liner thickened to serve also as insulator, if the insulator has structural properties superior to the liner and also is to serve as structure, or if the added safety of a separate insulator (should a delamination open up the liner) is deemed

desirable. Similar considerations should be applied in choosing a separate or combined structure. When a separate insulator is indicated, composite cure of the liner and insulator is recommended.

Reinforced plastics. — If maximum insulation properties are desired, a layup or tape-wrapped reinforcement with the plies perpendicular to the heat-transfer path should be specified. Slight compromise of this optimum orientation can be allowed, however, for economy in fabrication. Wrapping parallel to the thermal-liner back surface or parallel to centerline usually will reduce costs.

Further cost reduction by die molding of insulators should always be examined. Die molding should always be given first consideration unless the superior strength of a layup part is required.

Filled elastomers. — Filled elastomeric insulators are suitable as combined thermal liner and insulator in nozzle regions where the Mach number is less than 0.2 (e.g., on the chamber side of a submerged nozzle).

For economy in fabrication, trowelable, ambient-curing elastomers can be used for low-Mach-number regions of test nozzles.

Many elastomers, however, are not suitable for nozzles that will be stored or operated at low temperatures (e.g., in space). The designer must recognize this limitation.

Either die molding or layup followed by autoclave cure is recommended for the fabrication of elastomers for flight designs. The choice should be economic.

Ambient-curing trowelable elastomers should be used only for test-motor nozzles.

3.2.3 Structural and Mechanical Design

3.2.3.1 BASIC NOZZLE STRUCTURE

The nozzle structure shall be adequate for the most critical load requirement, all sources of loads and combinations of loads being considered.

The most critical design requirement may be strength limitation, deflection limitation, stability limitation, or economic limitation. Each component should be examined with respect to each possible critical limitation.

In general, in structural analysis of a nozzle, the following loads should be thoroughly evaluated:

- Loads due to internal pressure and flow
- Loads due to the thermal environment
- Loads imposed by nozzle actuation devices
- Inertial loads imposed by thrust and guidance maneuvers.

Maintain a checklist such as that presented in section 2.2.3.1, so that no load source can be overlooked.

Safety margins in a specific nozzle design should reflect the design philosophy of the overall system influenced by the following factors:

- The amount of analytical effort budgeted in the design and analysis phase
- The degree of characterization available for the elastic, thermal, and erosional properties of materials being used
- The similarity of the basic design to previous successful designs with respect to materials and geometry.

The lack of similarity to previous designs should be thoroughly compensated for by increased analytical effort that has been verified by experimental means or test data. Use of all experience that can be made applicable by analytical techniques will substantially reduce the development effort in a new nozzle design.

In general, when loading is well defined and strength is the critical design requirement, minimum factors of safety of 1.15 to 1.25 are recommended. If stability or deflection is the critical requirement, minimum factors of 1.25 to 1.50 are recommended.

3.2.3.2 STRUCTURAL MATERIALS

The structural materials shall, within the weight and envelope constraints, provide adequate structural properties at lowest cost.

Steel, aluminum, and glass composites should be considered first, because of their relatively low cost and extensive use history. Among these, aluminum and glass composites should be considered first (aluminum for entrance and throat, glass composite for exit) if the critical requirement is strength, as these materials have a better strength-to-weight ratio than steel. If stability or deflection is the critical requirement, steel is first choice because of its higher modulus.

If the structural components are expected to undergo a moderate temperature rise, steel usually is a better choice than aluminum or fiberglass because its properties do not decay as severely with increasing temperature. For greater temperature rises, titanium is recommended because it retains its strength better at high temperature than either aluminum or steel. Titanium also has a higher strength-to-weight ratio than either steel or aluminum and therefore should be considered when weight is critical, even if no structural temperature rise is expected.

For operation at very high temperature, structural tungsten, molybdenum, columbium, or various high-temperature alloys may be warranted despite their high cost.

In nozzles with exit diameters in excess of 100 in., honeycomb exit structure may provide the needed stability at lower weight than other structural materials.

Metallic structures must be protected against corrosion, especially if dissimilar metals are joined and moisture is present. Aluminum should be anodized on exposed surfaces but not on surfaces to be bonded (sec. 3.2.3.3). Steel and other metals should be protected by painting. Dissimilar metals should be isolated at joints, and corrosion-resisting joiners such as cadmium-coated bolts should be used.

3.2.3.3 ADHESIVES, SEALANTS, AND SEALS

Adhesives, sealants, and seals shall preclude gas leakage and provide adequate bonding between components.

Because of their extensive use history, epoxy adhesives that cure at room temperature should be first choice for adhesive or sealant. Adhesives that cure at high temperatures should be limited to the smaller nozzles, where development of high cooldown stresses is not a problem.

Adhesive bonds should not be depended on for retention of liner and insulator components. An additional mechanical retention system (e.g., pins through the structure) should be provided.

Adhesive gaps between components should be in the range 0.005 to 0.030 in. With the exception of stacks of pyrolytic graphite washers, all interfaces between components should be filled with sealant. If pressurization of an interface would lead to nozzle failure because of either thermal load or the resulting pressure-area load, then an O-ring seal should also be provided to seal the interface.

All surfaces to be bonded must be thoroughly cleaned, particularly aluminum surfaces, which should be acid etched by bath or by paste cleaning. Aluminum bonding surfaces

should not be anodized or, as an alternative, the anodized layer should be removed by grit blasting prior to bonding.

For maximum reliability, O-rings should be designed with a diametral rather than an axial squeeze. Provide a means to keep the O-ring free of adhesive during assembly, or cut the O-ring groove after the adhesive has cured. As a minimum, coat the O-rings lightly with grease to keep adhesive from bonding to them.

3.2.3.4 ATTACHED TVC SYSTEM

Designs for use with LITVC shall provide the special attachment and structural reinforcement required by this type of TVC system.

Use a circumferential metal ring that incorporates the mounting pads at the injection location. This ring should be stiff enough to withstand the side loads created by injection and limit the nozzle distortion produced by the side load to an acceptable value. If the nozzle is submerged, this injection ring and the nozzle-to-case attachment flange should be continuous, as in figures 18 and 34, or tied together with a conical metal structure. If the injection system is to be supported structurally by the nozzle, an additional circumferential ring between the injection ring and nozzle-to-case attachment flange may be necessary, as in figure 34.

With some injectants, the thermal liner must be compatible with the injectant to prevent excessive loss of the liner due to chemical reaction. The nozzle liner at and downstream of the injection ports should be silica/phenolic if the injectant is nitrogen tetroxide, and carbon/ or graphite/phenolic if it is strontium perchlorate; if the injectant is Freon, the injectant should not influence the liner choice. The path through the liner from the injector to the exhaust-gas interface similarly should be lined with silica/phenolic when the injectant is nitrogen tetroxide. Either silica/ or carbon/phenolic may be used with strontium perchlorate, because the perchlorate is relatively nonreactive until heated by the exhaust gas.

For all injectants, the liner must be thickened upstream of the injection ports, where the shock front forms, and from the ports to the exit plane, because liner loss will increase over that occurring in a firing with no injection. The added thickness necessary is a function of TVC duty cycle, but should not exceed a maximum of 25 percent. Base the increase on past experience with the same injectant. In a development and test program, test firings should be conducted both with and without injection, and the injection duty cycle varied. Compare the erosion to obtain a basis for predicting the probable erosion increase as a function of duty cycle.

3.2.3.5 MOVABLE-NOZZLE TVC SYSTEM

Designs incorporating flexible-joint TVC shall provide for the special load transmission and reaction requirements of this type of TVC system and provide adequate thermal protection for the flexible joint.

A folding elastomeric boot (fig. 35(a)) is sufficient thermal protection for the flexible-joint element if the expansion ratio at the boot is 10 or greater. If the expansion ratio is significantly less than 10, then it is recommended that the boot be supplemented with a protective cowl and splitline, as in figure 4, 19, and 35(b). Integral thermal protection (fig. 35(c)) is recommended if the flexible joint is made with composite rather than with metallic reinforcements.

The movable structure of the nozzle must be reinforced to react the side loads produced by vectoring and the point load applied by the actuator. A circumferential reinforcing ring is recommended at the point of application of the actuator load to react this load and to limit distortion of the exit. The acceptable distortion will depend on the stresses developed in the exit materials. The magnitude of the distortion depends on the location of the flexible-joint pivot point. If the pivot point is forward (fig. 4(a)), the actuator moment arm is relatively long, so the actuator force tending to produce nozzle distortion is small; an aft pivot point, however, with a shorter moment arm, (fig. 4(b)) requires a large force to overcome flexible-joint torque, and thus distortion of the nozzle is more likely.

The flexible-joint end rings must carry the nozzle ejection load as well as the side loads. Normally, sizing the rings to carry the ejection load and to fit the flexible-joint geometry ensures sufficient capability for side loads.

The nozzle fixed structure must react the actuator and side loads also. In general, the thickness of structure required for the internal pressure loads ensures capability for withstanding side and actuator loads.

3.2.3.6 NOZZLE-TO-CHAMBER ATTACHMENT

The nozzle-to-chamber attachment shall maintain the integrity of the nozzle-to-chamber interface under all motor operating and test conditions.

With respect to use, nozzles can be classified as motor-test, concept-demonstration, or flight type. For motor-test and concept-demonstration nozzles, low cost and ease of assembly and disassembly are primary considerations; simple methods such as shear pins, shear plates, shear bolts, retaining collar, segmented rings, or band clamps are recommended.

For flight designs, bolted, threaded, snap-ring, key, and lockwire joints should be traded off. For an interface diameter of 14 in. or more, the bolted joint is recommended; between 10

and 14 in., a threaded joint should also be considered unless components attached to the nozzle must be circumferentially oriented; below 10 in., snap-ring, key, and lockwire joints as well as bolted and threaded joints should be considered. The tradeoff among the various joints should consider the advantages and disadvantages previously discussed.

3.2.3.7 NOZZLE CLOSURES

In keeping with the intent of design, the nozzle closure shall, without adverse effect on the nozzle, serve as an environmental seal, an igniter platform, or a flow restrictor.

A snap-on cover (fig. 37(a)) is recommended as an environmental seal closure; it is simple and low in cost. The disk bonded between nozzle components (fig. 37(b)) has the advantage that it is an integral part of the design, but the disadvantage of difficult replacement in case of accidental puncture.

The igniter platform and flow-restrictor types of closures (figs. 37(c) and (d)) produce additional loads on the nozzle that must be considered in the structural design of the nozzle. Attention must also be given to provisions to ensure that the ejection of the closure does not damage the nozzle surfaces.

3.3 NOZZLE ANALYSIS

3.3.1 Aerothermal Analysis

3.3.1.1 THERMOCHEMICAL ANALYSIS

The thermochemical analysis shall identify the chemical composition and thermodynamic properties of the propellant exhaust mixture.

The thermodynamic properties and exhaust composition needed for subsequent material-response calculations should be determined by an established method. The method in reference 82 is recommended for either equilibrium- or frozen-composition assumptions. Use reference 87 to obtain data on enthalpy, free energy, and heat of formation.

3.3.1.2 TRANSPORT-PROPERTY ANALYSIS

The transport-property analysis shall identify the viscosity, thermal conductivity, diffusion coefficients, and Prandtl number of the propellant exhaust mixture.

When established propellants are used, obtain the transport properties from published data. When new propellant formulations are considered, determine the required properties by means of the EST 3, GASKET, or ACE programs (refs. 93, 94, and 95).

3.3.1.3 THEORETICAL AERODYNAMIC ANALYSIS

3.3.1.3.1 Inviscid Flow Field

The inviscid-flow-field analysis shall provide all flow-field properties required for calculation of the viscous-flow field.

Subsonic flow. — Nozzles with a convergent cone entrance of less than 45° half-angle and continuous geometry can be analyzed aerodynamically by one-dimensional isentropic-flow theory.

Entrances other than simple convergent cones should be analyzed by potential-flow theory as described in reference 97. If potential-flow theory (or experience) indicates a separated region of flow, a momentum-balance technique as described in reference 97 should be applied.

Transonic flow. — If the entrance contour produces relatively uniform acceleration, and if Mach 1.0 as predicted by potential-flow theory is reached less than 0.15 throat diameters upstream of the throat, then extrapolation of the potential-flow conditions through the transonic region normally is sufficiently accurate. If this is not the case, a more refined transonic analysis as presented in reference 98 is recommended.

Supersonic flow. — One-dimensional isentropic-flow theory will sufficiently define the supersonic flow field in most cases, particularly for conical exits up to 20° half-angle, for purposes of thermal analysis, aerodynamic-load calculation, and thrust-coefficient calculation. The method of characteristics as described in reference 99 defines the flow field more accurately and is recommended for all contoured nozzles and for conical nozzles with a half-angle greater than 20°.

The axisymmetric, two-phase, perfect-gas program (ref. 100) and the one-dimensional, two-phase, reacting-gas nonequilibrium program (ref. 101) are recommended for more sophisticated analysis. Flow fields containing shocks produced by TVC can be analyzed best with the computer program of reference 99.

3.3.1.3.2 Viscous Flow Field

The viscous-flow-field analysis shall define all properties necessary for the calculation of the convective heat-transfer coefficient.

The method of Elliott, Bartz, and Silver (ref. 102) or the ARGIEBL computer program (ref. 103) is recommended for calculation of properties of a turbulent boundary layer. The Bartz simplified solution (ref. 63) is recommended for rough sizing calculations.

3.3.1.4 EXPERIMENTAL AERODYNAMIC ANALYSIS

Experimental aerodynamic analysis, matching the flow conditions of the nozzle as closely as is practical and performed for geometries not amenable to theoretical analyses, shall define the properties necessary for calculation of the convective heat-transfer coefficient, aerodynamic loads, and aerodynamic efficiency.

Complex nozzle geometries, especially where flow separation is likely (e.g., in the splitline region of movable nozzles), cannot be analyzed accurately by theoretical methods and are better characterized by experimental methods. Two alternate techniques are available: cold-gas flow simulation, and water-table flow simulation. Cold-gas flow simulation should be given first consideration, since it more closely matches actual propellant exhaust flow.

The model geometry, Reynolds number at the throat, and Mach number throughout should match closely. The model should be as close to full scale as the cold-flow facilities will allow. Mach-number probes should be used in the subsonic region, and static-pressure taps and flow-visualization smears should be applied throughout the model. Aft case and grain geometry as well as the nozzle itself should be simulated in the model.

Water-table analysis is recommended as a less expensive (and less accurate) tool to develop an insight into flow patterns, particularly in separated-flow regions.

3.3.1.5 THEORETICAL THERMAL ANALYSIS

3.3.1.5.1 Heat Transfer

The heat-transfer analysis shall identify the heat transfer to the nozzle materials through convection, radiation, and particle impingement.

In the supersonic flow regime, the heat transfer is primarily convective. For most purposes, it is adequate to consider only the convective heating in this region. The convective heat-transfer coefficient should be determined by use of the boundary-layer procedure recommended in section 3.3.1.3.2.

If separation and reattachment occur in the supersonic portion of the nozzle, the effect of heating downstream of reattachment should be evaluated by restarting the boundary layer

at the point of reattachment. This practice will provide adequate definition of the convective heating downstream of the reattachment. However, analytical tools are not adequate for defining reattachment heating. It is therefore recommended that this region be further evaluated empirically.

Heat-transfer analysis of subsonic and transonic flow requires that radiation heating and particle-impingement heating as well as convective heating be considered. In the nozzle inlet, the radiant heating normally constitutes 25 to 50 percent of the total heating. In this case, use of an effective emissivity of 0.8 will account for all heating other than convective. Heating on the backside of submerged nozzles is nearly all radiative; therefore, an emissivity of 1.0 is recommended.

When complex grain designs (e.g., star) are combined with submerged nozzles, particle channeling down the axial slots can produce increases of as much as 300 percent in entrance erosion. Adjustments must be made in the heat-transfer assumptions to allow for this effect.

3.3.1.5.2 Material Response

The material-response analysis shall predict material recession and char and verify the integrity of the nozzle design.

The one-dimensional CMA technique of reference 117 is recommended for basic analysis of charring materials such as the various reinforced phenolics. The ASTHMA program in reference 118 should be used for more detailed analysis of charring materials and for analysis of noncharring materials.

3.3.1.6 EXPERIMENTAL THERMAL ANALYSIS

Test firings of the actual nozzle or of a test nozzle simulating the actual configuration and materials as closely as practical shall verify the integrity of the nozzle.

For throat diameters up to 18 in., full-scale testing of nozzles is recommended as most cost effective. If thermal, structural, performance, or weight design margins are very tight, a reduced propellant load is recommended, so that pressure, aerodynamic load, and flowrate are matched but duration is reduced. In this manner, incipient failure can be detected and appropriate design modifications made.

When the nozzle is very large, subscale testing is recommended as most cost effective. When subscale tests are conducted, the flow conditions of the subscale and full-scale nozzles must be matched as closely as practical.

3.3.2 Structural Analysis

The structural analysis shall verify the structural and thermal-mechanical integrity of the nozzle design.

The degree of analytical structural evaluation must be commensurate with the design complexity, risk philosophy, and program budget. All nozzle designs should be subjected to an evaluation of the basic structural shell and attachment flanges. This effort normally should consist of a simple compatibility analysis, with internal pressure loading applied. If the design is very similar in materials and geometry to previous successful designs, or if it is a heavy, conservative test design, then much of the thermal-mechanical analysis may be deleted. Even on the more conservative designs, if noncharring materials are included, it is recommended that analyses be performed for at least two critical conditions during firing. The first critical condition is the "thermal shock" condition, which typically occurs during the first few seconds of firing and is a result of the severe thermal gradients initially developed. The second critical condition from the standpoint of structural integrity occurs near the end of action time just before the pressure decays. At this time, all components are at the maximum temperature they will reach under load, and erosion and char are maximum.

Other critical conditions can occur; e.g., when external aerodynamic loads and TVC loads combine. Each condition should be evaluated at 4 or 5 critical stations; usually the critical stations are the throat, the nose of submerged nozzles, the inlet section, and various stations in the exit cone.

One of the major difficulties associated with all thermal-mechanical analyses is the lack of good material-property data. However, this lack should not deter the application of the finite-element analytical technique. Adequate estimates of properties can be made from data on similar classes of materials and, even when gross assumptions must be made, the technique has still proven very valuable as a qualitative tool when it is used to compare new designs with previously successful designs analyzed under the same assumptions.

When non-axisymmetric loading is applied to the nozzle shell, the techniques available for evaluation in general are quite complex and in a large majority of instances are of consequence only in the local area where the loads are applied to the nozzle shell. These effects usually can be evaluated with the basic structural techniques for point loads, moments, etc.

3.4 NOZZLE QUALITY ASSURANCE

Nozzle quality assurance shall verify that the nozzle components and assembly are built as designed and are free of unacceptable defects.

Good process controls as developed through experience in the various government and industry production and development programs are the best guarantee of quality. Checks of the adequacy of quality control by destructive and nondestructive testing are recommended as follows:

Nondestructive Testing

Reinforced-plastic composites. — Radiographic (X-ray) inspection (tangential) and complete alcohol wipe; no cracks allowed; delaminations and voids severely limited.

Graphites. — Radiographic inspection and complete dye-penetrant inspection; no cracks allowed; foreign inclusions not allowed if they penetrate the surface or are within the predicted erosion depth; voids limited to six times the average natural void size.

Elastomers. — Hardness and radiographic inspection; voids, delaminations, and foreign inclusions severely limited.

Metals. — Radiographic, magnetic particle, ultrasonic, and complete dye-penetrant inspection; one-hundred-percent radiographic inspection of critical welds; no cracks allowed. Hydrotest of nozzle metal shells should be considered.

Nozzle assembly. — Leak check on motor at 30 to 50 psia with throat plugged and, for movable nozzles, also test while vectoring at full pressure prior to installation on the motor.

Destructive Testing

The most reliable results are obtained if a representative number of randomly selected actual components are destructively tested. If the budget does not allow this kind of testing, second choice is testing of tag ends. Third choice is testing of separate test slabs processed with actual components.

Tests recommended for reinforced-plastic composites are density, volatile content, resin content, acetone-soluble content, tensile strength and modulus, compressive strength and modulus, flexure strength and modulus, interlaminar shear, and hardness.

Tests recommended for metals are density, hardness, tensile and compressive strength, modulus, percent elongation, and percent reduction of area. Metal quality assurance is covered in detail in reference 81.

APPENDIX A

GLOSSARY*

The nomenclature used in the preceding text basically is that presented in "Solid Propulsion Nomenclature Guide" (ref. 135). The guide should be reviewed for complete coverage of recommended solid propulsion symbols and subscripts; only those used in this monograph are presented below.

<u>Symbol</u>	<u>Definition</u>	<u>Appears in</u>
A	(1) empirical constant (2) wrap angle, deg	eq. (4) eq. (7)
a	blowing rate constant	eq. (8)
B	empirical constant	eq. (4)
B'	blowing rate parameter	eq. (8)
C _{F del}	delivered thrust coefficient	eq. (2)
C _{F vac}	vacuum thrust coefficient with no divergence loss	eq. (2)
CVD	chemical vapor deposition	text
D	inside diameter of part being tape wrapped, in.	eq. (7)
D _t	throat diameter of nozzle being designed, in.	eq. (3)
D _{tm}	throat diameter of nozzle in which erosion rate was measured, in.	eq. (3)
HGTVC	hot gas thrust vector control	text
ksi	1000 psi	tables II, III, and IV
L	throat-to-exit length, in.	fig. 27
LITVC	liquid injection thrust vector control	text
L/R _t	ratio of throat-to-exit length to throat radius	fig. 27

*Divided into three sections: Symbols, Material Designations, and Organization Abbreviations.

<u>Symbol</u>	<u>Definition</u>	<u>Appears in</u>
m	empirical constant	eq. (4)
MEOP	maximum expected operating pressure of motor, psi	text
NDT	nondestructive testing	text
P _{amb}	ambient pressure, psi	eq. (2)
P _c	chamber pressure, psi	eqs. (2) and (3)
P _{cm}	chamber pressure of motor in which nozzle erosion rate was measured, psi	eq. (3)
P _e	theoretical static pressure of exhaust gas at exit plane, psi	eq. (2)
Q	cold wall heat flux, Btu/(ft ² ·sec)	eqs. (4), (5), and (6)
R _t	nozzle throat radius, in.	fig. 27
St	local Stanton number	eq. (8)
St _D	Stanton number for zero blowing	eq. (8)
t _a	thickness allowed for erosion, in.	parameter $\frac{t_a - t_e}{t_e}$
t _e	expected erosion depth, in.	parameter $\frac{t_a - t_e}{t_e}$
TVC	thrust vector control	text
W	tape width, in.	eq. (7)
X	char depth, in.	eqs. (4), (5), and (6)
α	nozzle-divergence half-angle, deg	eq. (1)
γ	ratio of specific heats	fig. 27
ε	expansion ratio	eq. (2)

<u>Symbol</u>	<u>Definition</u>	<u>Appears in</u>
θ	firing duration, sec	eqs. (4), (5), and (6)
λ	divergence loss factor, $\lambda = \frac{1 + \cos \alpha}{2}$	eqs. (1) and (2)
ξ	tape-wrapping-capability index	eq. (7)

<u>Material¹</u>	<u>Identification</u>
AP	ammonium perchlorate
C-103	columbium-based alloy containing Hf, Ti, and Zr
Dacron	trade designation of E.I. duPont de Nemours & Co. for a polyester fiber made from polyethylene terephthalate
elastomer	polymersical material that at room temperature can be stretched to approximately twice its original length and on release return quickly to its original length
epoxy	thermosetting resin widely utilized as an adhesive and as a binder in the fabrication of glass-filament/resin composites
Freon 114-B2	trade designation for dibromotetrafluoroethane manufactured by E.I. duPont de Nemours & Co.
Haynes alloy	designation of certain cobalt- and nickel-base high-temperature alloys manufactured by Stellite Division of Cabot Corporation
HMX	cyclotetramethylene tetranitramine
Kevlar	trade designation for an aromatic polyamide fiber manufactured by E.I. duPont de Nemours & Co.
NBR	butadiene acrylonitrile rubber
NC	nitrocellulose

¹ Additional information on metallic materials herein can be found in the 1972 SAE Handbook, SAE, Two Pennsylvania Plaza, New York, N.Y.; in MIL-HDBK-5B, Metallic Materials and Elements for Aerospace Vehicle Structures, Dept. of Defense, Washington, D.C., Sept. 1971; and in Metals Handbook (8th ed.), Vol. 1: Properties and Selection of Metals, Am. Society for Metals (Metals Park, Ohio), 1961.

<u>Material</u>	<u>Identification</u>
NG	nitroglycerine ($C_3H_5(ONO_2)_3$), an oily explosive liquid obtained by nitrating glycerol
nitrogen tetroxide	N_2O_4 , propellant grade per MIL-P-26539
nylon	generic name for a family of polyamide polymers
PBAA	polybutadiene-acrylic acid polymer
PBAN	polybutadiene-acrylic acid-acrylonitrile terpolymer
PBCT	carboxy-terminated polybutadiene (also abbreviated as CTPB)
PU	polyurethane, any of various polymers that contain -NHCOO- linkages
rayon	any of a group of smooth textile fibers made in filament and staple form from regenerated cellulose or other cellulosic material
rubber	an elastomer, either a synthetic or a natural compound obtained from the hevea brasiliensis tree
Styrofoam	trade designation of The Dow Chemical Co. for expanded cellular polystyrene
Ta-10W	alloy consisting of 90% tantalum and 10% tungsten
Ti-6Al-4V	titanium-aluminum-vanadium alloy per AMS 4906
18%-Ni steel (200 class)	iron-nickel alloy processed to achieve 200 ksi tensile strength
90-percent-dense tungsten	tungsten possessing 90% of the density of the extruded or forged form

ORGANIZATIONS

AFBMD	Air Force Ballistic Missiles Division
AFFDL	Air Force Flight Dynamics Laboratory
AFML	Air Force Materials Laboratory

AFRPL	Air Force Rocket Propulsion Laboratory
AIAA	American Institute of Aeronautics and Astronautics
AIChE	American Institute of Chemical Engineers
ARPA	Advanced Research Projects Agency
ARS	American Rocket Society (now part of AIAA)
ASCE	American Society of Civil Engineers
ASD	Aeronautical Systems Division Wright-Patterson Air Force Base
ASME	American Society of Automotive Engineers
BSD	Ballistic Systems Division (Division of SAMSO)
CPIA	Chemical Propulsion Information Agency
ICRPG	Interagency Chemical Rocket Propulsion Group
IFP	Institute of Fluid Power
JANAF	Joint Army-Navy-Air Force
JANNAF	Joint Army-Navy-NASA-Air Force
JPL	Jet Propulsion Laboratory (California Institute of Technology)
LPIA	Liquid Propulsion Information Agency
NAA	North American Aviation Corp.
NOL	Naval Ordnance Laboratory
SAE	Society of Automotive Engineers
SAMSO	Space & Missile Systems Organization
WADD	Wright Air Development Division Wright-Patterson Air Force Base

APPENDIX B

Conversion of U.S. Customary Units to SI Units

Physical quantity	U.S. customary unit	SI unit	Conversion factor ^a
Density	lbm/in. ³	kg/m ³	2.768x10 ⁴
	gm/cm ³	kg/m ³	1.0x10 ³
Energy	Btu	J	1.054x10 ³
Force	lbf	N	4.448
Heat flux	Btu/(ft ² · sec)	J/(m ² · sec)	1.135x10 ⁴
Length	ft	m	0.3048
	in.	cm	2.54
	mil	μm	25.4
	μ in.	μm	25.4x10 ⁻³
Mass	lbm	kg	0.4536
Modulus (tensile; compressive)	ksi (1000 psi)	N/cm ²	6.895x10 ²
Pressure	psi	N/cm ²	0.6895
Specific heat	Btu/(lbm · °F)	J/(kg · K)	4.184x10 ³
Specific impulse	lbf-sec/lbm	N-sec/kg	9.807
Strength (compressive; shear; tensile; yield)	ksi (1000 psi)	N/cm ²	6.895x10 ²
Temperature	°C	K	K = °C + 273.15
	°F	K	K = $\frac{5}{9}(\text{°F} + 459.67)$
Temperature difference	°F	K	K = $\frac{5}{9}(\text{°F})$

(continued)

APPENDIX B (concluded)

Conversion of U.S. Customary Units to SI Units

Physical quantity	U.S. customary unit	SI unit	Conversion factor ^a
Thermal conductivity	Btu·ft/(hr·ft ² ·°F)	J/(sec·m·K)	1.730
Thermal diffusivity	ft ² /hr	cm ² /hr	9.29x10 ²
Thermal expansion	μ in./(in.·°F)	μ m/(m·K)	1.8
Thrust	lbf	N	4.448

^aMultiply value given in U.S. customary unit by conversion factor to obtain equivalent value in SI unit. For a complete listing of conversion factors for basic physical quantities, see Mechtrly, E.A.: The International System of Units. Physical Constants and Conversion Factors. Second Revision, NASA SP-7012, 1973.

REFERENCES

1. Desjardins, S. P.; and Wilson, J.: Evolution of Omniaxial Movable Nozzle Thrust Vector Control Systems (U). Paper presented at 3d ICRPG/AIAA Solid Propulsion Conference (Atlantic City, NJ), June 4-6, 1968, CPIA Publ. 167, vol. I, April 1968, pp. 257-293. (CONFIDENTIAL)
2. Anon.: Solid Rocket Motor Thrust Vector Control. NASA Space Vehicle Design Criteria Monograph, NASA SP-8114, December 1974.
3. Anon.: Final Test Results, First Stage MINUTEMAN Marquardt Corporation TVC Nozzle MA-103-XDA Using the TU-137-120 Rocket Motor. Rep. TW-217-3-62, Thiokol Chemical Corp. (Wasatch Div.), March 1962.
4. Strome, R. K.: Test Firing of a Supersonic Splitline Nozzle. AFRPL-TR-69-208, Air Force Rocket Propulsion Laboratory, October 1969.
5. Wilson, J. W.: Development of a Flexible Exit Cone Omniaxial Movable Nozzle TVC System. Paper presented at 5th AIAA Propulsion Joint Specialist Conference (Colorado Springs, CO), June 9-13, 1969.
6. Koballer, G. F.: Development of Expandable Rocket Nozzles. Paper presented at 1973 JANNAF Propulsion Meeting (Las Vegas, NV), Nov. 6-8, 1973, CPIA Publ. 242, vol. II, October 1973, pp. 67-85.
7. Carey, L.; and Ellis, R.: Extendible Exit Cone Development for the C4 Third-Stage Motor. J. Spacecraft Rockets, vol. 11, no. 9, September 1974, pp. 624-630.
8. Baker, W. H., Jr.; and Evanoff, P. D.: Development of Extendible Exit Cones for the Trident I (C4) Second Stage Nozzle. Vol. II – Metallic Extendible Exit Cone. Rep. TWR-8108, Hercules/Thiokol Joint Venture, June 15, 1974.
9. Anon.: Solid Rocket Motor Performance Analysis and Prediction. NASA Space Vehicle Design Criteria Monograph, NASA SP-8039, May 1971.
10. Ellis, R. A.: A Step Toward Automation of Nozzle Design. AIAA Paper 69-975, AIAA Aerospace Computer Systems Conference (Los Angeles, CA), Sept. 8-10, 1969.
11. Lund, R. K.: Final Report, Cold Flow Tests, Poseidon C-3 First and Second Stage. Rep. TWR-2320, Hercules Inc. and Thiokol Chemical Corp. (Wasatch Div.), February 1967.
12. Anon.: Final Report, Cold Flow Simulation Studies, Stage I MINUTEMAN Motors, Wing I and Wing II. Rep. TWR-554, Thiokol Chemical Corp. (Wasatch Div.), January 1964.
13. Anon.: 1965 Production Support Program (U), vol. I. BSD-TR-66-361, Hercules Powder Co., June 1967. (CONFIDENTIAL)

- *14. Haigh, W. S.; and Christenson, E. A.: Experimental Studies of the Effects of Solid Rocket Motor Nozzle Immersion and Entrance Shapes (U). Rep. TM-221 SRP, Aerojet-General Corp., May 1963. (CONFIDENTIAL)
- *15. Lund, R. K.; and Ellis, R. A.: Design of Entry Contours of Submerged Nozzles for Solid Rocket Motors. Rep. TWR-2117, Thiokol Chemical Corp. (Wasatch Div.), September 1966.
- *16. Gallas, S. B.; and Christenson, E. A.: Continuation of Aerodynamic Studies of Immersed Nozzle Design Parameters for 2nd Stage MINUTEMAN Wing VI Development. Rep. TM-160 SRP, Aerojet-General Corp., August 1963.
- 17. Crowe, C. T.; Dunlap, R.; Hermsen, R. W.; Wolff, H.; and Wooldridge, C. E.: High-Performance Nozzles for Solid-Propellant Rocket Motors (U). UTC Rep. 2025-FR, United Technology Center, Division of United Aircraft Corp., February 1967. (CONFIDENTIAL)
- 18. Lindsey, J. W.: A Cold Flow Study of Nozzle Feeding in a Four-Nozzle Rocket Case. AFBMD-TR-60, Hercules Powder Co., September 1961.
- *19. Haigh, W. S.: Aerodynamics Cold Flow Investigation of First Stage Polaris Model A-3 Nozzle-entrance and Closure-insulation Configurations. TM No. 197 SRP, Aerojet-General Corp., July 1962.
- 20. Anon.: AUM Propulsion System Design and Tradeoff Study (U). NOL Rep. E51-69, Thiokol Chemical Corp. (Elkton Div.), April 1969. (CONFIDENTIAL)
- 21. Lancaster, C. N.; and Desjardins, S. P.: Investigation of the Effects of Various Nozzle Transition Arc Radius Ratios. Final Report, Contract NAS7-706, Thiokol Chemical Corp. (Wasatch Div.), March 1969.
- 22. Winer, R.; and Morey, L.: Nozzle Design for Solid Propellant Rockets. Paper presented at Solid Propellant Rocket Research Conf., American Rocket Society, Princeton Univ., Jan. 28-29, 1960.
- 23. Thompson, H. D.: Design Procedure for Optimization of Rocket Motor Nozzles. Rep. TM-63-6, Jet Propulsion Center, Purdue Univ., May 1963.
- 24. Rao, G. V. R.: Optimum Thrust Performance of Contoured Rocket Nozzles. Bulletin of the First Meeting JANAF Liquid Propellant Group, vol. I, LPIA, Johns Hopkins Univ., November 1959, pp. 243-259.
- *25. Zeamer, R. J.; and Kimes, D. L.: Contoured Nozzles: Optimum Exit Cone Contour Curvature for Maximum Thrust with Two-Phase Flow and Recommended Design Methods. Rep. 17-10203/4/32/213, Hercules, Inc., October 1966.
- 26. Demuth, O. J.; and Ditore, M. J.: Graphical Methods for Selection of Nozzle Contours. Paper presented at Solid Propellant Rocket Research Conf., American Rocket Society, Princeton Univ., Jan. 28-29, 1960.

*Dossier for design criteria monograph "Solid Rocket Motor Nozzles." Unpublished. Collected source material available for inspection at NASA Lewis Research Center, Cleveland, Ohio.

- *27. Ehlers, F. E.: The Method of Characteristics Applied to the Design of Supersonic Axially Symmetric Nozzles. Mathematical Note No. 179, Document D2-2118, The Boeing Co., August 1957.
- 28. Foelsch, K.: The Analytical Design of an Axially-Symmetric DeLaval Nozzle for a Parallel and Uniform Jet. J. Aeron. Sci., vol. 16, no. 3, March 1949, pp. 161-166 and 188.
- *29. Anon.: Progress Report, Nozzle Contour Program, Rep. UER-373, Thiokol Chemical Corp. (Wasatch Div.), March 1960.
- 30. Ellis, R. A.; and Thomas, D.: Design and Test Results of a High Expansion Ratio Contoured Nozzle for the Surveyor Solid Propellant Retro Thrust Motor. Paper presented at 20th Interagency Solid Propulsion Meeting (Philadelphia, PA), July 13-15, 1964, CPIA Publ. 49B, vol. IV, October 1964, pp. 759-773.
- 31. Ellis, R. A.: Nozzle Efficiency Improvements with Advanced Materials. Paper presented at 1974 JANNAF Propulsion Meeting (San Diego, CA), Oct. 22-24, 1974.
- 32. Welch, H. C.; Kieth, B. C.; Freedman, I. H.; and Zeman, S.: SAM-D Propulsion Development (U). Paper presented at 4th ICRPG Solid Propulsion Meeting (Chicago, IL), May 20-22, 1969, CPIA Publ. 188, vol. I, April 1969, pp. 29-57. (CONFIDENTIAL)
- 33. Anon.: Analysis of the Divergent Section of the Dyna-Soar ARM Nozzle (U). Rep. TW-27-11-62, Thiokol Chemical Corp. (Wasatch Div.), November 1962. (CONFIDENTIAL)
- 34. Lafyatis, P. G.; Waters, C. W.; and Dull, R. B.: Final Report on the Development and Evaluation of Large Scale RVA and CFZ Graphite. AFML-TR-65-183, Union Carbide Corp., July 1965.
- 35. Digesu, F. J.; and Pears, C. D.: The Determination of Design Criteria for Grade CFZ Graphite. AFML-TR-65-142, Southern Research Inst., May 1965.
- 36. Wong, F. Y.: Solid Rocket Nozzle Design Summary. AIAA Paper 68-655, AIAA 4th Propulsion Joint Specialist Conference (Cleveland, OH), June 10-14, 1968.
- *37. Swope, L. M.: Properties of Selected Graphites. Rep. 461, Aerojet-General Corp., June 1963.
- 38. Baskins, Y.; Schell, D. C.; and Sumida, W. K.: Study of the Mechanism of Failure of Rocket Materials and Materials Research. ASD-TDR-62-314, Armour Research Foundation, May 1962.
- 39. Batchelor, J. D.; and Olcott, E. L.: Behavior of Nozzle Materials Under Extreme Rocket Motor Environments. Final Report, Contract NOW-64-393c (AD 467039), Atlantic Research Corp., June 1965.
- 40. Waylett, C. E.; Spring, M. A.; and Carter, M. B.: Research and Development on Advanced Graphite Materials. Vol. XXXI — High Performance Graphite by Liquid Impregnation. AFML-WADD-61-72, National Carbon Co., Div. of Union Carbide Corp., May 1964.

*Dossier for design criteria monograph "Solid Rocket Motor Nozzles." Unpublished. Collected source material available for inspection at NASA Lewis Research Center, Cleveland, Ohio.

41. Swope, L. M.; and Bernard, M. F.: Effects of Solid Rocket Propellant Formulations and Exhaust Gas Chemistries on the Erosion of Graphite Nozzles (U). Paper presented at AIAA Solid Rocket Conference (Palo Alto, CA), January 1964, CPIA Publ. 59, September 1964. (CONFIDENTIAL)
42. Lynch, J. F.; Ungar, E. W.; Bowers, D. J.; and Duckworth, W. H.: Investigation of Nozzle-Failure Mechanisms and of Parameters Affecting Nozzle-Material Suitability in Solid-Propellant Rockets. ASD-TDR-63-738, Battelle Memorial Inst., August 1963.
43. Jablansky, L.: Simulation and Control of Factors Influencing Rocket Nozzle Materials (U). Tech. Rep. DL-TR:1-62, Picatinny Arsenal, February 1962. (CONFIDENTIAL)
44. Armour, W. H.; and Hale, R. M.: Application of Materials to Advanced Rocket Propulsion Systems. AFML-TR-70-26, Philco-Ford Corp., March 1970.
45. Stephen, W. A.: Development of High-Performance Materials for High Chamber Pressure Rocket Motor Application. AFRPL-TR-69-222, United Technology Center, September 1969.
46. Ellison, J. R.; and Zorich, D. R.: High Temperature Evaluation of a Pyrolytic Graphite Coated Throat Insert (U). AFRPL-TR-69-103, Air Force Rocket Propulsion Laboratory, May 1969. (CONFIDENTIAL)
47. Ellison, J. R.; and Zorich, D. R.: Evaluation of Pyrolytic Coated Rocket Nozzle Throat Inserts (Test Nozzles 2 and 3). AFRPL-TR-69-237, Air Force Rocket Propulsion Laboratory, November 1969.
48. Anon.: High Chamber Pressure and Multiple Restart Nozzle Materials Investigation Interim Report (U). AFRPL-TR-70-18, Philco-Ford Corp., February 1970. (CONFIDENTIAL)
49. Batchelor, J. D.; Ford, E. F.; and Olcott, E. L.: Feasibility Demonstration of Pyrolytic Graphite Coated Nozzles (U). AFRPL-TR-65-57, Atlantic Research Corp., March 1965. (CONFIDENTIAL)
50. Olcott, E. L.: Pyrolytic Graphite Coatings for Rocket Nozzles (U). Paper presented at 26th JANNAF Solid Propulsion Meeting (Washington, DC), July 14-16, 1970, CPIA Publ. 196, vol. I, May 1970, pp. 811-819. (CONFIDENTIAL)
51. Payne, W.: Pyrolytic Graphite Coated Throat Inserts. AFRPL-TR-74-42, Air Force Rocket Propulsion Laboratory, August 1974.
52. Hove, J. E.; and Riley, W. C.: Ceramics for Advanced Technologies. Univ. of California Engineering and Physical Sciences Extension Series, John Wiley & Sons, Inc., 1965.
53. Ellison, J. R.: High Chamber Pressure Test Firing of a Wire Wound Tungsten Throat Insert Nozzle (Test No. 6) (U). AFRPL-TR-69-116, Air Force Rocket Propulsion Laboratory, June 1969. (CONFIDENTIAL)
54. Stephen, W. A.: High Chamber Pressure Evaluation of Wire-Wound Tungsten Nozzles (U). AFRPL-TR-69-79, United Technology Center, June 1969. (CONFIDENTIAL)

55. Greening, T. A.; Eppinger, E. D.; and Jacobs, S. M.: Wire Wound Plasma Spray Bonded Tungsten Solid Rocket Nozzle Insert Materials. AIAA Paper 68-536, ICRPG/AIAA 3rd Solid Propulsion Conf. (Atlantic City, NJ), June 4-6, 1968.
56. Anon.: Development and Demonstration of Flightweight Thrust Vector Control Hardware (U). AFRPL-TR-67-262, Thiokol Chemical Corp. (Wasatch Div.), November 1967. (CONFIDENTIAL)
57. Cannon, R. M.: Powder Metallurgy and Infiltration Technology of Self-Cooled Tungsten Rocket Nozzles. AVATD-0099-69-CR, AVCO Corp., March 1969.
- *58. Anon.: Hot-Pressed Tungsten for Rocket Nozzles – Final Report to Aerojet-General Corp., Haynes Stellite Co., April 1961.
59. Steigerwald, E. A.: Failure in Rocket Nozzle Inserts. Rep. ER-6866, TRW Equipment Lab., TRW, Inc. (Cleveland, OH), July 14, 1966.
60. Anon.: Space Program Summary 37-63, vol. III. JPL, Calif. Inst. Tech., June 1970.
61. Ellis, R. A.: Development of a Carbon-Carbon Nozzle for the Trident I C4 Third Stage Nozzle. Paper presented at JANNAF 1973 Propulsion Conference (Las Vegas, NV). Nov. 6-8, 1973, CPIA Publ. 242, vol. I, November 1973, pp. 89-115.
62. Schoner, R. J.: An Evaluation of Prepyrolyzed Plastics for Rocket Nozzle Applications (U). AFRPL-TR-68-203, Air Force Rocket Propulsion Laboratory, November 1968. (CONFIDENTIAL)
63. Bartz, D. R.: A Simple Equation for Rapid Estimation of Rocket Nozzle Convective Heat Transfer Coefficients. Jet Propulsion, vol. 27, no. 1, January 1957, pp. 49-51.
64. McDonald, A. J.; and Headman, P. O.: Erosion of Graphite in Solid Propellant Combustion Gases and Effects of Heat Transfer. AIAA J., vol. 3, no. 7, July 1965, pp. 1250-1257.
65. Barker, D. H.; Kordig, J. W.; Belnap, R. D.; and Hall, A. F.: A Simplified Method of Predicting Char Formation in Ablating Rocket Exit Cones. AIChE Chemical Engineering Progress Symposium Series, vol. 61, no. 59, 1965, pp. 108-114.
- *66. Warga, J. J.; et al.: The Effects of Material and Process Variables on the Properties of Three Carbon Fabric Reinforced Plastic Composites. FM-561, Aerojet-General Corp., Feb. 19, 1965.
- *67. Davis, H. O.; and Warga, J. J.: Mechanism of Failure in Carbon Fabric Reinforced Phenolics as Affected by Raw Material and Process Variables. FM-560, Aerojet-General Corp., September 1964.
- *68. Anon.: Some Special Considerations for Tape Wrapping. Haveg-Reinhold Inc., Oct. 1, 1964.
69. Warga, J. J.; Davis, H. O.; DeAcetis, J.; and Lampman, J. A.: Evaluation of Low-Cost Materials and Manufacturing Processes for Large Solid Rocket Nozzles. AFRPL-TR-67-310 (AD 825495), Aerojet-General Corp., December 1967.

*Dossier for design criteria monograph "Solid Rocket Motor Nozzles." Unpublished. Collected source material available for inspection at NASA Lewis Research Center, Cleveland, Ohio.

70. Mathis, J. R.; and Laramee, R. C.: Development of Low Cost Ablative Nozzles for Solid Propellant Rocket Motors. NASA CR-72641, Thiokol Chemical Corp. (Wasatch Div.), February 1970.
71. Anon.: 260-SL-3 Motor Program, Final Phase Report, Static Test Firing of Motor 260-SL-3. NASA CR-72284, Aerojet-General Corp., July 1967.
72. Anon.: Final Report, Demonstration of the 156-Inch Motor with Segmented Fiberglass Case and Ablative Nozzle (U). AFRPL-TR-68-159, Thiokol Chemical Corp. (Wasatch Div.), December 1968.
73. Anon.: Development of Manufacturing Processes for Reinforced Plastic Solid Propellant Rocket Nozzles. AFML-TR-65-345, TRW Structures Div., TRW, Inc., November 1965.
74. Ellison, J. R.; Schoner, R. J.; and Thrasher, D. J.: Test Firing of a Castable Carbon Rocket Nozzle. AFRPL-TR-69-39, Air Force Rocket Propulsion Laboratory, February 1969.
75. Laramee, R. C.; Mathis, J. R.; and Cardall, S. H.: Development of Low Cost Ablative Materials (U). Paper presented at 26th JANNAF Solid Propulsion Meeting (Washington, DC), July 14-16, 1970, CPIA Publ. 196, vol. I, May 1970, pp. 775-809. (CONFIDENTIAL)
76. Floral, R.: Sandwich Construction for Primary Structures of Ballistic Missile and Space Vehicles. Rep. R60-25, Martin Co., October 1960.
77. Ramroth, W. G.: 156-Inch Fiberglass Case LITVC Motor Program. AFRPL-TR-66-331, Thiokol Chemical Corp. (Wasatch Div.), January 1967.
78. Anon.: 156-Inch Diameter Motor Liquid Injection TVC Program (U). AFRPL-TR-66-109, Lockheed Propulsion Co., July 1966. (CONFIDENTIAL)
79. Anon.: Investigation of Compatibility of Injectants and Materials. NASA CR-72792, United Technology Center, December 1970.
80. Anon.: Development and Demonstration of an Omniaxial Flexible Seal Movable Nozzle for Thrust Vector Control (U). AFRPL-TR-66-315, Thiokol Chemical Corp. (Wasatch Div.), November 1966. (CONFIDENTIAL)
81. Anon.: Solid Rocket Motor Metal Cases. NASA Space Vehicle Design Criteria Monograph, NASA SP-8025, April 1970.
82. Zeleznik, F. J.; and Gordon, S.: A General IBM 704 or 7090 Computer Program for Computation of Chemical Equilibrium Compositions, Rocket Performance, and Chapman-Jouguet Detonations. NASA TN D-1737, 1963.
83. White, W. B.; Johnson, S. M.; and Danzig, G. R.: Chemical Equilibrium in Complex Mixtures. *J. Chem. Phys.*, vol. 28, no. 5, May 1958, pp. 751-755.
84. Oliver, R. C.; Stephanou, S. E.; and Baier, R. W.: Calculating Free-Energy Minimization. *Chem. Eng.*, vol. 69, no. 4, Feb. 19, 1962, pp. 121-128.

85. Crisman, P. A.; Goldwasser, S. R.; and Petrozzi, P. J.: Proceedings of the Propellant Thermodynamics and Handling Conference. Special Report 12, Engineering Experiment Station, Ohio State Univ., June 1960, pp. 293-313.
86. Hoffman, J. D.: An Analysis of the Effects of Gas-Particle Mixtures on the Performance of Rocket Nozzles. TM-63-1, Jet Propulsion Center, Purdue Univ., January 1963.
87. Anon.: JANAF Thermochemical Tables. Dow Chemical Co., Midland, Mich. (updated periodically).
88. Curtiss, C. F.; Hirschfelder, J. O.; and Bird, R. B.: Theories of Gas Transport Properties. Proc. Second Biennial Gas Dynamics Symposium, Northwestern Univ. Press, January 1958, pp. 3-11.
89. Lindsay, A. L.; and Bromley, L. A.: Thermal Conductivity of Gas Mixtures. Ind. Eng. Chem., vol. 42, no. 8, January 1950, pp. 1508-1511.
90. Svehla, R. A.: Estimated Viscosities and Thermal Conductivities of Gases at High Temperatures. NASA TR R-132, October 1961.
91. Butler, J. N.; and Brokaw, R. S.: Thermal Conductivity of Gas Mixtures in Chemical Equilibrium. J. Chem. Phys., vol. 36, no. 4, June 1957, pp. 1636-1643.
92. Nelson, J. D.: Determination of Kinetic Parameters of Six Ablative Polymers by Thermo-Gravimetric Analysis. NASA TN D-3919, April 1967.
93. Wool, M. R.: User's Manual — Aerotherrn Equilibrium Surface Thermochemistry Computer Program, Version 3. Vol. 1 — Program Description and Sample Problems. AFRPL-TR-70-93, vol. I (AD-875385), Aerotherrn Corp., April 1970.
94. Anon.: Aerotherrn Graphite Surface Kinetics Computer Program. Vol. I — Program Description and Sample Problems. AFRPL-TR-72-23, vol. 1 (AD-745440), Aerotherrn Div., Acurex Corp. (Mountain View, CA), January 1972.
95. Kendall, R. M.: A General Approach to the Thermochemical Solution of Mixed Equilibrium — Nonequilibrium, Homogeneous, or Heterogeneous Systems. Rep. 66-7, Part V (Contract NAS9-4599), Aerotherrn Corp., March 14, 1967.
96. Kliegel, J. R.: Gas Particle Nozzle Flows. Ninth Symposium on Combustion. Academic Press (New York and London), 1963, pp. 811-826.
- *97. Wright, C. H.; and Lund, R. K.: Internal Aerodynamics of Solid Rocket Motors. Paper presented at the 62nd National Meeting, AIChE (Salt Lake City, UT), May 21-24, 1967.
98. Hopkins, D. F.; and Hill, D. E.: Effect of Small Radius of Curvature on Transonic Flow in Axisymmetric Nozzles. AIAA J., vol. 4, no. 8, August 1966, pp. 1337-1343.

*Dossier for design criteria monograph "Solid Rocket Motor Nozzles." Unpublished. Collected source material available for inspection at NASA Lewis Research Center, Cleveland, Ohio.

99. Prozan, R. J.: Development of a Method of Characteristics Solution for Supersonic Flow of an Ideal Frozen or Equilibrium Reacting Gas. Rep. LMSC/HREC A782535-A, Lockheed Missiles and Space Co., April 1966.
100. Kliegel, J. R.; and Nickerson, G. R.: Axisymmetric Two-Phase Perfect Gas Performance Program. Vol. I: Engineering and Programming Description. Rep. MSC-1174, Systems Group, TRW, Inc., April 1967.
101. Kliegel, J. R.; Quan, V.; Cherry, S. S.; and Frey, H. M.: One-Dimensional Two-Phase Reacting Gas Non-equilibrium Performance Program. Vol. I: Engineering and Programming Description. Rep. MSC-1178, Systems Group, TRW, Inc., August 1967.
102. Elliott, D. G.; Bartz, D. R.; and Silver, S.: Calculation of Turbulent Boundary Layer Growth and Heat Transfer in Axisymmetric Nozzles. Tech. Rep. 32-387, JPL, Calif. Inst. Tech., February 1963.
103. Anon.: User's Manual, Aerotherm Real Gas Energy Integral Boundary Layer Program (ARGEIBL). Rep. 69-UM-6911, Aerotherm Corp., November 1969.
104. Coles, D. E.; and Hirst, E. A., eds.: Proceedings: Computation of Turbulent Boundary Layers. 1968 AFOSR-IFP-Stanford Conf., Vol. 2 — Compiled Data. Thermosciences Div., Dept. Mech. Eng., Stanford Univ., 1969.
105. Schorr, C. J.: Pressure Ratio Correction Factor when Utilizing the Hydraulic Analogy. J. Spacecraft Rockets, vol. 5, no. 9, September 1968, pp. 1119-1120.
106. Adams, D. M.: Application of the Hydraulic Analogy to Axisymmetric Nonideal Compressible Gas Systems. J. Spacecraft Rockets, vol. 4, no. 3, March 1967, pp. 359-363.
107. Adams, D. M.: The Application of the Hydraulic Analogy to Rocket Motor Analysis. Spec. Rep. U-66-8A, Thiokol Chemical Corp. (Huntsville Div.), February 1966.
108. Hoyt, J. W.: The Hydraulic Analogy for Compressible Gas Flow. Appl. Mech. Rev., Vol. 15, no. 6, June 1962, pp. 419-425.
109. Anon.: Low Cost Dual Area Nozzle (U). Report R-4514-1, Rocketdyne Div., North American Rockwell Corp., April 1969. (CONFIDENTIAL)
110. Anon.: Combined Thrust Vector Control (TVC) Dual Area Nozzle (DAN) for Application in Tactical Missiles (U). Report R-4595, Rocketdyne Div., North American Rockwell Corp., May 1970. (CONFIDENTIAL)
111. Anon.: Flexible Exit Cone Nozzle Development Program Phase I Report. AFRPL-TR-68-66, Thiokol Chemical Corp. (Wasatch Div.), April 1968.
112. Salmi, R. J.; and Pelouch, J. J.: Investigation of a Submerged Nozzle on a 1/14.2-Scale Model of the 260-Inch Solid Rocket. NASA TM-X-1388, May 1967.

113. Price, F. C.; Marple, V. A.; Williams, R. H.; Dupuis, R. A.; Moody, H. L.; Smallwood, W. L.; Peters, D. L.; Dobbins, R. A.; and Briggs, R. S.: Internal Environment of Solid Rocket Nozzles. AFRPL-TDR-64-140, Philco-Ford Corp., July 1964.
114. Adams, J. M.: On the Determination of Spectral Emissivity in an Optically Thick Particle Cloud. *J. Quantitative Spectroscopy and Radiation Transfer*, vol. 8, no. 2, January-April 1968, pp. 631-639.
115. Colucci, S. E.; et al.: Experimental Determination of Nozzle Heat Transfer Coefficient with Aluminized Propellants. Paper presented at Solid Propellant Rocket Conference, ARS (Salt Lake City, UT), Feb. 1-3, 1961.
116. Travis, L. P.; Fairall, R. S.; and Lorenc, S. A.: Performance of Solid Rocket Motors with Gas Particle Flow. ASME Paper No. 63-AHGT-99, Aviation and Space Hydraulic and Gas Turbine Conference and Products Show, ASME (Los Angeles, CA), March 3-7, 1963.
117. Anon.: User's Manual, Aerotherm Charring Material Thermal Response and Ablation Program, Version 3. AFRPL-TR-70-92, vol. I, Aerotherm Corporation, April 1970.
118. Anon.: User's Manual, Aerotherm Axisymmetric Transient Heating and Material Ablation Computer Program (ASTHMA 3). AFRPL-TR-72-24, Aerotherm Corporation, January 1972.
119. Freidman, H. A.: Effect of Rocket Engine Combustion on Chamber Materials. Part II: Two Dimensional Computer Program. NAA-RR-6050-2, Rocketdyne Div., North American Aviation, Inc., September 1965.
120. Anon.: Captive-Fired Testing of Solid Rocket Motors. NASA Space Vehicle Design Criteria Monograph, NASA SP-8041, March 1971.
121. Cox, D. M.: Hot Gas Secondary Injection Thrust Vector Control Demonstration (U). AFRPL-TR-68-166, Thiokol Chemical Corp. (Wasatch Div.), December 1968. (CONFIDENTIAL)
122. Shaefer, J. W.; Dahm, T. J.; Rodriguez, D. A.; Reese, J. J., Jr.; and Wool, M. R.: Studies of Ablative Material Performance for Solid Rocket Nozzle Applications. NASA CR-72429, Aerotherm Corp., March 1968.
123. Moody, H. L.; and Price, F. C.: Final Report, Prediction of Nozzle Material Performance for the 260-Inch Motor SL-3. Publ. UG-4239 (NAS7-567), Philco-Ford Corp., March 1968.
124. Pilkey, W. D., ed.: Structural Mechanics Computer Programs: Surveys, Assessments, & Availability. University Press of Virginia, 1974.
125. Becker, E. B.; and Brisbane, J. J.: Application of the Finite Element Method to Stress Analysis of Solid Propellant Rocket Grains. Rep. S-76, vol. II, pt. 1 (AD 476515) and pt. 2 (AD 476735), Rohm & Haas Co., January 1966.
126. Brisbane, J. J.; and Becker, E. B.: Stress Analysis of Solid Propellant Grains Under Transverse Acceleration Loads Rep. S-116, Rohm & Haas Co., March 1967.

127. Crose, J. G.; and Jones, R. M.: SAAS III, Finite Element Stress Analysis of Axisymmetric and Plane Solids with Different Orthotropic, Temperature-Dependent Material Properties in Tension and Compression. SAMSO-TR-71-103, The Aerospace Corp., June 22, 1971.
128. Weiler, F. C.: DOASIS User's Manual. Weiler Research Co. Inc. (Mountain View, CA). (To be published by AFML)
129. MacNeal, R. H., ed.: The NASTRAN Theoretical Manual. NASA SP-221(01), April 1972.
130. Bushnell, D.: Stress, Stability, and Vibration of Complex Shells of Revolution: Analysis and User's Manual for BOSOR3. N-SJ-69-1, Lockheed Missiles and Space Co., Sept. 6, 1969.
131. Almroth, B. O.; Brogan, F. A.; Meller, E.; Zele, F.; and Petersen, H. T.: Collapse Analysis for Shells of General Shape. Vol. II, User's Manual for the STAGS-A Computer Code. AFFDL-TR-71-8, AFFDL, March 1973.
132. Anon.: Hydrostatic Test of 260-SL-1 Motor Chamber and Nozzle Shell, Final Report. Rep. HTR-1 (NAS3-6284), Aerojet-General Corp., May 12, 1965.
133. Anon.: 260-SL-3 Motor Nozzle and Exit Cone Design, Fabrication and Assembly, Final Phase Report, Vol. III. NASA CR-72283, Aerojet-General Corp., June 14, 1967.
134. Warga, J. J.: Final Report, Investigation of Effects of Ablative Discrepancies on Nozzle Performance Reliability. NASA CR-72702, Aerojet Solid Propulsion Co., January 1970.
135. Anon.: Solid Propulsion Nomenclature Guide. CPIA Publ. 80, May 1965.

NASA SPACE VEHICLE DESIGN CRITERIA MONOGRAPHS ISSUED TO DATE

ENVIRONMENT

SP-8005	Solar Electromagnetic Radiation, Revised May 1971
SP-8010	Models of Mars Atmosphere (1974), Revised December 1974
SP-8011	Models of Venus Atmosphere (1972), Revised September 1972
SP-8013	Meteoroid Environment Model—1969 (Near Earth to Lunar Surface), March 1969
SP-8017	Magnetic Fields—Earth and Extraterrestrial, March 1969
SP-8020	Mars Surface Models (1968), May 1969
SP-8021	Models of Earth's Atmosphere (90 to 2500 km), Revised March 1973
SP-8023	Lunar Surface Models, May 1969
SP-8037	Assessment and Control of Spacecraft Magnetic Fields, September 1970
SP-8038	Meteoroid Environment Model—1970 (Interplanetary and Planetary), October 1970
SP-8049	The Earth's Ionosphere, March 1971
SP-8067	Earth Albedo and Emitted Radiation, July 1971
SP-8069	The Planet Jupiter (1970), December 1971
SP-8084	Surface Atmospheric Extremes (Launch and Transportation Areas), Revised June 1974
SP-8085	The Planet Mercury (1971), March 1972
SP-8091	The Planet Saturn (1970), June 1972
SP-8092	Assessment and Control of Spacecraft Electromagnetic Interference, June 1972
SP-8103	The Planets Uranus, Neptune, and Pluto (1971), November 1972

- SP-8105 Spacecraft Thermal Control, May 1973
SP-8111 Assessment and Control of Electrostatic Charges, May 1974
SP-8116 The Earth's Trapped Radiation Belts, March 1975
SP-8117 Gravity Fields of the Solar System, April 1975
SP-8118 Interplanetary Charged Particle Models (1974), March 1975

STRUCTURES

- SP-8001 Buffeting During Atmospheric Ascent, Revised November 1970
SP-8002 Flight-Loads Measurements During Launch and Exit, December 1964
SP-8003 Flutter, Buzz, and Divergence, July 1964
SP-8004 Panel Flutter, Revised June 1972
SP-8006 Local Steady Aerodynamic Loads During Launch and Exit, May 1965
SP-8007 Buckling of Thin-Walled Circular Cylinders, Revised August 1968
SP-8008 Prelaunch Ground Wind Loads, November 1965
SP-8009 Propellant Slosh Loads, August 1968
SP-8012 Natural Vibration Modal Analysis, September 1968
SP-8014 Entry Thermal Protection, August 1968
SP-8019 Buckling of Thin-Walled Truncated Cones, September 1968
SP-8022 Staging Loads, February 1969
SP-8029 Aerodynamic and Rocket-Exhaust Heating During Launch and Ascent, May 1969
SP-8030 Transient Loads From Thrust Excitation, February 1969
SP-8031 Slosh Suppression, May 1969
SP-8032 Buckling of Thin-Walled Doubly Curved Shells, August 1969
SP-8035 Wind Loads During Ascent, June 1970

SP-8040	Fracture Control of Metallic Pressure Vessels, May 1970
SP-8042	Meteoroid Damage Assessment, May 1970
SP-8043	Design-Development Testing, May 1970
SP-8044	Qualification Testing, May 1970
SP-8045	Acceptance Testing, April 1970
SP-8046	Landing Impact Attenuation for Non-Surface-Planing Landers, April 1970
SP-8050	Structural Vibration Prediction, June 1970
SP-8053	Nuclear and Space Radiation Effects on Materials, June 1970
SP-8054	Space Radiation Protection, June 1970
SP-8055	Prevention of Coupled Structure-Propulsion Instability (Pogo), October 1970
SP-8056	Flight Separation Mechanisms, October 1970
SP-8057	Structural Design Criteria Applicable to a Space Shuttle, Revised March 1972
SP-8060	Compartment Venting, November 1970
SP-8061	Interaction with Umbilicals and Launch Stand, August 1970
SP-8062	Entry Gasdynamic Heating, January 1971
SP-8063	Lubrication, Friction, and Wear, June 1971
SP-8066	Deployable Aerodynamic Deceleration Systems, June 1971
SP-8068	Buckling Strength of Structural Plates, June 1971
SP-8072	Acoustic Loads Generated by the Propulsion System, June 1971
SP-8077	Transportation and Handling Loads, September 1971
SP-8079	Structural Interaction with Control Systems, November 1971
SP-8082	Stress-Corrosion Cracking in Metals, August 1971

- SP-8083 Discontinuity Stresses in Metallic Pressure Vessels, November 1971
- SP-8095 Preliminary Criteria for the Fracture Control of Space Shuttle Structures, June 1971
- SP-8099 Combining Ascent Loads, May 1972
- SP-8104 Structural Interaction With Transportation and Handling Systems, January 1973

GUIDANCE AND CONTROL

- SP-8015 Guidance and Navigation for Entry Vehicles, November 1968
- SP-8016 Effects of Structural Flexibility on Spacecraft Control Systems, April 1969
- SP-8018 Spacecraft Magnetic Torques, March 1969
- SP-8024 Spacecraft Gravitational Torques, May 1969
- SP-8026 Spacecraft Star Trackers, July 1970
- SP-8027 Spacecraft Radiation Torques, October 1969
- SP-8028 Entry Vehicle Control, November 1969
- SP-8033 Spacecraft Earth Horizon Sensors, June 1970
- SP-8034 Spacecraft Mass Expulsion Torques, December 1969
- SP-8036 Effects of Structural Flexibility on Launch Vehicle Control Systems, February 1970
- SP-8047 Spacecraft Sun Sensors, June 1970
- SP-8058 Spacecraft Aerodynamic Torques, January 1971
- SP-8059 Spacecraft Attitude Control During Thrusting Maneuvers, February 1971
- SP-8065 Tubular Spacecraft Booms (Extendible, Reel Stored), February 1971
- SP-8070 Spaceborne Digital Computer Systems, March 1971
- SP-8071 Passive Gravity-Gradient Libration Dampers, February 1971

SP-8074	Spacecraft Solar Cell Arrays, May 1971
SP-8078	Spaceborne Electronic Imaging Systems, June 1971
SP-8086	Space Vehicle Displays Design Criteria, March 1972
SP-8096	Space Vehicle Gyroscope Sensor Applications, October 1972
SP-8098	Effects of Structural Flexibility on Entry Vehicle Control Systems, June 1972
SP-8102	Space Vehicle Accelerometer Applications, December 1972

CHEMICAL PROPULSION

SP-8087	Liquid Rocket Engine Fluid-Cooled Combustion Chambers, April 1972
SP-8113	Liquid Rocket Engine Combustion Stabilization Devices, November 1974
SP-8107	Turbopump Systems for Liquid Rocket Engines, August 1974
SP-8109	Liquid Rocket Engine Centrifugal Flow Turbopumps, December 1973
SP-8052	Liquid Rocket Engine Turbopump Inducers, May 1971
SP-8110	Liquid Rocket Engine Turbines, January 1974
SP-8081	Liquid Propellant Gas Generators, March 1972
SP-8048	Liquid Rocket Engine Turbopump Bearings, March 1971
SP-8101	Liquid Rocket Engine Turbopump Shafts and Couplings, September 1972
SP-8100	Liquid Rocket Engine Turbopump Gears, March 1974
SP-8088	Liquid Rocket Metal Tanks and Tank Components, May 1974
SP-8094	Liquid Rocket Valve Components, August 1973
SP-8097	Liquid Rocket Valve Assemblies, November 1973
SP-8090	Liquid Rocket Actuators and Operators, May 1973
SP-8080	Liquid Rocket Pressure Regulators, Relief Valves, Check Valves, Burst Disks, and Explosive Valves, March 1973

- SP-8064 Solid Propellant Selection and Characterization, June 1971
- SP-8075 Solid Propellant Processing Factors in Rocket Motor Design, October 1971
- SP-8076 Solid Propellant Grain Design and Internal Ballistics, March 1972
- SP-8073 Solid Propellant Grain Structural Integrity Analysis, June 1973
- SP-8039 Solid Rocket Motor Performance Analysis and Prediction, May 1971
- SP-8051 Solid Rocket Motor Igniters, March 1971
- SP-8025 Solid Rocket Motor Metal Cases, April 1970
- SP-8114 Solid Rocket Thrust Vector Control, December 1974
- SP-8041 Captive-Fired Testing of Solid Rocket Motors, March 1971